China Geology 7 (2024) 551−585

China Geology

Journal homepage: http://chinageology.cgs.cn
https://www.sciencedirect.com/journal/china-geology

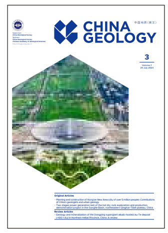

Formation, evolution, reconstruction of black shales and their influence on shale oil and gas resource

Shi-zhen Li[a, b, c,*], Qiu-chen Xu[a, b, c,*], Mu Liu[d,*], Guo-heng Liu[e], Yi-fan Li[f], Wen-yang Wang[g], Xiao-guang Yang[a, b, c], Wei-bin Liu[a, b, c], Yan-fei An[h], Peng Sun[i], Tao Liu[j], Jiang-hui Ding[k], Qian-chao Li[f], Chao-gang Fang[j]

[a] *State Key Laboratory of Continental Shale Oil*, *Beijing* 100083, *China*
[b] *The Key Laboratory of Unconventional Oil and Gas Geology*, *China Geological Survey*, *Beijing* 100083, *China*
[c] *Oil and Gas Survey*, *China Geological Survey*, *Ministry of Natural Resources*, *Beijing* 100083, *China*
[d] *State Key Laboratory of Lithospheric and Environmental Coevolution*, *Institute of Geology and Geophysics*, *Chinese Academy of Sciences*, *Beijing* 100029, *China*
[e] *School of Geosciences*, *China University of Petroleum (East China)*, *Qingdao* 266580, *China*
[f] *School of Energy Resources*, *China University of Geosciences (Beijing)*, *Beijing* 100083, *China*
[g] *Key Laboratory of Petroleum Resources Research*, *Institute of Geology and Geophysics*, *Chinese Academy of Sciences*, *Beijing* 100029, *China*
[h] *School of Resource and Environment Engineering*, *Anhui University*, *Hefei* 230601, *China*
[i] *Yangtze University*, *Wuhan* 430100, *China*
[j] *Nanjing Center*, *China Geological Survey*, *Nanjing* 210016, *China*
[k] *National Elite Institute of Engineering*, *CNPC*, *Beijing* 100096, *China*

A R T I C L E I N F O

Article history:
Received 19 April 2024
Received in revised form 4 July 2024
Accepted 9 July 2024
Available online 18 July 2024

Keywords:
Black shales
Shale oil and gas
Resource effects
Sedimentary environment
Sedimentary process
Organic matter accumulation
Diagenetic evolution
Thermal evolution
Organic matter and inorganic minerals
Tectonic reconstruction
Oil and gas exploration engineering
Veins
Fluid activity

A B S T R A C T

Black shales are important products of material cycling and energy exchange among the lithosphere, atmosphere, hydrosphere, and biosphere. They are widely distributed throughout geological history and provide essential energy and mineral resources for the development of human society. They also record the evolution process of the earth and improve the understanding of the earth. This review focuses on the diagenesis and formation mechanisms of black shales sedimentation, composition, evolution, and reconstruction, which have had a significant impact on the formation and enrichment of shale oil and gas. In terms of sedimentary environment, black shales can be classified into three types: Marine, terrestrial, and marine-terrestrial transitional facies. The formation processes include mechanisms such as eolian input, hypopycnal flow, gravity-driven and offshore bottom currents. From a geological perspective, the formation of black shales is often closely related to global or regional major geological events. The enrichment of organic matter is generally the result of the interaction and coupling of several factors such as primary productivity, water redox condition, and sedimentation rate. In terms of evolution, black shales have undergone diagenetic evolution of inorganic minerals, thermal evolution of organic matter and hydrocarbon generation, interactions between organic matter and inorganic minerals, and pore evolution. In terms of reconstruction, the effects of fold deformation, uplift and erosion, and fracturing have changed the stress state of black shale reservoirs, thereby having a significant impact on the pore structure. Fluid activity promotes the formation of veins, and have changed the material composition, stress structure, and reservoir properties of black shales. Regarding resource effects, the deposition of black shales is fundamental for shale oil and gas resources, the evolution of black shales promotes the shale oil and gas formation and storage, and the reconstruction of black shales would have caused the heterogeneous distribution of oil and gas in shales. Exploring the formation mechanisms and interactions of black shales at different scales is a key to in-depth research on shale formation and evolution, as well as the key to revealing the mechanism controlling shale oil and gas accumulation. The present records can reveal how these processes worked in geological history, and improve our understanding of the coupling mechanisms among regional geological events, black shales evolution, and shale oil and gas formation and enrichment.

First author: *E-mail address*: lishz2006@sina.com (Shi-zhen Li).

* Corresponding author: *E-mail address*: lishz2006@sina.com (Shi-zhen Li); qiuchenxu@126.com (Qiu-chen Xu); liumu@mail.iggcas.ac.cn (Mu Liu).

Literary editor: Li-qiong Jia
doi:10.31035/cg2024060
2096-5192/© 2024 China Geology Editorial Office.

1. Introduction

Black shales are extensively distributed throughout geological history and are significantly influenced by physical, chemical, and biological processes. They are essential products of material cycling and energy exchange between the lithosphere, atmosphere, hydrosphere, and biosphere. Until now, there is no unified and clear classification or definition of black shales, which are generally considered to be fine-grained sedimentary rocks containing a certain amount of organic matter (TOC > 0.5%), primarily composed of particles smaller than 0.0625 mm in diameter (Aplin AC and Macquaker JHS, 2011; Jiang ZX et al., 2013; Guo YH et al., 2021; Cao YC et al., 2023). The main components of black shales include clay minerals, quartz, carbonate minerals, organic matter, saline minerals, and volcaniclastic materials (Shao LY and Zhang TC, 2023; Jiang ZX et al., 2023a). Typically formed in reducing environments, black shales exhibit characteristics of mixed sedimentation. Although black shales appear very similar at the outcrop scale, they are complex in mineral composition and structure, diverse in sedimentary facies, intricate in depositional patterns, highly heterogeneous, fine-grained, and hard to be observed (Ilgen AG et al., 2017; Peng J et al., 2022). Black shales also act important record of the earth's evolution processes and enhancing our understanding of the earth. They also supply indispensable energy and mineral resources for human societal development, making them a long-standing focus of geological research.

Black shales were distributed worldwide during geological history, usually accounting for about 70% of basin fill (Aplin AC and Macquaker JHS, 2011). They act as a thick geological history book, faithfully recording the evolution of ancient marine environments, changes in paleogeography, and the occurrence and development of significant geological events. The aggregation and fragmentation of supercontinents, changes in earth's orbit, global sea-level fluctuations, alterations in ocean current circulation patterns, ice ages, and large-scale volcanic activities leading to oceanic anoxic events, as well as biological evolution, may have significantly influenced the large-scale formation of black shales on a plate scale or within specific sedimentary basins (Li MW et al., 2020; Pan SQ et al., 2021; Jin ZJ et al., 2023; Wen HJ et al., 2024). By studying the existing black shale fabric and geochemical characteristics in detail, it is possible to trace back the magnificent geological events of geological history and the formation and evolution of shales. It is noteworthy that the mineral, elemental, and isotopic abundances of black shales today are controlled by physical, chemical, and biological processes, which are facilitated by specific conditions at different times during the formation and evolution history of black shales (Rimstidt JD et al., 2017; Lev SM et al., 2008).

Black shales contain a variety of abundant mineral resources and trace elements, making them significant for economic utilization, elemental cycling, and environmental protection (Piper DZ and Calvert SE, 2009). In terms of mineral resources, some black shales are rich in Mn, Fe, Co, Ni, Cu, Zn, Mo, U, platinum group elements, or Au (Parviainen A and Loukola-Ruskeeniemi K, 2019; Jin ZJ et al., 2023; Wen HJ et al., 2024), and even contain He resources in shale gas (Nie HK et al., 2023; Wang XF et al., 2023), and have potential economic value. In terms of elemental cycling, the formation and erosion of shale would continuously sequestrate or release C, S, and some trace elements, affecting global biogeochemical cycling, and are products of material and energy exchange between different reservoirs of the Earth (Rimstidt JD et al., 2017; Jin ZJ et al., 2023). In terms of environmental protection, due to the abundance of various harmful elements in black shales, including radioactive nuclides, sulfides are highly susceptible to oxidation and dissolution, releasing protons and trace metals, becoming potential sources of pollution for soil, groundwater, and surface water, which have raised widespread concern for human health issues (Parviainen A and Loukola-Ruskeeniemi K, 2019; Zhang D et al., 2021; Wei W et al., 2024).

Black shales serve both as source rocks for conventional oil and gas and as reservoirs for unconventional oil and gas such as shale oil and gas (Aplin AC and Macquaker JHS, 2011; Bilgen S and Sarıkaya İ, 2016; Ilgen AG et al., 2017). According to a report by the U.S. Energy Information Administration (EIA, 2015), the technically recoverable shale gas resources in 46 countries worldwide amount to 21.45×10^{12} m^3, with shale oil at 57.39×10^9 t. Since the 21st century, shale oil and gas have achieved a series of significant exploration and development breakthroughs in the United States, helping the country become a net exporter of oil and gas, achieve "energy independence", and profoundly influence the global energy landscape (Li SZ, 2022; Zou CN et al., 2023). China has also made significant breakthroughs in the geological theory research and exploration and development of shale oil and gas. In 2023, the annual production of shale gas was about 25×10^9 m^3, accounting for more than 10% of the total natural gas output, and the production of shale oil exceeded 4×10^6 t, showing a rapidly increasing trend. From the exploration and development situation of shale oil and gas in China and the United States, it can be inferred that shale oil and gas will further play an important role in meeting global energy demands and will become an important part of the energy structure of most countries in the world. The exploration and development of shale oil and gas have not only promoted people's high attention to black shales but have also greatly promoted in-depth research on black shales. However, few literatures systematically elaborate on the series of mechanisms that occur throughout the life cycle of shale from formation to evolution and finally to reconstruction, as well as the effects of these mechanisms on the formation and enrichment of shale oil and gas, which is also the purpose of this paper.

This paper first reviews the main distribution characteristics of black shales worldwide in the geological history, then summarizes the current research hotspots and the latest progress in understanding from four aspects: Formation, composition, evolution, and reconstruction of black shales, and finally discusses the relationship between the formation, evolution, reconstruction of black shales and the generation and enrichment of shale oil and gas. This study is based on petroleum geology, with the causes and mechanisms in the processes of sedimentation, composition, diagenesis, and reconstruction of black shales as the main line, striving to reveal the macro and micro mechanisms in the life history of shale, aiming to improve the overall understanding of black shales from a new perspective.

2. Distribution of black shales in geological history

From a temporal perspective, the earliest black shales are believed to have formed during the Archean Eon, exemplified by the Duffer Formation, Nullagine Group, Hardey Formation in the Pilbara, Western Australia, dating back approximately 3.46 Ga to 2.76 Ga (Wille M et al., 2013). During the Proterozoic Eon, the evolution of life in the marine chemical environment, particularly represented by the emergence and development of oxygenic photosynthetic organisms such as cyanobacteria (Fig. 1b), significantly enhanced marine primary productivity. Consequently, the distribution of black shales expanded, with some, like the Xiamaling Formation and Hongshuizhuang Formation black shales in China and the Velkerri Formation black shales in Australia, possessing industrial hydrocarbon source rock potential (Zhao WZ et al., 2019).

Compared to the Precambrian, the distribution of black shales during the Phanerozoic Eon is considerably more extensive (Fig. 1). It is estimated that over 90% of hydrocarbon source rocks were formed after the Ediacaran (Klemme HD and Ulmishek GF, 1991). Several factors may contribute to this phenomenon: (1) The enhanced preservation condition of younger shales by overlying sediments, resulting in less intense subsequent alteration or recycling compared to the older Precambrian black shales (Cawood PA, et al., 2022). (2) The rapid evolution of metazoans and the increasing complexity of biological systems during the Phanerozoic provided a diverse organic matter foundation. (3) The heterogenization of marine chemical structures promoted the geographically differentiated distribution of black shales.

Klemme HD and Ulmishek GF (1991) conducted a comprehensive study on the temporal and spatial distribution of the world's hydrocarbon source rocks, summarizing six major global depositional sequences of source rocks: (1) The Silurian (Llandovery-Pridoli), (2) the Upper Devonian-Carboniferous (Frasnian-Tournaisian), (3) the Carboniferous-Lower Permian (Bashkirian-Kungurian), (4) the Upper Jurassic (Callovian-Tithonian), (5) the Cretaceous (Aptian-Turonian), and (6) the Paleocene-Eocene. These strata, which only account for 35% of the Phanerozoic Eon, contribute to 91.5% of the world's original reserves of oil and natural gas. The Silurian, Upper Devonian, Upper Jurassic, and middle Cretaceous source rocks were deposited during transgressive periods, while the Carboniferous-Lower Permian and Paleocene-Eocene source rocks were deposited during regressive periods. From a tectonic perspective, these six shale sequences were primarily deposited in passive continental margin basins and rift basins formed under extensional tectonics (Wen ZX et al., 2014; Zhu RX, 2024). Particularly within the Tethyan and Laurasian tectonic domains, the continuous and stable subsidence under extensional environments, coupled with the control of global sea-level changes, led to the formation of black shale segments primarily within the condensed section (CS) at the top of the transgressive systems tract (TST), where the TOC content is relatively high. During the deposition of the Upper Jurassic, Paleocene-Eocene, Cretaceous, and Upper Devonian shale sequences, global temperatures and humidity were high, favoring the formation and preservation of Type I and II organic matter, making these sequences the main enriched layers of global shale oil, accounting for 87.83% of the total resource volume (Zou CN et al., 2023).

The geochemical, physical, and petrological characteristics of black shales exhibit spatial and temporal variability, manifesting as regional distribution in different strata over geological time and local deposition under specific tectonic patterns. The factors controlling the formation of black shales also vary by stratum and region, and it is clear that they are not the result of a single mechanism. The main factors controlling shale deposition may be influenced by a variety of processes, including tectonics, climate, hydrology, biology, and sea level (Klemme HD and Ulmishek GF, 1991; Li MW et al., 2020; Jin ZJ et al., 2023). These factors have interacted in complex ways across different periods and regions, resulting in the heterogeneous distribution of black shales temporally and regionally.

3. Formation of black shales

3.1. Sedimentary environment

The sedimentary environment of black shales can be divided into three facies: Marine, terrestrial, and marine-terrestrial transitional.

3.1.1. Marine

Marine is the most important sedimentary environment for the formation of high-quality fine-grained sedimentary rocks, and the deposition of black shale is mostly controlled by autogenesis. A reducing sedimentary environment is conducive to the preservation of organic matter, especially in marine shelf, continental slope-basin, and enclosed basin, which are the most favorable sedimentary environments for the formation of thick black shales (Trabucho Alexandre J, 2015).

The marine shelf is located between the outer edge of the continental shelf and the slope break zone, with an upper limit near the wave base and a lower limit of about 200 m in water depth, with a width ranging from several kilometers to hundreds of kilometers (Jiang ZX, 2003). Due to surface

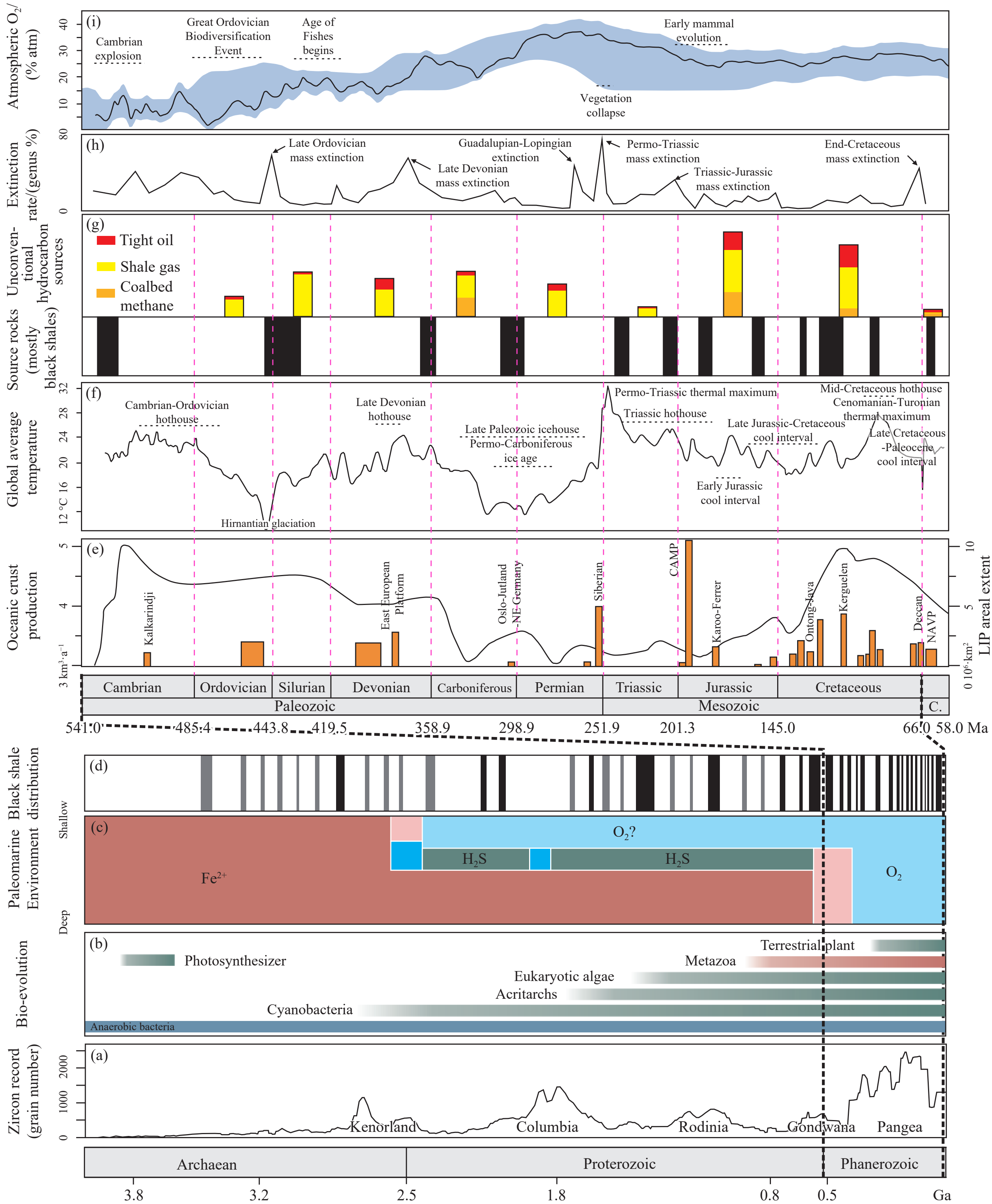

Fig. 1. Paleoecological changes of the deep-time Earth, major biological and geological events, and distribution of black shales. a–tectonic evolution phases and zircon record (Cawood PA et al., 2022); b–biological evolution timescale; c–oceanic redox conditions, with pink and light blue representing the transition between iron-rich (Fe^{2+}) and oxygenated (O_2) conditions, as well as sulfidic waters (H_2S) (Planavsky NJ et al., 2011); d–stratigraphic distribution of black shales, with black bar codes indicating the global distribution of black shales, and grey intervals representing local development (Jin ZJ et al., 2023); e–volume of new oceanic crust (Stanley SM, 2015) and the extent of large igneous province areas (Kidder DL and Worsley TR, 2010); f–global average temperature (Scotese CR et al., 2021); g–unconventional oil and gas resource volumes and the distribution of major black shale formations (Pan SQ et al., 2021); h–extinction rate of Genus-level (Sepkoski JJ, 1984); i–changes in atmospheric oxygen content (Mills BJW et al., 2023).

runoff and upwelling, water column is rich in nutrients and have high productivity. The deposition pathway of organic matter is shorter, the deposition rate is higher, and it is not easy to be oxidized during transportation and deposition, which helps to preserve organic matter (Fig. 2a). The shale in the continental slope-basin is mainly formed by deep-sea sedimentation, and the high yield of planktonic organisms in surface water, reducing sedimentary bottom water environment, and relative lack of terrestrial debris are necessary conditions for the formation of black shales (Fig. 2b; Guo W et al., 2022; Trabucho Alexandre J, 2015). The enclosed basin is surrounded by continents and islands, but there are narrow waterways or straits that connect with the ocean, resulting in poor water exchange and renewal capabilities, leading to water stratification and widespread anoxic bottom water (Fig. 2c; Arthur MA and Sageman BB, 1994).

3.1.2. Terrestrial

The terrestrial shale is mainly formed in large and medium-sized inland lakes, and the massive organic matter provides a basis for the formation of high-quality source rocks. However, due to the complexity of terrigenous detrital and organic matter input, the diversity and heterogeneity of terrestrial shale are distinct (Li MW et al., 2020; Wang EZ et al., 2022).

The terrestrial black shales mainly develop in the semi-deep lake to deep lake facies (Guo XS et al., 2023), where wave action is no longer involved and the water is quiet. Under the combination factors of suitable biological yield, redox environment, and terrestrial input (Tyson RV and Pearson TH, 1991), it forms in two modes: Lake transgression and water stratification. The lake transgression leads to a rise in lake level, resulting in extensive hypoxia in the area where organic matter was originally developed, forming a reducing environment and enhanced preservation conditions (Fig. 2d). The water stratification is caused by rapid alteration of chemocline and thermocline, which make it difficult for the upper and lower water bodies to circulate and exchange. Bottom water stagnancy creates an anoxic environment, and organic matter can be buried and preserved (Fig. 2d; Guan QZ et al., 2016).

3.1.3. Marine-terrestrial transitional

The marine-terrestrial transitional shale is influenced by both marine and terrestrial processes, and is sensitive to climate and environmental changes. Therefore, it has a small scale, frequent changes in lithology, strong heterogeneity, and is usually interbedded with coal seams, tight sandstone layers, etc. It is rich in organic matter, has moderate maturity, and has good resource prospects (Luo W et al., 2018; Liang JT et al, 2020).

The marine-terrestrial transitional shale is mainly deposited in shallow water environments, including swamp in river delta systems, and lagoons in barrier systems (Luo W et al., 2018; Liang JT et al, 2020). Delta is formed at the intersection of marine and land, and swamps are low-lying areas of delta plains that are periodically submerged underwater and in a reducing environment. Under the influence of warm and humid climate and sufficient vegetation, black shales interbedded with coal seams can be deposited (Fig. 2e; Jasper K et al., 2010). A lagoon is a shallow water basin enclosed by coastlines and barrier islands, connected to or semi-isolated from the open sea by a waterway. The water body is in a low-energy state, and anaerobic bacteria often breed in the lower part, forming a reducing environment (McLaughlin MR et al., 2009), which is conducive to the preservation of organic matter (Fig. 2f). The two systems have high similarities in lithology, sedimentary structures, paleontological associations, trace fossils, geochemical parameters, etc. (Dong DZ et al., 2021).

3.2. Sedimentary processes

3.2.1. Eolian input

Aeolian inputs primarily include dust and volcanic ash. Dust deposits into offshore oceans due to dust storms, such as

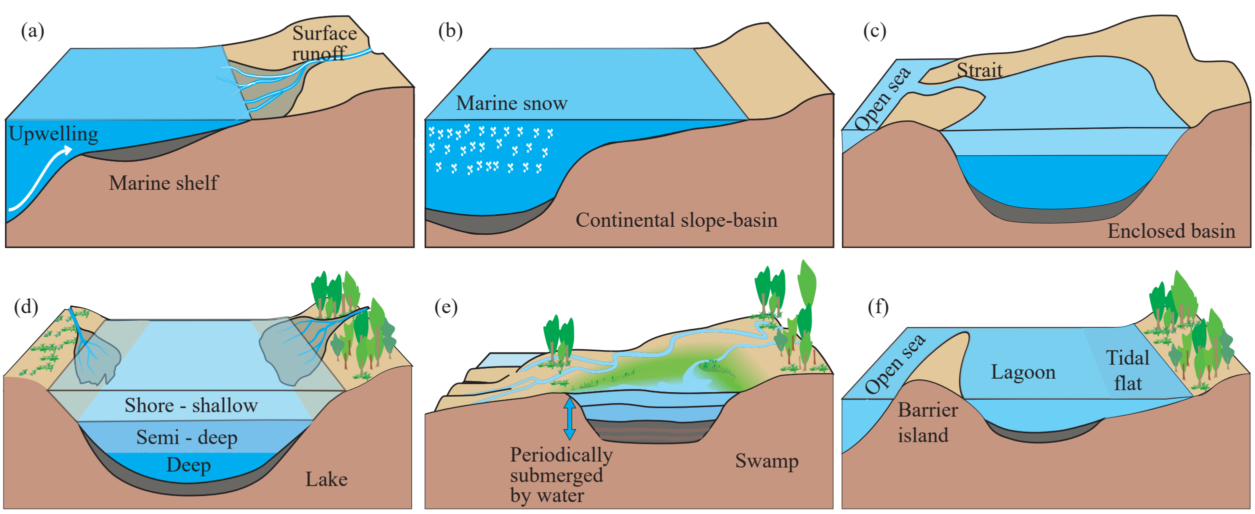

Fig. 2. Sedimentary schematic diagram of black shales in different sedimentary environments (modified from Arthur MA and Sageman BB, 1994; Trabucho Alexandre J, 2015). a–marine shelf; b–slope basin; c–enclosed basin; d–lake; e–swamp; f–lagoon.

aeolian sediments from the Sahara Desert found in the central Atlantic (Middleton NJ and Goudie AS, 2001). Intense volcanic eruptions produce vast amounts of volcanic ash, drifting to the open sea and depositing to form layers of volcanic ash (K-Bentonite layer) (Rose WI and Durant AJ, 2009). Volcanic ash layers in fine-grained sedimentary rocks serve as excellent chronostratigraphic markers, such as those found in the Wufeng-Longmaxi formations in the Upper Yangtze region and the Upper Cretaceous shales in Utah, USA, which are valuable for stratigraphic correlation (Su WB et al., 2007; Zelt FB, 1985). Generally, the deposition of dust and volcanic ash would preserve the original sedimentary features; however, some may be reworked by bottom currents during deposition, exhibiting certain bedding characteristics.

3.2.2. Hypopycnal flow

Hypopycnal plumes primarily consist of mud-rich suspended sediments from river inputs, floating over saline and denser seawater at shallow depths（Fig. 3a）. Their floating range generally extends several tens of kilometers offshore (Warrick JA et al., 2007; Falcieri FM et al., 2014), and under the influence of coastal currents, can even reach several hundred kilometers offshore (Weight RWR et al., 2011). Hypopycnal plumes, not impacted by other hydrodynamic conditions (like waves, bottom currents), settle as suspended sediments, forming laminated bedding (Fig. 3i). Characteristics of laminated bedding include no grain-size grading internally, weak sorting, and blurry bedding boundaries with gradual transitions, indicating a passive deposition process under weak hydrodynamic conditions. Horizontal laminations are commonly observed in shale deposition spanning from the Wufeng-Longmaxi, Niutitang Formations (or Qiongzhusi Formation), to Dalong organic rich shales in the Upper Yangtze region (Fig. 3j).

3.2.3. Gravity-driven

(i) Delta front turbidity current

When rivers form deltas and enter the sea, relatively steep slopes are created in the delta front regions, leading to surge-type turbidity currents caused by slope failures (Pattison SAJ, 2005). As the energy of the turbidity current diminishes, its dominant sediment transport mechanism transfers from sediment gravity flow to traction and finally to suspension, resulting in a typical vertical variation sequence. Key sedimentary features include bioturbation at the top with relatively integrated contacts. Internally, a general coarsening upward sequence divided into five lamina groups, with the finest grains at the bottom transitioning to coarser grains towards the top; and erosional bases often featuring channels and tool marks (Lazar OR et al., 2015; Fig. 3c–d).

(ii) Density flow

Density flows refer to high-density fluid inputs from rivers, denser than seawater, thus moving as bottom currents from the delta front slopes towards the offshore (Mulder T and Alexander J, 2001). These flows, generated by high-density river waters, can result from extreme floods or in mountainous rivers in humid environments (Mulder T and Syvitski JPM, 1995). The formation of density flows is influenced by seawater salinity, climate changes, and the degree of weathering (Schieber J, 2016). A complete density flow deposit shows symmetrical grain-size variations, with the lower part displaying inverse grading and the upper part showing normal grading, reflecting the transport capacity cycle of density flows from weak to strong and then back to weak. However, due to intense erosion during peak flood periods, the upper part of density flow deposits often exhibits an incomplete depositional sequence dominated by inverse grading features (Mulder T and Alexander J, 2001).

(iii) Wave-influenced sediment gravity flow

Wave-influenced sediment gravity flows result from the secondary transport and deposition of sediments settled from hyperpycnal or density flows (near delta regions) under the action of waves and bottom currents (Bhattacharya JP and MacEachern JA, 2009; Friedrichs CT and Scully ME, 2007; Bentley SJ, 2003). The deposition and transport mechanism of wave-influenced sediment gravity flows is characterized by a large number of fine-grained sediments being suspended to form high-density flows under the agitation of storm waves or bottom currents, maintaining suspension due to wave action, and the slope-induced gravity causing the sediments to be advected offshore, showing a vertical transition from traction, to sediment gravity flow, to suspension. Hence, their overall deposition also presents a set of normal grading sequences (Bhattacharya JP and MacEachern JA, 2009; Martin DP et al., 2008) (Fig. 3e–f). Sedimentary features include bioturbation on the top. Internally, clay-rich laminae with normal grading changes, extremely thin curved or wavy laminae transitioning from silt to clay with gradual contacts at the top, and rich silt, homogeneous laminae with vague grading features at the top with gradual contacts; and erosional bases, curved interfaces with low relief (Fig. 3e–f; Macquaker JHS et al., 2010).

(iv) Storm flow

Storm flows refer to bottom currents moving offshore under the influence of storm waves, mainly depositing fine-grained sediments in offshore regions (Aigner T and Reineck HE, 1982). Unlike the sediment gravity flows mentioned above, the transport dynamics of storm flows are primarily driven by coastal downwelling, with gravity playing a relatively minor role. However, as these flows move away from the shoreline, their transport capacity gradually decreases, and the sediment transport mechanism transitions from mixed flow erosion and traction to suspension, thus, the depositional sequence also exhibits normal grading characteristics. Sedimentary features include bioturbation on the top with signs of wave modification. Internally, the sequence gradually fines upward, with laminae curving at the bottom and becoming straighter upwards; bottom laminae overlying erosional surfaces and filling depressions; and upper laminae with more obscure layering; and erosional bases, curved to wavy, with high relief and common small channels (Fig. 3g–h).

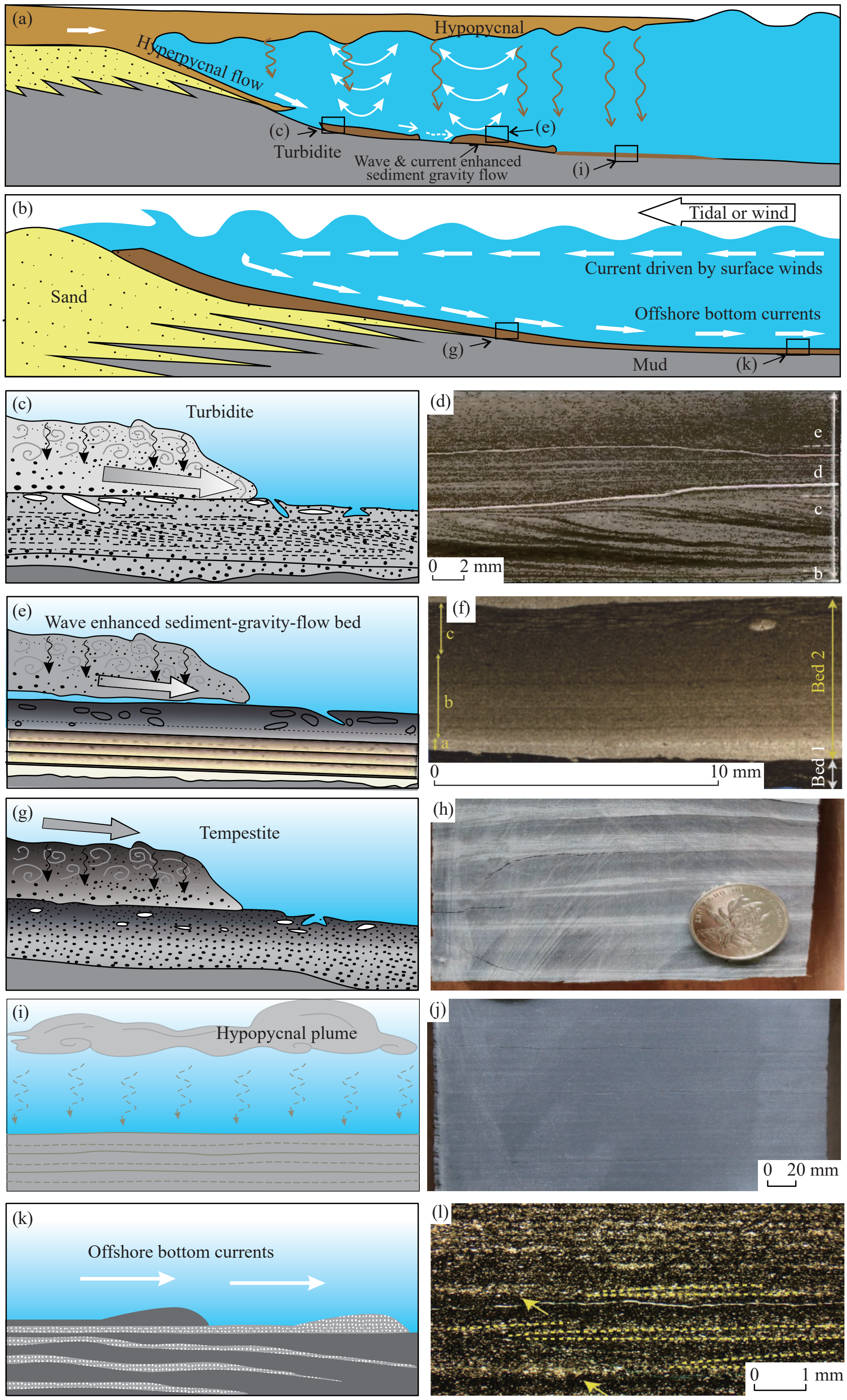

Fig. 3. Schematic model of sedimentary processes and sedimentary characteristics of mudstones and shales. a–schematic model of subaqueous sedimentary density flows (modified from Schieber J, 2016); b–schematic model of offshore flowing bottom currents due to wind-set up in the coast (modified from Schieber J, 2016); c–schematic illustration of a turbidite (Lazar OR et al., 2015); d–turbidite example in the Sonyea Group of New York, U.S. (Lazar OR et al., 2015); e–schematic illustration of a wave-enhanced sediment-gravity-flow bed (Lazar OR et al., 2015); f–a wave-enhanced sediment-gravity-flow bed in the Mowry Shale of Wyoming, U.S. (Macquaker JHS et al., 2010); g–schematic model of a mud tempestite (Lazar OR et al., 2015); h–multiple tempestite layers in the Qiongzhusi Formation of Jingyan, Sichuan (Li XS et al., 2021); i–conceptual view of hypopycnal flow; j–horizontal bedding in the Qiongzhusi Formation, Jingyan, Sichuan (Li XS et al., 2021); k–schematic model of offshore bottom current ripples (modified from Yawar Z and Schieber J, 2017); l–current ripples in the Longmaxi Formation (marked by yellow dashed lines), Xishui, Guizhou (Li YF et al., 2017).

3.2.4. Offshore bottom currents

Recent studies suggest that the mechanism for transporting fine-grained sediments in large epicontinental sea areas mainly involves offshore bottom currents formed under tidal or monsoonal influences (Li YF et al., 2017; Fig. 3b). Flume experiments have shown that under the influence of bottom currents, fine-grained sediments can form flocculate-sized particles, transporting forward as bed load and forming current ripples (Yawar Z and Schieber J, 2017; Fig. 3k). Sedimentary features of current ripples include asymmetric crests with overcutting or truncation. Internally, the foreset at certain angles (<27°) overlying the bottom interface, with a clear distinction between coarser and finer laminae; and erosional or abrupt bases, curved to straight shape. However, the typical features of current ripple layering are not apparent in ancient marine mudstones. These features often appear in relatively coarser silty segments, whereas flume experiments reveal more evident current ripple (Yawar Z and Schieber J, 2017). This contrast mainly arises because fine-grained sediments have a high-water content, exceeding 80%, and early-formed current ripples may develop into "parallel" laminations or low-angle cross-bedding under later compaction. The "parallel" laminations or low-angle cross-bedding widely distributed in ancient continental shelf shales, such as the Wufeng-Longmaxi formations in the Upper Yangtze region of China (Li YF et al., 2017; Fig. 3l), could be indicative of current ripples formed under the influence of bottom currents. Recent flume experiments show that the morphology differences of current ripples (layer thickness and the foreset angles) are mainly controlled by fluid velocity and sedimentation rate (Yawar Z and Schieber J, 2017).

3.3. Geological events and black shales formation

Major geological events in geological history usually include volcanic eruptions, tectonics, sea level changes, climate changes, and biological extinction and evolution. These major geological events often affect a wide range, and do not exist in isolation but interact with each other, and leave conspicuous records in the strata, providing important information to interpret the earth's past.

The extension, rupture and uplift of the lithosphere promoted the formation of the deep water basin. Volcanic eruption, hydrothermal activity and continental glaciation would have brought abundant nutrients to the water; suitable climate and the development of ocean currents promoted the flourishing of organisms, all of which provided favorable conditions for the formation of black shales (Fig. 4). At the same time, the large-scale carbon sequestration into black shales would also affect the CO_2 concentration in the atmosphere and the O_2 content in the ocean, which will promote climate change and biological evolution.

Black shales, as rock sequence with high organic matter content, is mainly formed under anoxic conditions, and its deposition is thought to be the result of the interaction of crustal evolution, orbital change, weathering, photosynthesis and organic matter degradation. They are often closely related to some key global geological events (such as large-scale volcanic activity, widespread oceanic anoxia, and mass extinctions), so they have extremely important implications for the interpretation of paleoenvironment, tectonics, and paleontological evolution (Ernst RE and Youbi N et al., 2017; Liu R et al., 2021; Jin ZJ et al., 2023). The earliest black shale appeared about 3.5 Ga ago (Fig. 1d). During this period, frequent global volcanic activity brought about extensive hydrothermal circulation in the lithosphere, resulting in the collapse of craters and the formation of a series of basins with limited seawater circulation. Provided suitable habitat for early life (Van Kranendonk MJ, 2006). Between 2.2 Ga and 1.8 Ga, the famous Great Oxidation Event (GOE) occurred on Earth, the concentration of oxygen in the atmosphere increased significantly, and multiple periods of comparable carbon isotope migration events occurred around the world. The rise of oxidizing photosynthetic organisms such as cyanobacteria (Fig. 1b), which produce large amounts of organic matter through photosynthesis, has resulted in the development of black shale deposits in major blocks around the world (Chi FE et al., 2016; Asael D et al., 2018). Similarly, plate movement has had a significant impact on the formation of black shales, such as with the formation of the Rodinia supercontinent about 1 Ga ago (Fig. 1a), which led to the reorganization of the crust and accelerated nutrient circulation. As a result, black shales were widely deposited in Siberia, the Baltic Sea, India, and West Africa (Zhao WZ et al., 2019).

Interestingly, the formation of large-scale black shales in the Phanerozoic is often closely related to major biological evolution events. After the Cambrian explosion of life 500 Ma ago, a geological event, the record of black shales became more extensive, with significant increases in TOC content compared to older shales (Jin JZ et al., 2023). Studies have shown that in geological history, the Cambrian life explosion and major biological events at the end of the Ordovician, Late Devonian, Late Permian, Late Triassic and Late Cretaceous correspond to the formation of a wide range of black shale formations around the world (Pan SQ et al., 2021; Fig. 1h). For example, the black shale of the Cambrian Niutitang Formation in South China roughly corresponding to the Cambrian life explosion (Zhang GJ et al., 2021), the Wufeng-Longmaxi Formation in China at the turn of the Ordovician-Silurian period, and the Hot Shale in North Africa and the Middle East (Li SZ et al., 2023b), the widespread Bakken and Woodford shale of North America during the Late Devonian (Liu M and Philp RP, 2023), the Dalong Formation at the end of the Permian (Ge XT et al., 2022), and the widespread black shales in the west coast of the Tethys Ocean during the Late Triassic and Late Cretaceous (El-Shafeiy M et al., 2024). In addition, several global Oceanic Anoxic Events (OAEs) occurred frequently during the Jurassic and Cretaceous periods, due to abnormal perturbations in the carbon cycle, changes in ocean productivity, and expansion of anoxic environments. It also promoted the preservation of organic

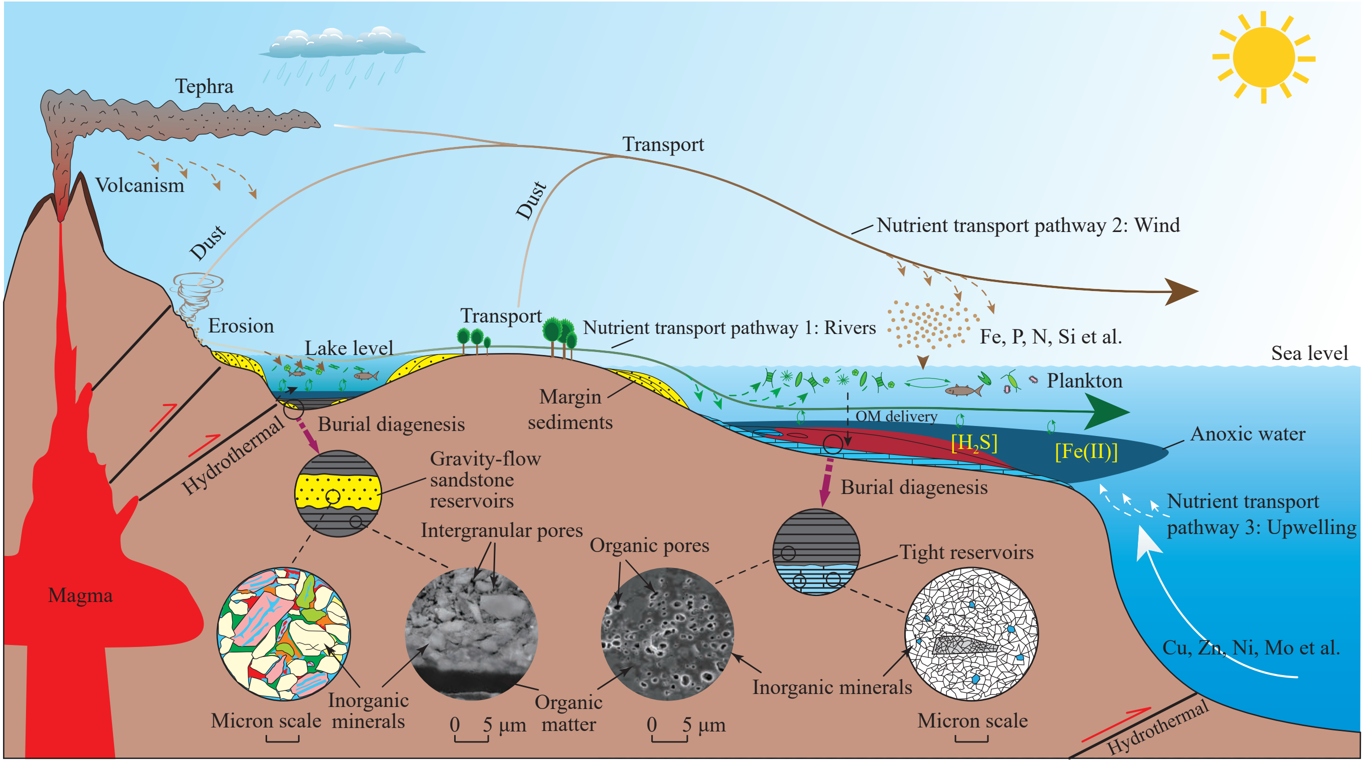

Fig. 4. Schematic diagram of sedimentary route of black shales (Zou CN et al., 2022). The nutrients provided by three sources - rivers, wind and upwelling - are key determinants of surface water primary productivity. Volcanic and hydrothermal activity can promote the flow of nutrients into oceans and lakes. Suboxic and anoxic bottom water is conducive to the preservation of organic matter.

matter and the formation of black shales to varying degrees (Jenkyns HC, 2010; Liu W et al., 2022; Chen X et al., 2022). The driving mechanisms of these major evolutionary and extinction events may vary, but the end result is often dramatic changes in Marine and terrestrial ecosystems, which may include mass extinctions, niche iterations, and shifts in the Marine environment (Rong JY and Huang B, 2014; Shen SZ and Zhang H, 2017). Such ecosystem turbulence provided the material basis for organic matter. In particular, biological pumping in the ocean promoted Marine carbon sink and organic carbon into sediments, while the formation of anoxic environment provided conditions for the preservation of organic matter, and with appropriate sedimentation rate, further promoted the formation of black shales at the same time (Xie SC et al., 2022).

3.4. Mechanisms of organic matter accumulation

Organic matter (OM) accumulation is a complex physical and chemical process. More and more scholars have realized that the enhanced accumulation of organic matter is not determined by a single factor, but is the result of the mutual coupling interactions of multiple factors such as biological productivity, paleoredox condition of bottom water, and sedimentation rate (Qiu Z and Zou CN, 2020; Ding JH et al., 2021; Li SZ et al., 2023a; Zhang SC et al., 2023).

The level of biological productivity is closely related to the nutrient degree of the water body. The more abundant the nutrient supply, the more prosperous the biological life activities, the stronger the ability to fix carbon through photosynthesis, and the greater the biological productivity. Volcanic eruption, submarine hydrothermal, terrestrial clastic input, and upwelling ocean currents often carry or decompose and release large amounts of nutrient elements such as N, P, Fe, Cu, and Zn (Fig. 4), which can provide abundant nutrients for the bloom of low aquatic organisms such as algae and contribute to improving the biological productivity. Some scholars represented by Pedersen TF and Calvert SE (1990), Sageman BB et al. (2003), and Gallego-Torres D et al. (2007) believed that organic matter enrichment is mainly controlled by the primary productivity of the ocean surface, and the impact of paleoredox condition is limited, with typical examples of rising ocean currents on the continental margin. High biological productivity can provide sufficient material basis for organic matter accumulation, and the anoxic environment formed by the early oxidation of organic matter is a necessary condition for the effective preservation of the original sedimentary organic matter (Chen DZ et al., 2011; Liu QY et al., 2022; Li SZ et al., 2023b).

The paleoredox condition of water column is also a key factor controlling the preservation of organic matter. The oxygen content determines the distribution of anaerobic microbial communities and the type of benthic organisms (Woulds C et al., 2007). The formation and preservation of organic matter refer to a complicated process, during which it is further degraded by both aerobic and anaerobic microorganisms, resulting in only about 1% of the original biogenic organic matter being preserved (Middelburg JJ and Meysman FJR, 2007). Some scholars demonstrated that the low biological productivity at the ocean surface in anoxic environments, especially in euxinic environments, can also form the black shales, with modern anoxic basins such as the Black Sea and the Cretaceous Oceanic Anoxic Event (OAE) as typical representatives (Arthur MA and Sageman BB, 1994; Mort H et al., 2007). Overall, anoxic environments are commonly favorable for organic matter preservation, which may be caused by consumption of dissolved oxygen due to biological blooms in the water, massive degradation of organic matter, water column stratification caused by closed environments, a decrease in dissolved oxygen caused by rising ocean temperatures, and changes in salinity or pH values of seawater.

The sedimentary rate (SR) has a significant influence on organic matter enrichment and preservation (Ding JH et al., 2021). Several studies (e.g., Ibach LEJ, 1982; Murphy AE et al., 2000) demonstrated that a low sedimentary rate causes organic matter to suffer oxidation decomposition and benthic consumption under an oxic environment, while a high sedimentary rate tends to enhance the dilution of organic matter by minerals, so the appropriate sedimentary rate is a key factor causing the enrichment of organic matter. When SR < 5cm/ky, TOC increases with the increase of sedimentary rate, thus indicating that a relatively high deposition rate in a certain range is conducive to the preservation of organic matter. When SR > 5cm/ky, TOC decreases with the increase of deposition rate, deciphering that the excessive deposition rate is unfavorable for organic matter preservation in a reducing environment since sufficient sedimentary materials would result in organic matter dilution (Ibach LEJ, 1982). The influence of sedimentary rate on organic matter is mainly determined by sea level fluctuation, distance from terrigenous source, input of riverine runoffs, and so on.

4. Composition of black shales

4.1. Mineral composition

Black shales mainly contain clay minerals (such as illite, illite smectite mixed layer, kaolinite, chlorite), quartz, feldspar, carbonate minerals (such as calcite, dolomite, siderite), sulfides (mainly pyrite), and organic matter, etc. (Aplin AC and Macquaker JHS, 2011). Chemical and mineralogical variability manifests itself in terms of silt/clay ratios and also the proportions of materials derived from different source regions, from biologic production in the water column and from diagenetic reactions.

Minerals are the most basic components of black shales, and its composition affect many properties such as the structure and texture, pore structure characteristics, physical properties, and fracturing ability of the shales. When studying shale as an unconventional reservoir, scholars often classify the mineralogical composition of shales into three major categories: Clay minerals, felsic minerals, and carbonate minerals (Borcovsky D et al., 2017; Milliken KL and Olson T, 2017; Wu P et al., 2021; He WY et al., 2024; Liu HM, 2018; Li SZ et al., 2023b). The distribution of mineralogical composition in the three terminal elements (Fig. 5) shows strong heterogeneity in different shales and within the same set of shales. For example, the quartz content in some sections of the Wufeng-Longmaxi Formation shale can reach up to 68.34% (Li SZ et al., 2023b), commonly referred to as siliceous shale; The shale of the Shahejie Formation in the Jiyang Depression of the Bohai Bay Basin is mainly composed of carbonate minerals, mainly including calcite and a small amount of dolomite, accounting for 45% to 55% of the total mineral content (Liu HM et al., 2018), commonly referred to as calcareous shale; while the Shanxi Formation shale in the eastern Ordos Basin have the highest clay mineral content, which can reach up to 90% (Wu P et al., 2021), commonly referred to as argillaceous shale.

4.2. Mineral sources

4.2.1. Detrital (allochthonous) components

From the perspective of composition sources, the components in black shales can be divided into detrital (allochthonous) components and production-derived (autochthonous) components (Aplin AC and Macquaker JHS, 2011; Jiang ZX et al., 2023a; Cao YC et al., 2023). Detrital (allochthonous) components originate from outside the sedimentary basin, including terrigenous clastic materials formed by the weathering of parent rocks, volcaniclastic materials formed by volcanic eruptions, and terrestrial organic matter (the organic matter will be discussed in detail in Section 4.3). The weathered terrestrial debris material of the parent rock is transported to the basin through rivers, winds, and other means. Among them, fine-grained debris material (mainly silt and mud) can remain suspended in the water for a long time and gradually deposit in deep water areas (Jiang ZX et al., 2023a). Almost all shales in the basin contains terrestrial debris material. Compared to the marine shale, terrestrial sediments are more sensitive to climate, detrital inputs, and the physical and chemical properties of the water body, showing greater variability in detrital (allochthonous) components in its spatial and temporal dimensions (Li MW et al., 2022; Cao YC et al., 2023). In terms of shale mineral composition, detrital components mainly include clay minerals, quartz, feldspar, etc. Volcanic eruptions produce volcanic debris, which can be divided into volcanic bombs, volcanic blocks, volcanic gravel, and volcanic ash according to their particle size.

The main factors controlling the content of detrital components in black shales mainly include the supply of detrital in the source area and the distance from the source area. The material composition, physical and chemical weathering intensity of the source area determine the supply of detrital components, while the hydrodynamic conditions and monsoon intensity of runoff determine the transportation distance of detrital components. Generally, the closer to the source area, the higher the content of detrital components.

4.2.2. Production-derived (autochthonous) components

Production-derived (autochthonous) components are the products of chemical or biochemical precipitation of dissolved

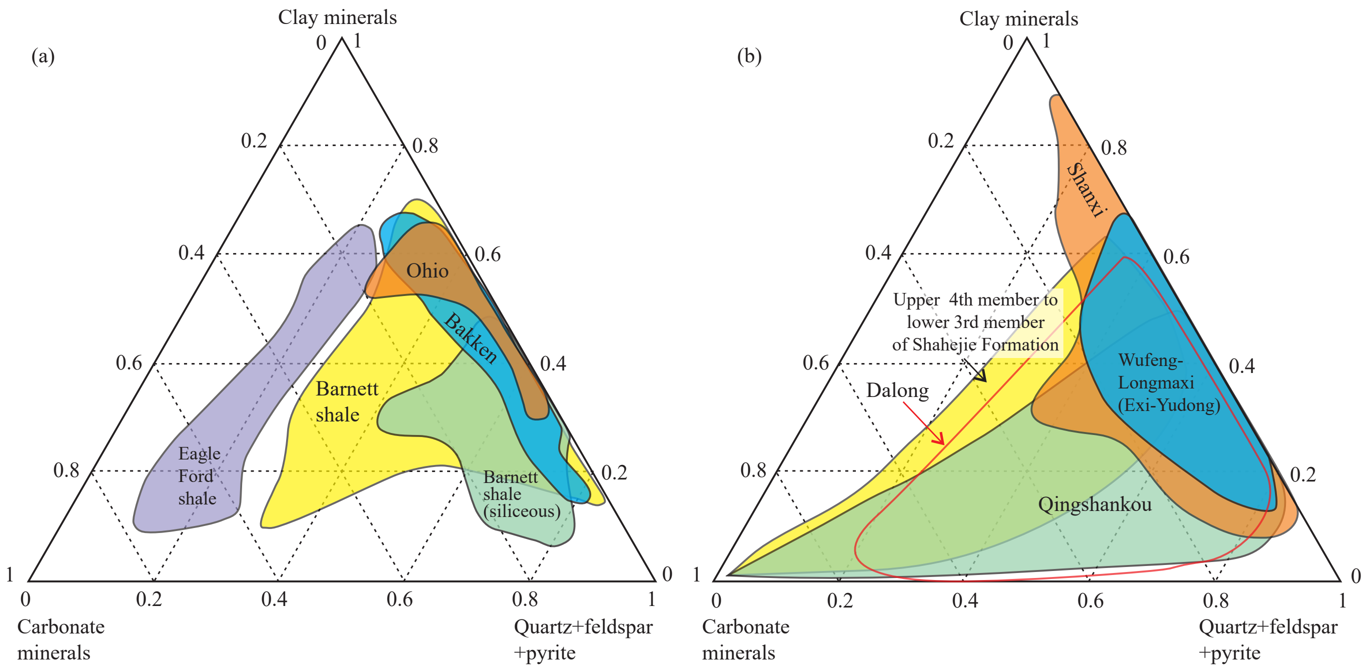

Fig. 5. Lithofacies classification of black shales. a–main shales in the United States (Borcovsky D et al., 2017); b–main shales in China (Wu P et al., 2021; He WY et al., 2024; Liu HM, 2018; Li SZ et al., 2023b).

substances in sedimentary basins. The main minerals include carbonate minerals, phosphate minerals, gypsum, and opal, among others. Under specific physical, chemical, and biochemical conditions, microbial metabolism can typically produce various authigenic minerals such as carbonates, pyrite, quartz, etc. The degree of their development is related to periodic climate changes and changes in water media (temperature, salinity, nutrients) (Jiang ZX et al., 2023a). Among them, in deep-water environments, organisms such as planktonic, microalgae, radiolarians, foraminifera, diatoms, and dinoflagellates, whose shells and skeletons can dissolve or form debris in seawater (lake water), and then precipitate to form sediment. Some biological debris directly forms complexes with clay and other organisms (Macquaker JHS et al., 2010). Biogenic quartz is one of the most important autochthonous minerals in marine black shales. Given the diversity of quartz sources, this paper specifically discusses it in section 4.2.3. In addition, there are also some biogenic substances, namely organisms formed in the basin and organic-inorganic complexes related to organisms. Taking the Wufeng Longmaxi Formation as an example, a large number of graptolite fossils developed within shale are a type of biogenic debris, belonging to the organic-siliceous complex (Liu GH et al., 2021; Fig. 6).

The main factors controlling the content of autochthonous components in black shales are the reduction of detrital input and the bloom of organisms in the water. In environments where the detrital input is limited, the supply of autochthonous components exceeds that of detrital components, which is more common in marine black shale. In lacustrine black shale, there is also a high proportion of autochthonous components, such as in the black shale of the Shahejie Formation (Sha-4 upper to Sha-3 lower) in the Jiyang Depression of the Bohai Bay Basin, where the highest amount of chemical precipitates in the basin can reach over 60% (Cao YC et al., 2023). The blooming of organisms in the water provides a large amount of calcareous or siliceous skeletal, providing an important material basis for the dissolution and reprecipitation of seawater to form autochthonous minerals.

4.2.3. Quartz types

Quartz is one of the main minerals in black shales, and its content, type, and morphology are considered to be of great significance for interpreting the source of sediments. As a research hotspot, it is attracting extensive research by numerous geologists (Peng JW et al., 2024; Gao P et al., 2024). Given that quartz is the most dominant mineral in black shales and its sources are diverse, this section focuses on discussing its characteristics and origins separately.

In the classification of genetic types, quartz mainly includes detrital quartz, biogenic quartz, and diagenetic authigenic quartz. Detrital quartz is primarily the product of weathering of source area parent rocks, transported into the sedimentary basin by wind, water, and other agents, and then accumulated and buried, with particles ranging from clay (<4 μm) to sand (>62.5 μm) distributed in shales. Biogenic quartz, also known as silica sponge needles, radiolarians, and other organisms, absorbs Si^{4+} from water during their growth. During burial, the silica in the organisms undergoes a series of transformations from unstable opal-A to more stable opal-CT, ultimately forming stable quartz (Schieber J et al., 2000); Zhao JH et al., 2017). Some studies suggest that the transformation of Opal-A to Opal-CT (transformation temperature: 33°C–45°C) was completed in the early diagenetic stage A, while the transformation of Opal CT to

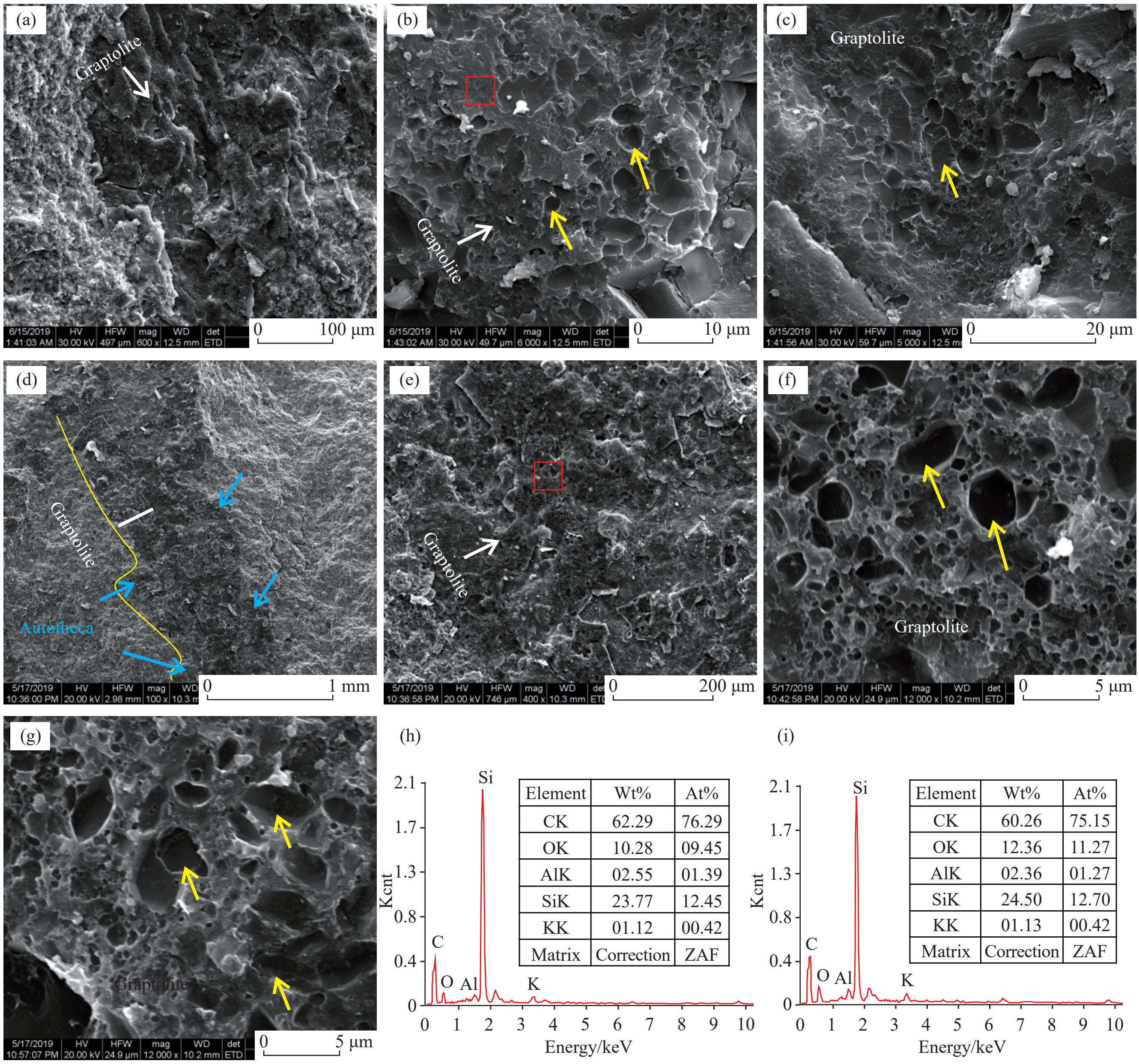

Fig. 6. Scanning electron microscopy image of shale samples in the LM1-4 graptolite belt of the Longmaxi Formation (after Liu GH et al., 2021). a–g–Sample 1, LGH-1, 2851.00 m, LM4. a–c and d–g correspond to the same graptolite body, respectively. The white arrow indicates the graptolite body, and the yellow arrow indicates quartz. The blue arrow indicates the positive cell tube of the graptolite, and the yellow curve marks the outline of the graptolite body. h–Fig. (b) energy spectrum analysis at the red box position; i–Fig. (e) energy spectrum analysis at the red box position.

quartz was completed in the early diagenetic stage B (Ishii E et al., 2011; Zhao JH et al., 2017). Biogenic quartz is often widely distributed throughout the shale matrix as microquartz and nanoquartz, and appears in large volume fractions (Peng JW et al., 2024). Diagenetic authigenic quartz is formed during the diagenetic process by the transformation of clay minerals, dissolution of detrital quartz, dissolution of feldspar, devitrification of volcanic ash, and precipitation of SiO_2 generated by hydrothermal activity (Bjørlykke K, 2011; Yasser MM and Evgeni MC, 2012; Liu GH et al., 2019a; Liu GH et al., 2023).

Quartz of different types has different morphologies and occurrence characteristics in shale (Fig. 7), and there are also differences in element geochemistry, such as particle size, cathodoluminescence intensity, and Si, Al and other element contents. In research, techniques such as field emission scanning electron microscopy, energy spectrum analysis, and cathodoluminescence are often used to distinguish quartz types, combined with element geochemical characteristics (Mei JF et al., 2024; Gao P et al., 2024).

4.3. Organic matter and its sources

One of the most typical characteristics of black shales is that it contains a certain amount of organic matter (Tissot BP and Welte DH, 1984; Jiang ZX et al., 2023b; Cai C et al., 2023). Compared to the mineral components in shales, although the organic matter content is generally not high, the

TOC content of a few types of samples can even be as low as 0.5%. However, the types and sources of organic matter in shale are crucial for oil and gas resource exploration (Taylor GH et al., 1998; Mastalerz M et al., 2018; Liu B et al., 2022）。

There are various classification schemes for the organic matter in black shales, but the earliest research scheme relied on coal petrology. In the field of coal rock research, organic macerals are classified into four major categories based on reflection color, morphology, structure, elemental composition, and fluorescence characteristics: Vitrinite, Inertinite, Humite, and Lipinite (ICCP, 1998, 2001; Pickel W et al., 2017; Dai SF et al., 2021a, 2021b, 2021c, 2021d). However, unlike coal rock, which is dominated by a large accumulation of Vitrinite and Inertinite, the organic composition of black shales, although also containing a certain amount of vitrinite and inertinite, is often dominated by dispersed particles (Liu B, 2023). In the field of organic geochemistry, organic components in black shales are divided into soluble and insoluble organic components based on the compositional characteristics of shale organic matter. The former is mainly composed of chloroform extracts and is often divided into four groups of components: Saturated hydrocarbons, arene, non-hydrocarbons, and bitumen, used to evaluate the organic matter abundance and hydrocarbon generation ability of shale (Durand B, 1980). The latter mainly refers to kerogen, which are insoluble in non-oxidizing acids, bases, and organic solvents. Based on the composition and proportion of C, H, and O elements, kerogen is often divided into Type I (sapropel-type), Type II (humic-sapropel type), and Type III (humic-type).

To explore the origins of organic matter, the classification of organic matter types in shales also often draws on palynology and modern oceanography. In palynological morphological studies, the organic matter in mud shales is divided into amorphous organic matter (AOM), structured organic matter (STOM), and palynomorph organic matter, which are used to determine the sedimentary environment of the organic matter (Tyson RV, 2001; Li JG and Batten DJ, 2005). In the field of oceanography, organic matter is physically classified based on whether it can pass through a filter membrane, divided into dissolved organic matter (DOM) that can pass through a 0.45 μm filter pore, particulate organic matter (POM) that cannot pass through a 0.45 μm filter pore, and colloidal organic matter (COM) that transforms between the former two (Rimmer SM, 2004; Guo S and Sun J, 2020). Obviously, according to this standard, most of the aforementioned organic matter types belong to particulate organic matter (POM). Although a large amount of dissolved organic matter and colloidal organic matter may aggregate into fixed forms and be classified as such, dissolved organic matter, which accounts for the majority of organic

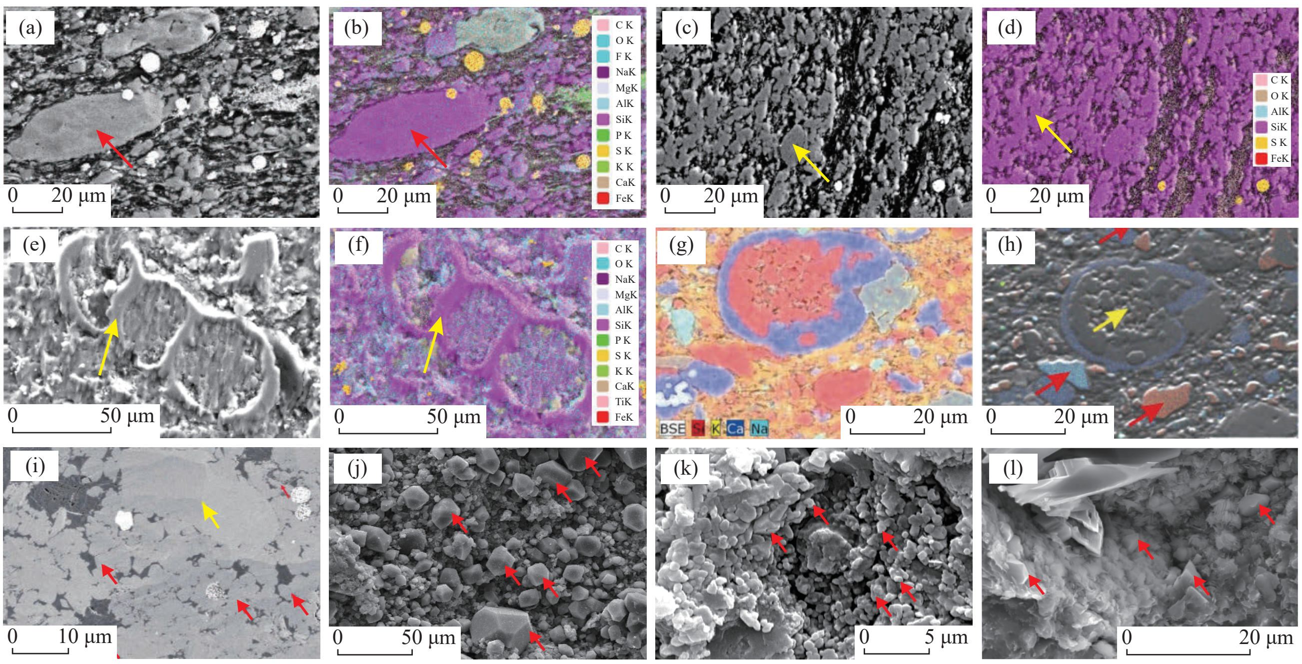

Fig. 7. Scanning electron microscopy image of quartz in black shales. a–detrital quartz in the shale of the Permian Gufeng Formation (red arrow); b–energy spectrum scanning of (a); c–microquartz (yellow arrow) in the shale of the Permian Gufeng Formation, biogenic quartz; d–energy spectrum scanning of (c); e–foraminiferal framework in the shale of the Permian Dalong Formation, replaced by quartz during diagenesis (yellow arrow); f–energy spectrum scanning of (e); g–SEM-based EDS map showing chambers of a bioclast filled with euhedral quartz cement (red). Pennsylvanian cline shale, Midland Basin, U.S (Peng JW et al., 2024). h–SEM-based cathodoluminescence (CL) image of the same area in (g). Intragranular quartz cement (yellow arrow) exhibits dark greyish CL color that is similar to the silicified biosiliceous allochems. Note that silt- to clay-sized detrital quartz in the matrix (red arrows) exhibits variable CL color (from reddish to light blue) (Peng JW et al., 2024); i–biogenic quartz (red arrow) and detrital quartz (yellow arrow) from the Wufeng Formation- Longmaxi Formation (Liu GH, 2021); j–Permian Lucaogou Formation shale contains authigenic quartz (red arrow), which is of volcanic ash devolatification origin and has a good crystal structure(Liu GH, 2017); k–amorphous quartz of the Lucaogou Formation (red arrow) is caused by volcanic ash devitrification(Liu GH, 2017); l–quartz in the shale of the Yanchang Formation, formed by the transformation of clay minerals(Liu GH, 2017).

matter in seawater, is mostly deposited and stored in ultrafine and dispersed forms, such as within minerals or pores, and is often overlooked in shale.

In general, shale organic matter can be divided into five categories based on its source and genesis: Vitrinite, inertinite, liptinite, zooclasts, and secondary organic matter (Mastalerz M et al., 2018; Liu B et al., 2022; Liu B, 2023). Among them, the definitions of vitrinite and inertinite are basically consistent with coal petrology, including multiple subcategories, mostly derived from lignin and cellulose rich in higher plants (Fig. 8a–d), and are the main hydrogen deficient components, mainly contributing to terrestrial higher plants (ICCP, 1998, 2001; Dai SF et al., 2021a, 2021b). Liptinite mainly refer to hydrogen rich components such as alginite, bituminite, and liptodetrinite, etc. which are not only the main organic components of shale, but also the main hydrocarbon generating components (Fig. 8e, f; Hackley PC et al., 2017; Pickel W et al., 2017; Dai SF et al., 2021d). Alginite are the foundation of high-quality marine hydrocarbon source rocks and an important source material for marine oil generation (Tissot BP and Welte DH, 1984; Xie XM et al., 2015; Brocks JJ et al., 2017). Bituminite, also known as amorphous bodies, refers to microscopic components without a fixed structure, which is different from both secondary bitumen and organic geochemical bitumen (Kus J et al., 2017; Teng J et al., 2021). Zooclasts is also an important component of shale organic matter, which is the body or organ fragments of planktonic or benthic organisms (Fig. 8g), including graptolites, chitins, foraminifera, and trilobites, with low hydrocarbon generation potential. The characteristics observed under the microscope of zooclasts are similar to those of vitrinite. When vitrinite is not developed, reflectance of zooclasts is often used as a substitute for vitrinite reflectance for maturity characterization (Goodarzi F and Norford BS, 1989; Petersen HI et al., 2013). Secondary organic matter mainly refers to the solid bitumen, pyrobitumen, and petroleum formed by the thermal evolution of shale organic matter during oil generation (Fig. 8h, i). After the peak of oil generation (R_o 0.8%–1.0%), they gradually become the main types of shale organic matter and develop organic matter pore (Mastalerz M et al., 2018; Liu B et al., 2022).

5. Evolution of black shales

5.1. Diagenetic evolution of inorganic minerals

After deposition, with changes in burial depth, formation temperature, fluid conditions, and other environmental

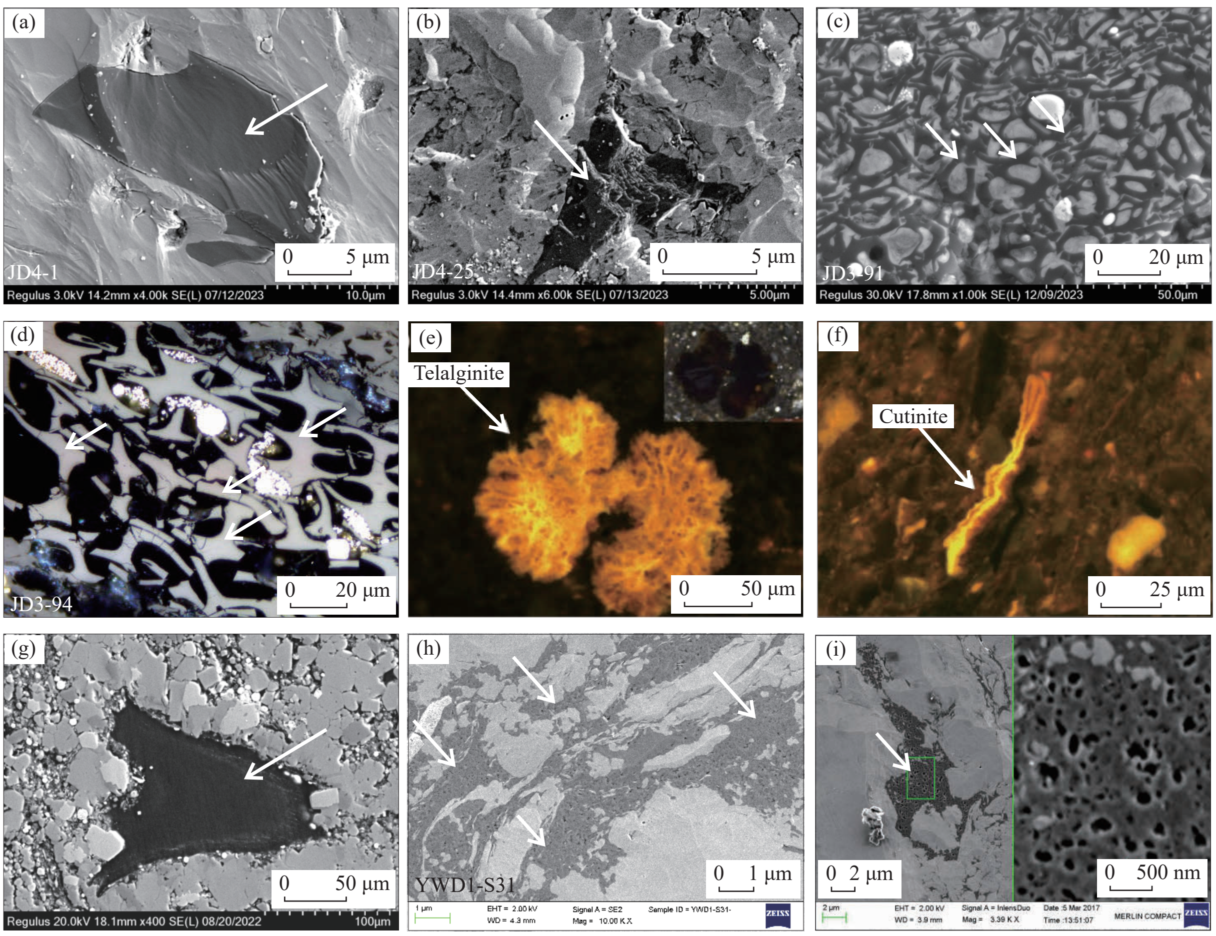

Fig. 8. Scanning electron microscopy and optical microscopy images of different types of organic matter in black shales. a–vitrinite structure in Daye Formation; b–vitrinite structure in Dalong Formation; c–inertinite fragments in Longtan Formation; d–inertinite fragments in Longtan Formation, reflected light; e–liptinite (telalginite), Chang 7 unit of Yanchang Formation, fluorescent light (Chen G et al., 2020); f–liptinite (cutinite), Chang 7 unit of Yanchang Formation, fluorescent light (Chen G et al., 2020); g–zooclasts in Gufeng Formation; h–secondary bitumen in Dalong Formation; i–secondary bitumen in Longmaxi Formation (Li SZ et al., 2022).

factors, loose sediments consolidate to form rocks, accompanied by a series of physical and chemical changes (Ehrenberg SN, 1997; Bjørlykke K, 2014). The diagenetic evolution process is complex and prolonged, playing a decisive role in the formation, loss, and preservation of post-sedimentary reservoir spaces (Dutton SP and Loucks RG, 2010; Ma BB et al., 2015), and significantly impacting changes in reservoir performance.

5.1.1. Diagenetic fluids and environments

Diagenetic fluids are shale pore fluids, and their compositional characteristics, properties, and sources are of great significance for the study of diagenesis. The composition of diagenetic fluids and their changing patterns help to further infer the timing of diagenetic events, as well as the openness/closedness and acidity/alkalinity of the fluid system during the formation and evolution of shale (Bjørlykke K and Jahren J, 2012; Ma BB et al., 2015). Diagenetic fluids include hydrocarbons (oil and gas) and ion-rich pore water can fill the pores. There are five main sources of diagenetic fluids: original sedimentary water of strata, meteoritic water, crystal water from mineral transformation or chemical transformation related fluids (Worden RH et al., 2018), deep thermal fluids, and hydrocarbons formed by the thermal evolution of organic matter. Diagenetic fluid interacts with (aluminum) silicate minerals and carbonate minerals in rocks, resulting in dissolution or precipitation, which is the key to influencing diagenetic evolution. In particular, acidic fluid dissolution is an important factor in forming effective reservoir space. This includes atmospheric freshwater leaching, organic acids and CO_2 from organic matter thermal evolution, bacterial sulfate reduction (BSR), thermochemical sulfate reduction (TSR), clay mineral transformations such as illitization acid dissolution, and deep hydrothermal dissolution (Machel HG, 2001; Bjørlykke K and Jahren J, 2012; Liu QY et al., 2019).

5.1.2. Diagenesis and diagenetic evolution

Shale diagenesis can be divided into mechanical diagenesis and chemical diagenesis. Mechanical diagenesis mainly includes compaction, which is manifested as pore water removal, rock volume reduction, porosity and permeability variation, and mineral orientation arrangement. This mainly occurs in the early diagenesis stage and has a significant effect on pore reduction. Chemical diagenesis includes cementation, dissolution, recrystallization, metasomatism, and clay mineral transformation (Mastalerz M et al., 2013; Liu GH et al., 2019b). Among these, clay mineral transformation and unstable mineral dissolution are relatively important positive diagenetic processes. The temperature and pressure increase caused by the increase in burial depth, as well as the resulting discharge of interlayer water and interlayer cations of clay minerals, lead to conversions between clay minerals, thus causing rock volume shrinkage. Additionally, the conversion of clay minerals can produce a large amount of silica (Thyberg B et al., 2010), and the secondary increase of quartz produced has a positive effect on the preservation of primary pores. Recrystallization and mineral metasomatism, accompanied by the exchange of materials between minerals, follow the law of conservation of materials and have no obvious effects on the reservoir.

The diagenetic evolution process of shale can be divided into early diagenetic stage (A, B), middle diagenetic stage (A, B), and late diagenetic stages (Fig. 9) by referring to the criteria of diagenetic stages of clastic rocks in China. The indexes of diagenetic stages are R_o, Tmax, clay mineral types and their combination characteristics, carbonate mineral crystallization degree, authigenic mineral types, and oxygen isotope values.

5.2. Thermal evolution of organic matter (hydrocarbon generation)

The thermal evolution of organic matter in black shales, also known as hydrocarbon generation evolution, refers to the biological, physical, and chemical changes of sedimentary organic matter during diagenesis and metamorphism as burial depth, temperature, duration, and pressure increase (Tissot BP and Welte DH, 1984; Taylor GH et al., 1998).

In this process, although the five major types of organic matter in shales gradually change from biological organic matter to geological organic matter and oil and gas, different types of organic matter behave differently. In black shales, type I kerogen has the strongest hydrocarbon generation capacity, type II has a medium hydrocarbon generation capacity, and type III has the worst hydrocarbon generation capacity (Fig. 10). Inertinite comes from higher terrestrial plants and basically does not undergo significant morphological changes and hydrocarbon formation evolution during thermal evolution (ICCP, 1998; Dai SF et al., 2021a). The vitrinite increases with the degree of metamorphism, gradually darkens in color, and increases in reflectance in the process of thermal evolution, which is the most prominent feature. With the intensified metamorphism, the reflection color of the vitrinite gradually becomes lighter, and the reflectance gradually increases from <0.5% to >2.0% or even higher. Based on this, the vitrinite reflectance is often used as an important indicator of the maturity of organic matter in coal petrology and organic petrology studies (ICCP, 2001; Dai SF et al., 2021b). Liptinite, as the main hydrocarbon-bearing component and hydrocarbon-generating body, exhibit more significant changes in microscopic optical characteristics during thermal evolution compared to the vitrinite. With the enhancement of thermal evolution, the fluorescence characteristics of liptinite gradually weaken, the reflection color becomes lighter, and the reflectance gradually increases, eventually approaching the level of the associated vitrinite components. Animal detritus is similar to those of vitrinite and the reflectance gradually increases during the thermal evolution process (Pickel W et al., 2017; Dai SF et al., 2021c). Therefore, the reflectance of animal detritus is often used to characterize maturity when vitrinite is absent

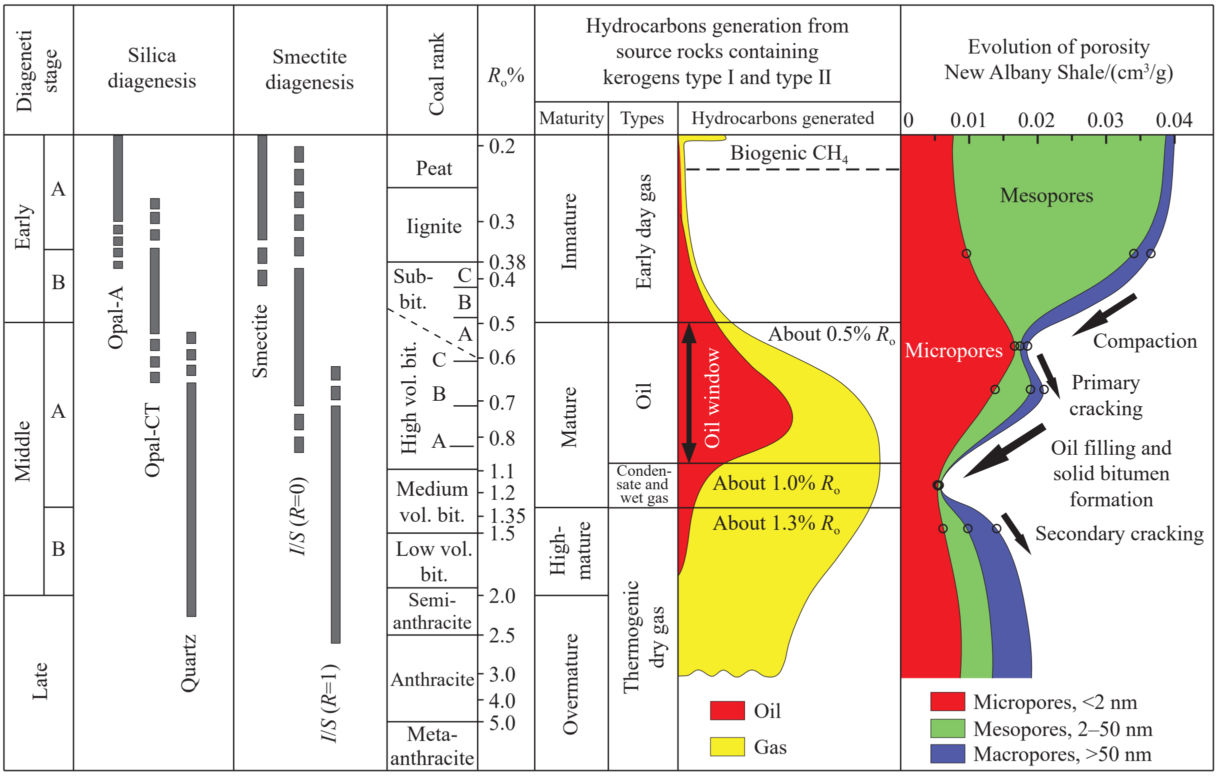

Fig. 9. Evolution of minerals, organic matter, and pores during shale diagenetic evolution (modified from Mastalerz M et al., 2013; Pollastro RM, 1993; Zou CN et al., 2022). vol.–volatile; bit.–bituminous; Opal-A–amorphous opal; Opal-CT–crystalline opal.

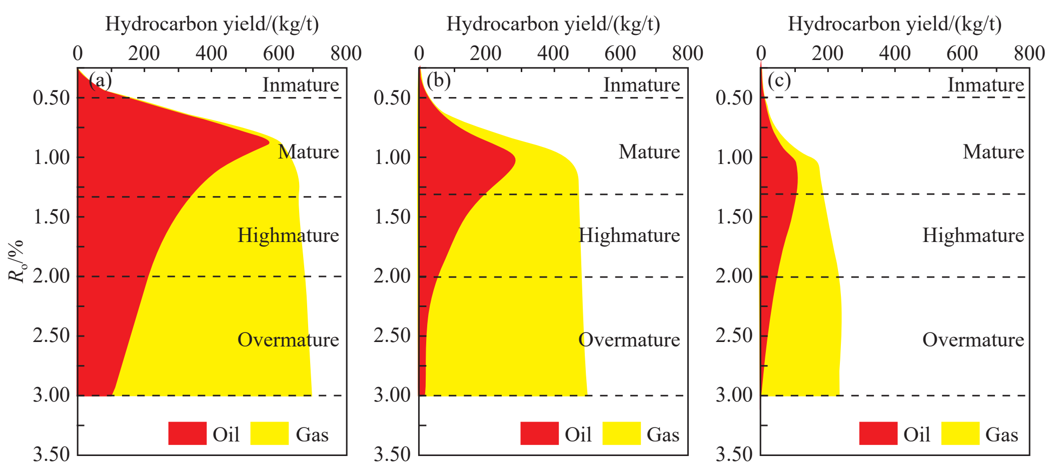

Fig. 10. Hydrocarbon generation models of different types of kerogen (modified from Qin JZ and Liu BQ, 2003; Qin JZ and Liu BQ, 2005). a–marine type I kerogen; b–marine type II kerogen; c–lacustrine type III kerogen.

(Goodarzi F and Norford BS, 1989; Petersen HI et al., 2013). Secondary organic matter, no matter solid bitumen, pyrobitumen, or petroleum, represents the product of thermal evolution of original organic matter, and gradually evolves into the main body of shale organic matter in the later stage of thermal evolution (Mastalerz M et al., 2018; Liu B et al., 2022).

The thermal evolution of organic matter in black shales is not only manifested in microscopic morphology but also in chemical composition. According to the theory of organic hydrocarbon generation, the hydrocarbon evolution of organic matter is mainly manifested in component condensation, polymerization, aromatization, loss of Nitrogen-Sulfur-Oxygen (NSO) functional groups, increase of carbon content, and decrease of moisture and volatile content (Tissot BP and Welte DH, 1984; Taylor GH et al., 1998). The characterization of hydrocarbon generation evolution of black shales is often characterized by vitrinite reflectance (R_o) or bitumen reflectance, and can also be defined by biomarker parameters.

In 1970s, Tissot B et al. (1974) summarized the process of hydrocarbon generation of organic matter and put forward the theory of late hydrocarbon generation of kerogen. This theory is the classic theory of hydrocarbon generation to guide oil and gas exploration at present, which can be roughly divided into four main evolutionary stages: Immature stage, mature stage, high mature stage, and over-mature stage (Figs. 9, 10). In recent years, the discovery of immature crude oil and early mature oil has challenged the classic Tissot hydrocarbon generation model (Huang DF, 1996; Liu WH et al., 1999). In order to investigate this issue, scholars have proposed different hypotheses or models, such as early hydrocarbon generation of resinite, early hydrocarbon generation of suberinite, early hydrocarbon generation of alginite, early hydrocarbon generation of kerogen degradation, and bacterial activities. Studies have found that resinite and suberinite contributed by higher plants have the characteristics of low polymerization degree and long chain liptinite, and can act as chemical reactants with low activation energy under low thermodynamic conditions to generate hydrocarbons with mainly chain structures (Liu WH et al., 1999). In addition, bacterial action will degrade and transform terrestrial organic matter, and the addition of metabolites such as liptodetrinite will increase its H/C atomic ratio, increase the degree of hydrogen enrichment and sapropelization, and reduce the activation energy of organic matter, resulting in the generation of low-mature oil and gas (Huang DF, 1996).

In addition, the hydrocarbon generation evolution process is not only affected by the types and biological processes of organic matter, but also goes through multi-stage thermal evolution and secondary hydrocarbon generation with tectonic uplift and subsidence and magmatic intrusion (Wang WY et al., 2022). Second hydrocarbon generation refers to the process of source rock entering the threshold of hydrocarbon generation in geological history, experiencing the initial process of hydrocarbon generation, and then heating up again after stopping hydrocarbon generation due to low temperature reduction (Xiong YQ et al., 2001; Hackley PC and Cardott BJ, 2016). The evolution process of secondary hydrocarbon generation of organic matter is the superposition of the pyrolysis evolution of residual kerogen and the thermal pyrolysis transformation of residual oil, which are both interrelated and completely different physicochemical processes.

5.3. Interaction between organic matter and inorganic minerals

The study of interaction between organic matter and inorganic minerals has a long history. Grim RE (1947) had long noticed that clay minerals had a catalytic effect on hydrocarbon generation from organic matter when studying petroleum generation. Curtis CD (1978) and Surdam RC et al. (1989) proposed when studying conventional oil and gas reservoirs in sandstone and carbonate rocks that organic acids formed by organic matter can dissolve inorganic minerals (Fig. 11). In different stages of diagenetic evolution in geological environments, the magnitude of their interaction is different. With the development of shale oil and gas exploration, the organic-inorganic mechanism in the source rocks has once again attracted the attention and discussion from unconventional oil and gas geologists.

Regarding the catalytic effect of inorganic minerals on hydrocarbon generation of organic matter, Johns WD and Shimoyama A (1972), Horsfield B and Douglas AG (1980) carried out a series of thermal simulation experiments on clay minerals such as montmorillonite and illite and model compounds such as source rocks, kerogen, and fatty acids. In the experiment, it was observed that the presence of minerals such as montmorillonite would have shortened the formation duration of long-chain alkanes and the duration for further cracking to produce short-chain alkanes, and the distribution of the generated long and short-chain alkanes was very similar to the composition of petroleum. Clay minerals are widely existing in shales, and the catalytic principle of clay minerals for decarboxylation of organic matter is different from that for thermal cracking of organic matter (Wang XX et al., 2006; Zhang P, 2020). During the decarboxylation of organic matter, clay minerals participate in the decarboxylation of organic matter as oxidants. Fe^{3+} in clay minerals is reduced to Fe^{2+}, organic matter is oxidized, and free hydrocarbons with shorter chain lengths are formed. During the thermal cracking of organic matter, clay minerals provide H^+ to organic matter to the reaction. The catalytic activity of clay minerals in the reaction is not affected by the medium conditions, and acid catalytic activity is still present on the surface of clay minerals in alkaline formation water (Wang XX et al., 2006). Lewan MD (1997) believed that formation water promoted the hydrocarbon generation and expulsion process of organic matter by providing H^+ and increased hydrocarbon production, while dehydration in the conversion process of clay minerals may have acted as source of formation water as well.

Thermal evolution of organic matter is a unique type of diagenesis in black shales, which is different from other sedimentary rocks, and is an important promoter of various diagenetic processes (Wang Y, 2020). Organic acids are products in the evolution of organic matter. With the increase of burial depth and the thermal evolution of organic matter, organic acids will be formed during the deoxidation process

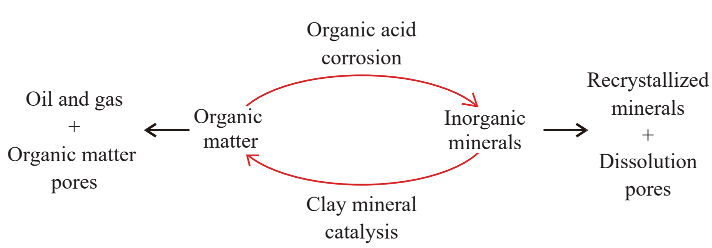

Fig. 11. Mechanism model of interaction between organic matter and inorganic minerals.

of kerogen, and organic acids will be released when hydrocarbons are generated (Xu HM et al., 2000). Corrosion in shale reservoirs is mostly related to organic acids produced by organic matter (Zhang P, 2020). These acids would dissolve aluminosilicate and carbonate minerals vigorously, often promoting the dissolution of feldspar, calcite, dolomite, and other minerals, generating secondary pores. When organic matter evolves into a mature stage, the decarboxylation of organic acids will release CO_2. At this time, the content of CO_2 in the reservoir increases, which leads to the weakening of the dissolution reaction of organic acids on carbonate minerals. Additionally, the pH of pore water continues to rise, and the acidic environment weakens. The Ca^{2+}, Mg^{2+}, and HCO^{3-} released during the illitization of montmorillonite will precipitate and recrystallize carbonate minerals, thus increasing the content of carbonate minerals in shale (Xue LH et al., 1996; Zhang P, 2020). This cycle of organic acid formation (weakening) drives the dissolution (precipitation) of minerals, further redistributing mineral composition (Rimstidt JD et al., 2017). Studies have shown that changes in ambient temperature, pressure, and pH have a certain control effect on the dissolution rate of minerals. An increase in temperature and pressure would enhance the dissolution effect of alkaline feldspar (Li T et al., 2018; Gudbrandsson S et al., 2014), while an increase in pH value will promote the recrystallization of carbonate minerals (Zhang P, 2020).

5.4. Pore evolution

The pore development of black shales is different from that of conventional oil and gas reservoirs. The fine-grained composition and structure of shale determine the pore body of black shales is dominated by nano-sized pores (Guo XW et al., 2019; Zhao JH et al., 2017; Yu BS, 2013). In addition to a small number of intergranular pores, shale pores are mostly found in common matrix minerals such as quartz, feldspar, calcite, pyrite, and clay minerals, and are also heavily enriched in organic matter. Therefore, the diagenesis of shale matrix minerals and hydrocarbon generation of organic matter are closely related to the formation and evolution of the shale pore system (Zheng YJ et al., 2024; Lin W et al., 2024; Wan XF et al., 2023). However, due to differences in sedimentary and tectonic environments and material sources, the mineral composition and organic matter characteristics of black shales differ across regions and times are different, leading to distinct formation and evolution of pore systems.

The shale pore system is mainly composed of organic and inorganic pores, and the complex pore network system is the result of the dynamic evolution of black shales under various geological processes during their formation and evolution (Liu WP et al., 2017; Sun LN et al., 2019; Xu LW et al., 2019). Among the influencing factors, sedimentary and structural settings determine the material basis of shale pore development, including mineral components and sources of organic matter. The hydrocarbon generation and diagenesis of organic matter are the primary driving mechanisms of pore evolution. The evolution of hydrocarbon generation from organic matter does not simply affect the development of organic pores. Organic acids generated in the process of hydrocarbon generation are one of the important conditions for the occurrence of corrosion (Ji LM et al., 2016), and the solid bitumen generated in the process of hydrocarbon generation can easily block the inorganic pores (Mastalerz M et al., 2013). Diagenesis is not limited to inorganic minerals, among which compaction is an important mechanism leading to the reduction of organic pores and inorganic pores in shale. Rigid minerals can prevent both organic and inorganic pores from being destroyed by compaction (Zhao JH et al., 2017). In summary, the relationship between hydrocarbon generation and diagenesis of organic matter is complex, with pore evolution from multiple interrelated mechanisms.

Throughout geological history, organic pores do not simply increase with maturity (Guo SB and Mao WJ, 2019). Thermal simulation experiments of shale indicate that secondary organic pores begin to develop in the low-mature to mature stage (Fig. 12b). However, during the oil-generating stage, asphaltane filling is prone to cover up part of the pores, which is especially obvious in marine shale rich in oil content (Fig. 12c). As maturity continues to increase, hydrocarbon generation shows a good correlation with the evolution of organic matter pores. After the oil peak generation, the secondary cracking of hydrocarbons or bitumen occurs, and the development of organic matter pores becomes more pronounced (Figs. 12a, b). During this process, organic matter forms numerous micropores with hydrocarbon generation and expulsion, while also decreasing in volume and generating shrinkage cracks that form a significant number of macro pores. The organic pores show polarized characteristics (Figs. 12b, d). However, when entering the overmature stage (R_o > 3.0%), the organic porosity tends to decrease, which is mainly related to late thermal alteration and compaction (Loucks RG et al., 2012).

The evolution of inorganic pores in shale is mainly controlled by diagenesis, and the difference in components and diagenetic paths is the main factor of the evolution difference of inorganic pores (Zhao JH et al., 2017; Liu WP et al., 2017). Current studies have shown that the diagenesis types of shale reservoirs are similar to conventional reservoirs, including compaction, cementation, metasomatism, dissolution, and clay mineral transformation. Among which compaction and cementation are the two primary porosity reduction processes, while dissolution is the main porosity increase process (Zhang YF et al., 2017). In general, the inorganic pores of shale gradually decrease with the increase of burial depth, but the compaction effect gradually weakens with the increase of burial depth and shale densification. In the deep high-over-maturity stage, the illitization and recrystallization of clay minerals increase the volume of mesopores (Fig. 12c). The dissolution of organic acids made the secondary inorganic pores grow in stages.

Based on the results of previous studies, the evolution models of shale pore systems established at present are mainly

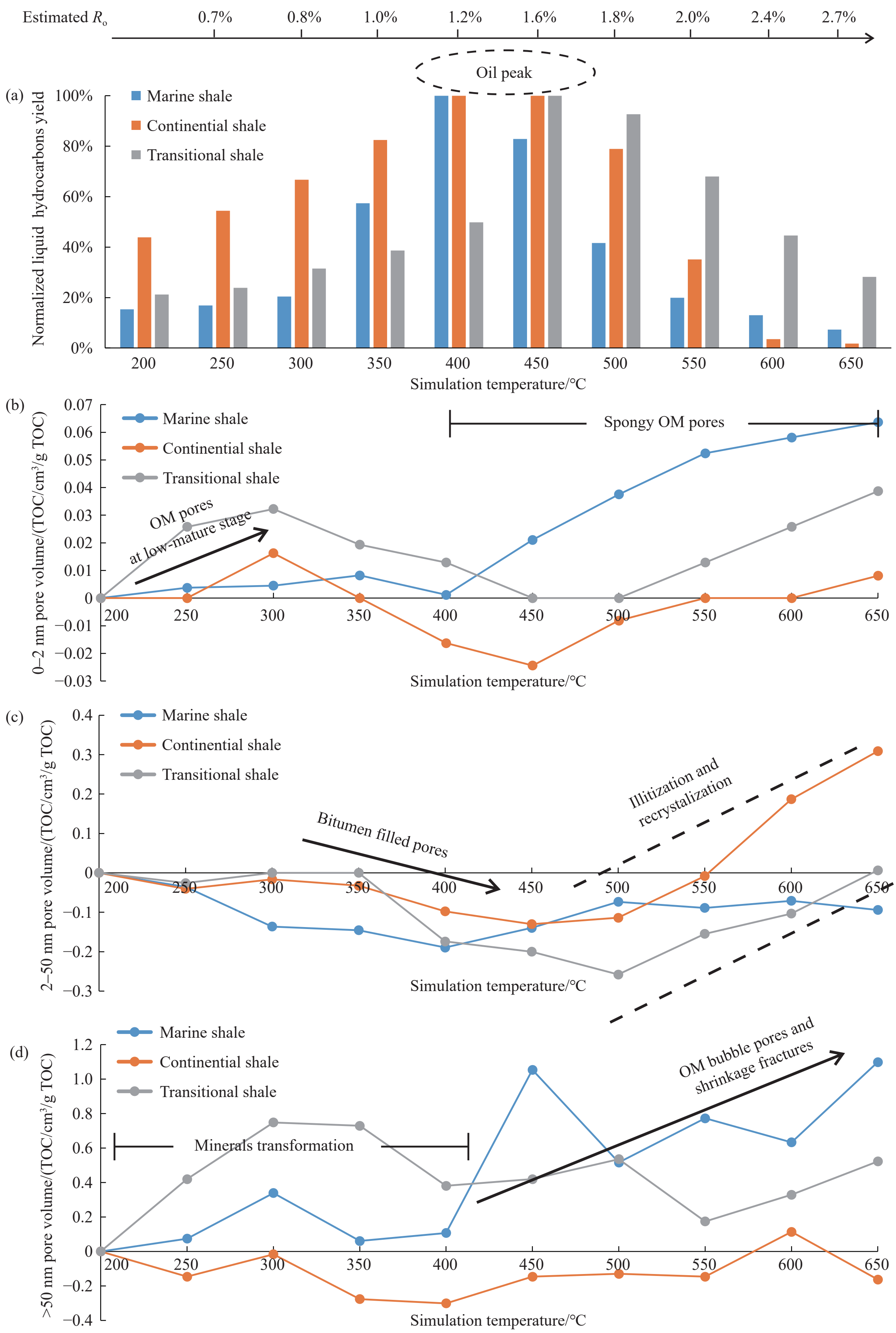

Fig. 12. Hydrocarbon generation and pore co-evolution process in marine, terrestrial, and transitional black shales thermal simulation experiments, R_o estimated according to thermal simulation heating flow (modified from Guo SB et al., 2019; Yang XG et al., 2020; Wang ZL et al., 2024). a–change of normalized liquid hydrocarbon yield with simulated temperature (liquid hydrocarbon yield at the peak of normalized hydrocarbon generation =1); b–change of pore volume of 0–2 nm with simulated temperature; c–change of pore volume of 2–50 nm with simulated temperature; d–change of pore volume > 50 nm with simulated temperature.

based on maturity (Liu WP et al., 2017; Sun LN et al., 2019; Xu LW et al., 2019; Ji LM et al., 2016; Guo SB and Mao WJ, 2019; Huang WK et al., 2023). Under the complete evolutionary sequence, the total pore size of shale is affected by the evolution of organic and inorganic pores, and the overall evolution trend is first decreasing, then increasing, and finally decreasing (Xu L et al., 2022; Mastalerz M et al., 2013; Ji LM et al., 2016; Guo SB and Mao WJ, 2019; Huang WK et al., 2023). Before the shale reaches the hydrocarbon generation threshold, the pores are predominantly inorganic pores and are rapidly reduced by the compaction. During the oil-gas generation stage, the organic pores of shale gradually develop, and the inorganic pores increase due to the hydrocarbon generation of organic matter and the dissolution of organic acids, correspondingly. It is noteworthy that in the early stage of this process, the pores of shale may be blocked by solid bitumen, resulting in phased reduction of shale pores. In the over-mature stage, hydrocarbon generation ceases, and processes such as shale graphitization and strong compaction cause pores to collapse and shrink, leading to further reduction of pores and their size (Fig. 9).

6. Reconstruction of black shales

6.1. Tectonic reconstruction

Tectonic action controls the burial and uplift of shale reservoirs, as well as horizontal compression and extension, through stress actions (Emmanuel S and Day-Stirrat RJ, 2012). By forming various structural patterns (folds, faults, etc.), they alter the stress structure of the reservoir, significantly modifying the pore structure of the shale (Guo TL, 2016).

6.1.1. Compressional deformation and uplift erosion

The compressional deformation caused by structural compression typically enhances both the horizontal and vertical permeability of the shale. The degree of compressional deformation also affects the scale and size of tensile fractures. Influenced by primary sedimentation, the shale develops internal laminae, and the pressure relief from subsequent structural uplift leads to the development of tensile fractures along these laminae. During deformation, all pore types become interconnected, forming microfractures ranging from a few nanometers to several tens of micrometers. This connectivity enhancement due to deformation significantly increases the lateral permeability of the shale compared to its vertical permeability. Generally, structural locations with higher layer curvature, such as the axial and hinge zones of folds, have a higher degree of fracture development, whereas areas with lower layer curvature, like the limbs, show less fracture development (Zeng LB et al., 2023). In the absence of vertical fractures, natural gas migrates along the shale laminae, resulting in variations in gas content across different parts of the folds. Typically, the broad anticlinal axes and the cores of residual synclines exhibit better gas content compared to the limbs (Cui Y et al., 2023). Under the same porosity conditions, the permeability of deformed shale is significantly higher than that of undeformed shale, with stronger deformation correlating to higher permeability (Li XS et al., 2021).

Uplift and erosion reduce the overburden and regional caprock thickness above the shale layers, decreasing vertical stress and disrupting the original formation pressure equilibrium. This results in elastic strain relaxation proportional to the Young's modulus, causing vertical expansion that reopens closed fractures, thereby increasing horizontal permeability (Rimstidt JD et al., 2017; Gale JFW, 2014; He ZL et al., 2020; Feng QQ et al., 2022). Due to the Poisson effect, the rock contracts horizontally, creating new joints and reactivating pre-existing fractures, which increases vertical permeability and reduces sealing capacity (Gale JFW et al., 2014). The tendency for shale to fracture depends on its mineral composition; thus, shale with high quartz, feldspar, and carbonate content is more brittle and prone to fracturing compared to clay-rich shale (Bourg IC, 2015). Fractures resulting from uplift and erosion increase both horizontal and vertical macroscopic permeability, transforming the shale from a nearly closed system to an open system, leading to the loss of shale oil and gas and a decrease in formation pressure coefficients (Gao J et al., 2022). In this scenario, it is also possible for brine from surrounding formations or meteoric water to infiltrate the shale (Engle MA et al., 2016), or for hydrothermal fluids to enter the shale, depositing sulfide minerals or carrying away metals to form mineral deposits elsewhere.

6.1.2. Faults and fractures

Faulting is a common structural deformation in shale development areas, typically accompanied by numerous fractures that significantly enhance the permeability of the shale. These fractures allow shale oil and gas to escape through the fracture-fault system until they are dissipated (Li WP et al., 2017; Xiang J et al., 2021). The development of fractures is closely related to the presence of faults. Faults represent the macroscopic manifestation of fractures, with the relationship between faults and fractures characterized by two aspects: (1) The development of faults originates from structural fractures, which act as precursors to fault formation. (2) During the formation and development of faults, relative movement between the fault blocks generates local stress fields, leading to the creation of new fracture systems. During fault formation, secondary structures or induced fractures develop within a certain range on either side of the main fault. These fracture zones are directly influenced by the main fault and are also referred to as induced fracture zones. The rock masses within fault influence zones exhibit distinct physical and mechanical characteristics compared to the surrounding normal rock, featuring lower strength, greater deformation, and higher permeability. Structural processes significantly impact the pore types and pore structure evolution in black shales (Zhu HJ et al., 2018). The total pore volume in shale within fault zones increases with the degree of deformation, characterized by a notable decrease in organic pores and the significant development of larger intergranular pores, microfractures, and microchannels. This greatly enhances the storage capacity and permeability of the shale reservoir (Liang ML et al., 2020; Shang FH et al., 2023). Compared to shale in structurally stable zones, shale in deformation zones exhibits higher average pore size, total pore volume, and the proportion of medium to large pores (Sun WJB et al., 2020; Sun WJB et al., 2023; Zhu HJ et al., 2019).

Natural fractures represent a unique type of storage space in black shales, exhibiting strong heterogeneity in their macroscopic to microscopic multi-scale distribution and arrangement. This variability is dictated by the depositional, diagenetic, and structural environments that control the interfaces and mechanical properties (Gale JFW et al., 2014). Fracture growth may result from one or more mechanisms, including differential compaction, local and regional stress changes related to structural events, strain adjustment around large structures, secondary processes, and tectonic uplift (Ding WL et al., 2011; Ding WL et al., 2012; Gale JFW et al., 2014; Zeng LB et al., 2023). Structural fractures, the most common type, are often filled with calcite and may intersect different generations of fractures, forming complex fracture networks with observable features such as folding and microfaulting, indicating multiple phases of tectonic activity (Ma J et al., 2022). The degree of development and scale of structural fractures are greater in areas with concentrated tectonic stress. Statistical analysis of fractures in different parts of faults shows that the upper fault block has a higher degree and width of fracture development than the lower fault block, with fracture density highest near the fault plane and gradually decreasing with distance from it (Zeng LB et al., 2023). Microfractures have a dual impact on shale reservoirs: they can enhance local connectivity, facilitating shale gas accumulation, but if they penetrate the layers extensively and connect to the surface, they may lower reservoir pressure and lead to significant gas dissipation, thus hindering gas accumulation (Ding WL et al., 2012; Zeng LB et al., 2023).

6.2. Fluid-induced reconstruction

After diagenesis, shales continue to experience multiple phases of fluid activity. The interactions between water and rock, as well as the fluid content, significantly modify the mineral composition, pore structure, and permeability of black shales. The main types of diagenetic fluids include seawater, formation water, hydrothermal fluids, and meteoric freshwater (Wu AB et al., 2020). Seawater influences rock primarily during the early diagenetic stage, and it does not appear in highly mature hydrocarbon-bearing black shales. Formation water refers to atmospheric freshwater and seawater that have been trapped within sediments. As burial continues, under gradually changing temperature and pressure conditions, these waters undergo long-term water-rock interactions, resulting in basin brines which are complex chemically. Hydrothermal fluids are defined as fluids with temperatures higher than the formation temperature sourced from deep brines or magmatic origins (Xie XN et al., 2009). Meteoric freshwater infiltrates into formations from surface outcrops through precipitation and is typically found in shallow strata. Fluid-induced reconstruction in shales is characterized by various type of fluid and the depth and structural position within the formation (Fig. 13).

Research on ancient fluid activities primarily based on the petrographic and geochemical characteristics of fracture veins to reconstruct ancient fluid temperature, salinity, isotopic composition, and potential existence of hydrocarbons. Determining the formation ages of fracture veins in shales is crucial for understanding the processes of ancient fluid activities, identifying the origins of ancient fluids, and elucidating the fluid reconstruction effects on shale.

6.2.1. Mechanisms of vein formation

Veins are aggregates of minerals precipitated from fluids in rock expansion areas, typically consisting of one or more mineral types and usually taking on tabular or lenticular shapes. During the formation of veins, fluid flow and diffusion are the two fundamental mechanisms of material transport (Okamoto A and Sekine K, 2011).

Fluid flow is a more effective mean of material transport than diffusion, capable of moving materials over long distances at the crustal scale (Bons PD et al., 2012). There are three basic types of fluid flow (Oliver NH and Bons PD, 2001): (1) Percolation through rock pore media: This type of fluid flow follows Darcy law. Due to the extensive contact interface between the pore fluid and the rock, there is strong water-rock interaction. (2) Fluid flow through pre-existing fractures or faults: This flow type is faster and more effective than percolation, but the interaction between fluid and rock is very limited. (3) Fluid flow in hydraulically induced fractures: In this case, the flow rate of the fluid is approximately the same as the rate of fracture propagation (Bons PD, 2001). The presence of numerous crack-seal structures in veins indicates that episodic or cyclic fluid flow is common (Cox SF, 1995). High fluid pressure can generate hydraulic fractures, suggesting that under certain pressures, fluid pathways are ubiquitous in the sediments. Fluid flow is generally controlled by fluid potential, flowing from regions of high fluid potential to regions of low fluid potential (Chi GX and Xue CJ, 2011). Numerically, fluid potential is equivalent to fluid overpressure, meaning that fluid typically flows from high overpressure areas to low overpressure areas.

Diffusion is another crucial mechanism of material transport in the formation of veins, though the amount of material transported by diffusion is much smaller compared to fluid flow (Parnell J et al., 2000). Consequently, veins formed by diffusion are usually smaller, with lengths typically ranging from 0 to 10 cm (Fisher DM et al., 1995). The direct driving force for diffusion transport is the chemical potential gradient, primarily related to concentration. Diffusion always occurs spontaneously from areas of high concentration to areas of low concentration. Due to the diffusion between the vein and the surrounding rock, elements are notably depleted in the rock surrounding the vein (Elburg MA et al., 2002). Additionally, diffusion is influenced by pressure, temperature, and crystal structure conditions (Bons PD et al., 2012). For instance, pressure significantly impacts the solubility of quartz. When a fracture occurs, fluid pressure is released, and the pressure differential between the fluid in the vein and the surrounding rock can cause chemical disequilibrium, leading to material transport from the wall rock to the vein by diffusion (Fisher DM et al., 1995).

Mineral precipitation initially occurs at fluid flow sites, where crystals fill the fractures. As the fractures are gradually filled with crystals, further fluid flow is impeded, making it difficult to completely fill the vein through fluid flow alone (Hilgers C and Urai JL, 2002). Therefore, to fully fill the vein, diffusion transport may occur simultaneously with fluid flow or in alternating phases.

6.2.2. Reconstructive impact of fluid activity on shales

Fluids act as a medium for interactions between minerals and organic matter within shale, with frequent fluid activity promoting organic-inorganic interactions and the redistribution of substances within the shale (Dehghanpour H et al., 2013; Zhao JZ et al., 2017). During the maturation of organic matter, a large amount of hydrocarbon and organic acids are generated. Excessive hydrocarbons and high pressure can inhibit further degradation of organic matter, while organic acids increase the solubility of minerals in formation water. These substances, released under high-pressure conditions, precipitate during fluid environment changes, forming hydrocarbon reservoirs or metal deposits.

Fluid activity affects the physical properties and heterogeneity of shale in various complex ways. When substances like water and oil come into contact with shale, they are absorbed and alter the shale's composition and structure (Dehghanpour H et al., 2013). Without the creation of new fractures, an increase in non-hydrocarbon fluids and the intrusion of external fluids typically have a negative impact on quality of shale reservoirs. The clay minerals in shale are hydrophilic, and the ingress of water causes these minerals to swell (Geng LK et al., 2022), leading to throat blockage and a significant reduction in permeability. Under high-temperature and high-pressure conditions, the solubility of minerals increases, causing more calcium and silica to dissolve in hydrothermal fluids. Excessive minerals precipitate as cementation, secondary overgrowths, and recrystallized minerals within the pores or fractures of the shale (Fig. 14), would significantly reduce porosity and permeability. Additionally, an increase in the proportion of aqueous phase occupies limited space within the shale, resulting in multiphase fluids with oil and gas, thereby decreasing the single-phase permeability of hydrocarbons (Zou C et al., 2023).

In another scenario, fluid activity induces the formation of new microfractures in shale, improving the reservoir quality (Shen YH et al., 2017). Shale often experiences abnormal overpressure during its evolution, primarily due to hydrocarbon generation, clay mineral dehydration, and tectonic activities. Veins in mature shale often capture hydrocarbon-bearing fluid inclusions, indicating that fracture formation is related to hydrocarbon generation. During uplift, the associated pressure release causes the internal fluid potential of the shale to exceed that of the external environment. If the matrix permeability is poor or highly heterogeneous, this forces the shale to develop microfractures. Some studies also suggest that the dehydration of montmorillonite coincides with the thermal evolution of source rocks in terms of temperature, time, and depth (Wang M et al., 2018). Combined with tectonic forces altering the stress state of shale, this composite mechanism is likely a common cause of shale overpressure and fracture formation (Zhao JZ et al., 2017).

7. Shale oil and gas resource effects in the formation, evolution and reconstruction of black shales

7.1. Depositional scale and quality of black shales determine shale oil and gas resources

One of the most critical factors determining the shale oil and gas content in black shales is the Total Organic Carbon (TOC). Regardless of facies, high production of a single well requires a considerable thickness of organic-rich (TOC > 2%) shale (Curtis JB, 2002; Ross DJK and Bustin R, 2008; Hao F et al., 2013). The duration of favorable conditions and the extent of low-oxygen zones during the formation of black shales determine the thickness and extent of high-quality shale (Li SZ et al., 2022). This forms a solid geological foundation for shale oil and gas formation and directly influences their resource potential.

During deposition, fine-grained materials form through biological, biochemical, and mechanical processes. These materials, including individual particles, flocculated particles, clasts within the shale, rock fragments, organic-mineral aggregates ("marine snow"), and zooplankton fecal pellets, are transported to the ocean by wind, low-density flows, gravity flows, and bottom currents. They eventually settle vertically and/or laterally (Shi ZS et al., 2021). Although the deposition process of mudstone and shale is complex, relatively stable hydrodynamic conditions, especially suspension deposition (hypopycnal flow), facilitate the formation of extensive, organic-rich black shales during geological history.

Different depositional facies may result in shales with similarities in hydrocarbon content but significant differences in formation environment, thickness, distribution, and lithological characteristics (Table 1). Marine shales dominate the shale oil and gas production layers worldwide (Dong DZ et al. 2021). Deepwater shelf-deposited black shales include the Woodford Shale, Marcellus Shale, Fayetteville Shale, and Eagle Ford Shale in North America and the Wufeng-Longmaxi formations in southern China. The Barnett Shale and Haynesville Shale are thought to have been deposited in

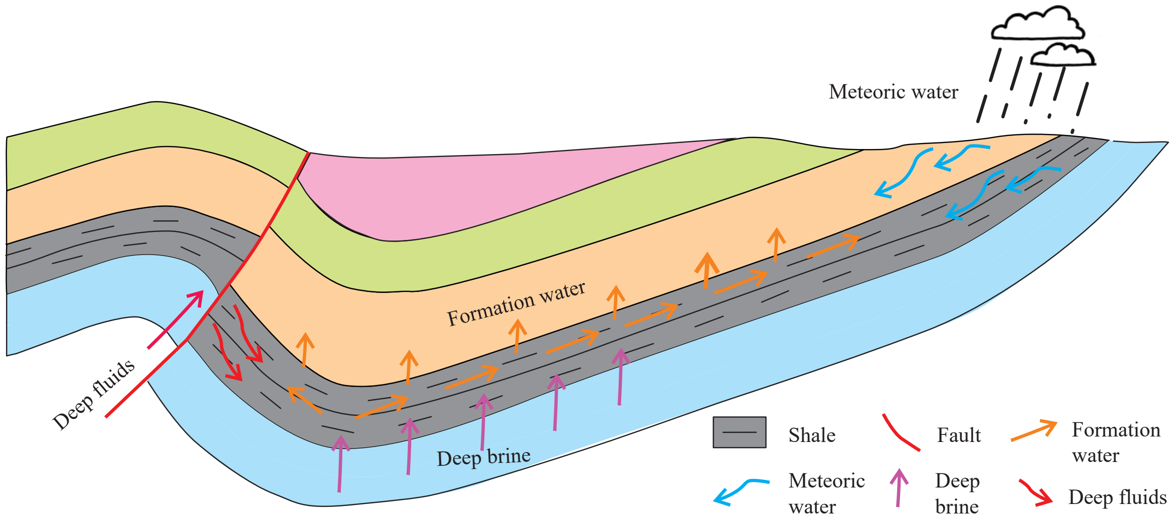

Fig. 13. Modes of diagenetic fluid activity in shale during tectonic reconstruction.

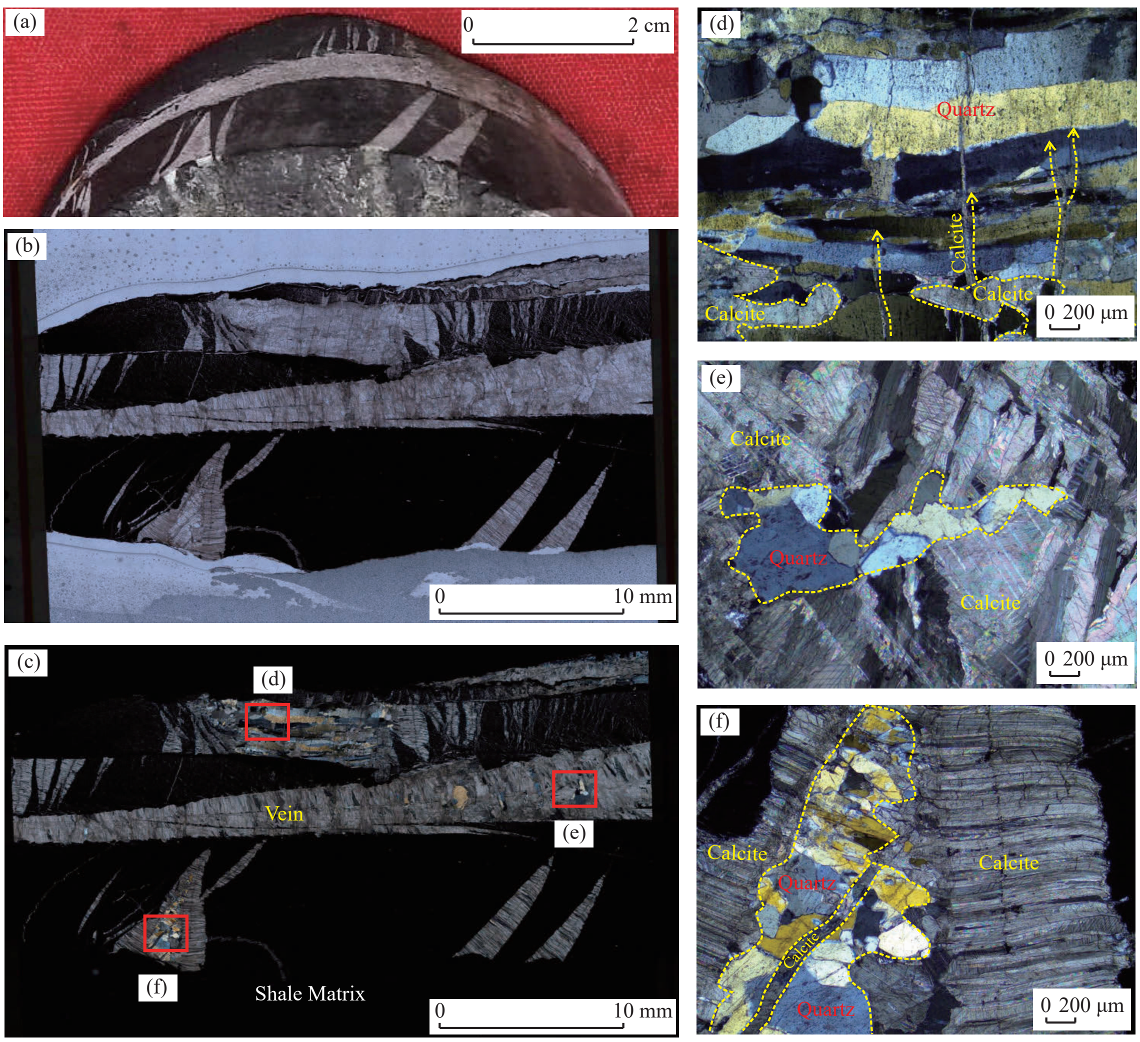

Fig. 14. Characteristics of veins in structurally altered black shales, Hedi-1 Well, Dalong Formation, 1288.2 m. a–photograph of core specimen, showing veins filled in horizontal and high-angle fractures; b–thin section overview under plane-polarized light, with horizontal veins appearing as tabular and stable in thickness, while high-angle veins appear triangular or semi-lenticular, decreasing in thickness towards the horizontal veins; c–thin section overview under cross-polarized light, with the periphery of the veins filled with calcite and the thicker central parts filled with quartz; d–elongated blocky quartz veins, with quartz grains elongated towards both sides, indicating the opening direction of the veins. The central part of the quartz grains is penetrated by fine calcite veins, representing multiple phases of tectonic-fluid activity; e–fibrous calcite and blocky quartz veins in horizontal veins, with coarser calcite and quartz grains; f–blocky quartz and fibrous calcite veins, with finer calcite veins and quartz grains. The quartz grains are later cracked and refilled with calcite.

deepwater slope-basin environments (Slatt MR and Rodriguez ND, 2012; Guo W et al., 2022). The Carboniferous Dawuba Formation shale in the Dianqiangui region and the Permian Dalong Formation shale in the western Hubei trough are formed in more enclosed bay environments (Yuan K et al., 2023; Li SZ et al., 2024). Terrestrial black shales, major hydrocarbon source rocks in China's oil and gas basins, include the Upper Cretaceous Qingshankou Formation shale in the Songliao Basin, the Paleogene Shahejie Formation shale in the Bohai Bay Basin, and the Upper Triassic Yanchang Formation shale in the Ordos Basin (Ju YW et al., 2016; Li QQ and Xu S, 2022). Transitional facies shales from the Mesozoic era include the Upper Cretaceous Lewis Shale in the Powder River Basin, the Mungaroo Formation in the Upper Triassic of the North Carnarvon Basin in Australia, and the Bonaparte Basin's Middle Jurassic Elang and Upper Jurassic Frigate formations. In China, transitional facies shales are primarily developed in the Late Paleozoic in the Ordos and Sichuan basins (Dong DZ et al., 2021). Significant amount of shale oil and gas resources have been discovered in these areas and formations.

7.2. Diagenesis and thermal evolution of black shales promote shale oil and gas formation and storage

The organic matter in black shales gradually converts to oil and gas with increasing burial depth, influenced by temperature, duration, and pressure. In source-reservoir symbiotic shale reservoirs, the reservoir comprises inorganic minerals and a significant amount of organic matter. The interactions between pore fluids, minerals, and organic matter evolution products are relatively complex, and they play a decisive role in the formation and evolution of organic-inorganic pores (Yang T et al., 2018).

High-quality reservoirs and favorable shale oil and gas storage require the spatial arrangement and temporal co-evolution of organic and inorganic components (Nie HK et al., 2020a; Zhao JH and Jin ZJ, 2021). During the diagenesis and pore evolution of shale, inorganic mineral diagenesis and organic hydrocarbon generation coexist in micro-nanoscale spaces, necessitating the study of diagenesis and hydrocarbon generation within a unified spatial and temporal framework (Hu ZQ et al., 2021). If hydrocarbon generation occurs earlier than reservoir formation, the oil expulsion would be extensive, leading to low present-day oil and gas content. Conversely, if high-porosity-permeability reservoirs form first and are later filled with hydrocarbons, the shale oil and gas content will be high.

The main terrestrial shale formations in China are mainly in the middle diagenetic stage A, such as the Qingshankou Formation in the Songliao Basin (Feng ZH et al., 2020) and the Shahejie Formation in the Bohai Bay Basin (Hu WX et al., 2019). These stages, with paleotemperatures ranging from 85°C–140°C and R_o values between 0.5%–1.3%, allow the organic matter to enter the "oil window". Significant amount of organic acid was released from kerogen catalyzed by temperature and clay minerals, leading to substantial dissolution of unstable minerals like feldspar, forming secondary dissolution pores. Marine shale formations in China are mainly in the middle diagenetic stage B to late diagenetic stage, such as the Wufeng-Longmaxi formations in the Sichuan Basin (Wang RY et al., 2022), with paleotemperatures over 140°C and R_o values above 1.3%, where the organic matter reaches a mature to over mature stage. The secondary cracking of kerogen and bitumen leads to significant development of organic pore, dominating the storage space (Mastalerz M et al., 2013).

7.3. Tectonic and fluid-induced reconstruction on black shales lead to differential enrichment and dissipation of shale oil and gas

Tectonic reconstruction impact shale oil and gas migration and preservation through four main aspects. (1) Improving shale reservoir quality: Regions with large stress gradient changes are likely to develop microfractures, increasing shale

Table 1. Characteristics of black shales in different depositional facies.

Depositional facies	Marine facies	Terrestrial facies	Transitional facies
Age	Paleozoic - Mesozoic	Mesozoic - Cenozoic	Late Paleozoic - Early Cenozoic
Depositional environment	Marine shelf, slope-basin, enclosed basin	Semi-deep lake, deep lake	Swamp, barrier-lagoon
Lithological characteristics	Shale with thin carbonate interlayers, low clay mineral content	Variable lithology, clay mineral content between marine and transitional facies	Interbedded with limestone, coal, and sandstone, frequent changes, high clay mineral content with kaolinite dominance
Thickness	Single layer > 10 m	Thin single layers with clear interbeds < 3 m	Thin single layers with clear interbeds, large cumulative thickness
Distribution size	Extensive, stable	Small scale	Small scale
Organic matter type	Mainly type I kerogen, some type II	Mainly type II kerogen, some type I	Mainly type III and type II
Shale oil and gas characteristics	High thermal maturity, oil cracked to gas	Moderate thermal maturity, mainly oil generation	Mainly gas generated from Type III kerogen
Typical shales	Woodford shale, Marcellus shale, in North America; and Wufeng - Longmaxi shale in China, etc.	Qingshankou shale in Songliao Basin, China; Shahejie Formation in Bohai Bay Basin, China	Lewis shale in San Juan, America; Mungaroo Formation of Upper Triassic in North Carnarvon, Australia; Shanxi Formation of Permian in Ordos Basin; Longtan Formation of Permian in Sichuan Basin, etc.

porosity and enhancing multiphase fluid storage and migration (Feng QQ et al., 2022). (2) Forming more sealed systems: Structural activities may create sealed structures, such as uplift converting mudstone to brittle over consolidated material, enhancing shale seal properties and aiding long-term oil and gas preservation (Nygård R et al., 2006). (3) Damage and refracturing: Structural activities cause rock fragmentation and deformation, forming new or reopening old fractures, promoting shale oil and gas dissipation. Exploration practice shows that shorter and smaller fractures favor preservation, whereas intense deformation with large faults and high-angle fractures is detrimental (He ZL et al., 2020; Wei XF et al., 2017). (4) Altering oil and gas migration paths: Structural deformation may change migration paths and directions, significantly impacting oil and gas preservation in shale. For example, structural stress can compress rigid minerals into adjacent pores, altering migration paths and affecting oil-gas-water distribution and storage (Gou QY et al., 2021).

Fluid-induced reconstruction has dual effects on shale oil and gas migration. (1) Reducing shale porosity and permeability: Increased non-hydrocarbon fluids and external fluid invasion cause pore throat blockage and a significant drop in permeability. (2) Improving shale porosity and permeability: Fluid activities create new microfractures, enhancing reservoir quality and facilitating oil and gas migration and accumulation or dissipation.

Geological history shows that almost all black shales have undergone tectonic and fluid-induced reconstruction. For example, the main Cambrian and Silurian shales in southern China experienced multiple tectonic activities during the Caledonian, Hercynian, Indosinian, Yanshanian, and Himalayan periods, leading to uplift, erosion, and deformation, along with fluid activity evidence. The major shale layers reached maximum burial depths during the late Yanshanian period, generating significant gas, followed by folding and faulting that caused differential enrichment in the Sichuan Basin’s shale layers. Intense later tectonic activities can make organic-rich shales more open, leading to the complete loss of free gas, which is a primary risk in marine shale gas exploration in China (Hao F et al., 2013; Guo TL, 2016; Ma YS et al., 2018; Chen L et al., 2019; Li SJ et al., 2020; Yu GC et al., 2020). Nie HK et al. (2020b) studied vein types and formation times in the Wufeng-Longmaxi formations, finding that earlier and deeper veins favor shale gas preservation, while multiple late-stage veins with a wide temperature range and lower temperatures indicate significant deep shale gas reservoir damage. Therefore, stable, weakly deformed shale preservation areas would be the ideal exploration targets.

8. Perspectives

The variable shales exhibit spatiotemporal heterogeneity from the nanoscale to the basin scale, due to each set of shale or different parts of the same shale undergoing unique and complicated formation and evolutionary processes. Investigating the formation mechanisms at different scales is key to in-depth study of shale formation and evolution, and crucial for revealing the patterns of shale oil and gas formation and enrichment.

Looking ahead, the research focus in macroscopic mechanisms will include: (1) How the interaction of earth’s multiple spheres further controls the formation of black shales; (2) the coupling depositional process of black shales and drastic environmental changes under the drive of global or regional significant geological events (such as large-scale volcanic activity, widespread ocean anoxic, and mass extinction events) ; (3) the feedback of black shale formation on climate, environment, and organic carbon cycles; (4) the internal material and structural changes of shale after formation due to tectonic alteration.

In terms of micro-scale mechanisms, the research focus including the following points are strongly encouraged: (1) The typical physical-chemical-biological action processes during the formation of black shale; (2) the synergistic evolution of organic-inorganic components within the life cycle of black shale and their impact on structure and composition; (3) the competitive coexistence mechanisms and changes of various fluids in shale reservoirs, etc.

In terms of mineral resources, shale oil and gas will still be a long-term research focus, including: (1) The dynamic evolution process and controlling factors of oil and gas in black shale; (2) differential enrichment mechanism of shale oil and gas. In addition, as various mineral resources in shale are increasingly valued, the occurrence state, enrichment mechanism, and relationship with biological activities of important metal elements will be further studied. Importantly, macro- and micro- scale investigation should all be included relying on the development and improvement of microanalysis techniques, as well as the continuous enrichment of big data for statistical analysis and simulation, striving for a more comprehensive, systematic, and in-depth understanding of black shales.

9. Conclusions

This study extensively reviewed the literatures on black shales, including the progress in their distribution throughout geological history, depositional environments, material composition, evolution, alteration, and the impact on shale oil and gas resources. The following conclusions have been drawn:

(i) The distribution of black shales exhibits diversity and heterogeneity in geological time and space. Black shales first formed approximately 3.46 Ga to 2.76 Ga ago in the Archean. However, compared to the Proterozoic, the distribution of black shales in the Phanerozoic is more extensive. Six major sets of hydrocarbon source rocks widely deposited during the Phanerozoic have contributed over 90% of the world’s original reserves of oil and natural gas.

(ii) Black shales are formed in marine, terrestrial, and marine-terrestrial depositional environments. Marine shelves, continental slope-basin, and enclosed basin being the most favorable settings for the formation of thick black shales. The depositional process of black shales is a complexation involving eolian input, hypopycnal currents, gravity-driven, and offshore bottom currents. Global or regional significant geological events have driven the formation of black shales, and the enhanced accumulation of organic matter is the result of the interactions and coupling of multiple factors such as primary productivity, the redox of bottom water, and sedimentation rate.

(iii) The material composition of black shales can be classified as allochthonous components, autochthonous components, and organic matter. Quartz, as one of the most important mineral components in black shales, includes types such as terrigenous quartz, biogenic quartz, and diagenetic authigenic quartz, each with different morphologies, characteristics, and elemental composition. The sources of organic matter are even more variable, with different types of organic matter exhibiting significantly different oil and gas generation capabilities.

(iv) After deposition, black shales undergo complex physical and chemical processes, including diagenetic evolution, thermal evolution of organic matter, and hydrocarbon generation, as well as complex organic-inorganic interactions. As these processes proceed, the shales' organic and inorganic pore networks also undergo complex dynamic evolution, typically showing a trend of first decreasing, then increasing, and then decreasing again during the complete evolutionary process.

(v) Post-deposition, black shales generally experience compressional deformation and uplift, erosion, fracturing, and alteration, which all increase shale permeability. Frequent fluid activity can promote organic-inorganic interactions and redistribution of materials within the shale, affecting the shales' properties and heterogeneity in various complex ways. Fluids can both plug pore throats, reducing porosity and permeability, and generate micro-fractures to improve reservoir quality.

(vi) The formation, evolution and reconstruction of black shales have substantial impacts on the shale oil and gas resources. The depositional scale and quality of black shales lay the foundation for shale oil and gas resources, while the diagenetic and thermal evolution of black shales promote shale oil and gas generation and storage. Tectonic and fluid-induced reconstruction on black shales lead to differential enrichment and dissipation of shale oil and gas.

CRediT authorship contribution statement

Shi-zhen Li: Conceptualization, writing - original draft, writing - review & editing, funding acquisition, project administration. Qiu-chen Xu, Mu Liu: Conceptualization, writing - original draft, writing - review & editing. Guo-heng Liu, Yi-fan Li, Wen-yang Wang, Xiao-guang Yang, Wei-bin Liu, Peng Sun, Tao Liu, Yan-fei An, Jiang-hui Ding, Qian-chao Li: Writing - original draft, writing - review & editing. Chao-gang Fang: writing - review & editing.

Declaration of competing interest

The authors declare no conflicts of interest.

Acknowledgement

This study was supported by the projects of the China Geological Survey (DD20230043, DD20240048), and the project of the National Natural Science Foundation of China (42102123).

References

Aigner T, Reineck HE. 1982. Proximality trends in modern storm sands from the Helgoland Bight (North Sea) and their implications for basin analysis. Senckenbergia Maritima, 14(5–6), 183–215.

Aplin AC, Macquaker JHS. 2011. Mudstone diversity: Origin and implications for source, seal, and reservoir properties in petroleum systems. AAPG Bulletin, 95(12), 2031–2059. doi: 10.1306/03281110162.

Arthur MA, Sageman BB. 1994. Marine black shales: Depositional mechanisms and environments of ancient deposits. Annual Review of Earth and Planetary Sciences, 22, 499–551. doi: 10.1146/annurev.ea.22.050194.002435.

Asael D, Rouxel O, Poulton SW, Lyons TW, Bekker A. 2018. Molybdenum record from black shales indicates oscillating atmospheric oxygen levels in the early Paleoproterozoic. American Journal of Science, 318(3), 275–299. doi: 10.2475/03.2018.01.

Bentley SJ. 2003. Wave-current dispersal of fine-grained fluvial sediments across continental shelves: The significance of hyperpycnal plumes. In: Scott ED, Bouma AH, Bryant WR (eds.), Siltstones, mudstones and shales: Depositional processes and characteristics. SEPM/GCAGS Joint Publication: 35–48. doi: 10.2110/sepmmisc.01.0099.

Bhattacharya JP, MacEachern JA. 2009. Hyperpycnal Rivers and prodeltaic shelves in the Cretaceous seaway of North America. Journal of Sedimentary Research, 79(4), 184–209. doi: 10.2110/jsr.2009.026.

Bilgen S, Sarıkaya İ. 2016. New horizon in energy: Shale gas. Journal of Natural Gas Science and Engineering, 35, 637–645. doi: 10.1016/j.jngse.2016.09.014.

Bjørlykke K. 2011. Open-system chemical behaviour of Wilcox Group mudstones. How is large scale mass transfer at great burial depth in sedimentary basins possible? A discussion. Marine and Petroleum Geology, 28, 1381–1382. doi: 10.1016/j.marpetgeo.2011.01.009.

Bjørlykke K, Jahren J. 2012. Open or closed geochemical systems during diagenesis in sedimentary basins: Constraints on mass transfer during diagenesis and the prediction of porosity in sandstone and carbonate reservoirs. AAPG Bulletin, 96(12), 2193–2214. doi: 10.1306/04301211139.

Bjørlykke K. 2014. Relationships between depositional environments, burial history and rock properties. Some principal aspects of diagenetic process in sedimentary basins. Sedimentary Geology, 301, 1–14. doi: 10.1016/j.sedgeo.2013.12.002.

Bons PD. 2001. Development of crystal morphology during unitaxial growth in a progressively widening vein: I. The numerical model. Journal of Structural Geology, 23(6–7), 865–872. doi: 10.1016/S0191-8141(00)00159-0.

Bons PD, Elburg MA, Gomez-Rivas E. 2012. A review of the formation of tectonic veins and their microstructures. Journal of Structural Geology, 43, 33–62. doi: 10.1016/j.jsg.2012.07.005.

Borcovsky D, Egenhoff S, Fishman N, Maletz J, Boehlke A, Lowers H. 2017. Sedimentology, facies architecture, and sequence stratigraphy of a Mississippian black mudstone succession—The upper member of the Bakken Formation, North Dakota, United States. AAPG Bulletin, 101(10), 1625–1673. doi: 10.1306/01111715183.

Bourg, IC. 2015. Sealing shales versus brittle shales: A sharp threshold in the material properties and energy technology uses of fine-grained sedimentary rocks. Environmental Science & Technology Letters, 2(10), 255–259. doi: 10.1021/acs.estlett.5b00233.

Brocks JJ, Jarrett AJM, Sirantoine E. Hallmann C, Hoshino Y, Liyanage T. 2017. The rise of algae in Cryogenian oceans and the emergence of animals. Nature, 548, 578–581. doi: 10.1038/nature23457.

Cai C, Cai JG, Liu HM, Wang XJ, Zeng X, Wang YS. 2023. Occurrence of organic matter in argillaceous sediments and rocks and its geological significance: A review. Chemical Geology, 639, 121737. doi: 10.1016/j.chemgeo.2023.121737.

Cao YC, Liang C, Han Y, Xi KL, Wang JR, Ji SC, Mei JF. 2023. Discussions on classification scheme for fine-grained sedimentary rocks based on sediments sources and genesis. Journal of palaeogeography, 25(4), 729–741 (in Chinese with English abstract). doi: 10.7605/gdlxb.2023.04.079.

Cawood PA, Chowdhury P, Mulder JA, Hawkesworth CJ, Capitanio FA, Gunawardana PM, Nebel O. 2022. Secular evolution of continents and the Earth system. Reviews of Geophysics, 60, e2022RG000789. doi: 10.1029/2022RG000789.

Chen DZ, Wang JG, Yan DT, Wei HY, Yu H, Wang QC. 2011. Environmental dynamics of organic accumulation for the principal Paleozoic source rocks on Yangtze block. Chinese Journal of Geology, 46(1), 5–26 (in Chinese with English abstract). doi: 10.3969/j.issn.0563-5020.2011.01.003.

Chen G, Gang WZ, Chang XC, Wang N, Zhang PF, Cao QY, Xu JB. 2020. Paleoproductivity of the Chang 7 unit in the Ordos Basin (North China) and its controlling factors. Palaeogeography, Palaeoclimatology, Palaeoecology, 551, 109741. doi: 10.1016/j.palaeo.2020.109741.

Chen L, Lu YC, Li JQ, Guo XS, Jiang S, Luo C. 2019. Comparative study on the Lower Silurian Longmaxi marine shale in the Jiaoshiba shale gas field and the Pengshui area in the southeast Sichuan Basin, China. Geosciences Journal, 24, 61–71. doi: 10.1007/s12303-019-0014-y.

Chen X, Guo HF, Yao HW, Han KB, Wang HH. 2022. Processes and forcing mechanisms of the carbon cycle perturbation during Cretaceous Oceanic Anoxic Event 2. Chinese Science Bulletin, 67, 1677–1688 (in Chinese with English abstract). doi: 10.1360/TB-2021-0806.

Chi FE, Rodríguez NP, Partin CA, Lalonde SV, Andersson P, Weiss DJ, Albani AE, Rodushking I, Konhause KO. 2016. Cu isotopes in marine black shales record the Great Oxidation Event. Proceedings of the National Academy of Sciences, 113(18), 4941–4946. doi: 10.1073/pnas.1523544113.

Chi GX, Xue CJ. 2011. Principles, methods and applications of hydrodynamic studies of mineralization. Earth Science Frontiers, 18(5), 1–18 (in Chinese with English abstract).

Cox SF. 1995. Faulting processes at high fluid pressures: An example of fault valve behavior from the Wattle Gully Fault, Victoria, Australia. Journal of Geophysical Research: Solid Earth, 100(B7), 12841–12859. doi: 10.1029/95JB00915.

Cui Y, Li XZ, Guo W, Lin W, Hu Y, Han LL, Qian C, Zhao JM. 2023. Enlightenment of calcite veins in deep Ordovician Wufeng-Silurian Longmaxi shales fractures to migration and enrichment of shale gas in southern Sichuan Basin, SW China. Petroleum Exploration and Development, 50(6), 1199–1208 (in Chinese with English abstract). doi: 10.11698/PED.20230033.

Curtis CD. 1978. Possible links between sandstone diagenesis and depth-related geochemical reactions occurring in enclosing mudstones. Journal of the Geological Society, 135(1), 107–117. doi: 10.1144/gsjgs.135.1.0107.

Curtis JB. Fractured shale-gas systems. 2002. AAPG Bulletin, 86(11), 1921–1938. doi: 10.1306/61EEDDBE-173E-11D7-8645000102C1865D.

Dai SF, Tang YG, Jiang YF, Liu JJ, Ren DY, Zhao FH, Zhao L, Wang XB. 2021a. An in depth interpretation of definition and classification of macerals in coal (ICCP system 1994) for Chinese researchers, I: Vitrinite. Journal of China Coal Society, 46(6), 1821–1832 (in Chinese with English abstract).

Dai SF, Wang SQ, Tang YG, Jiang YF, Ren DY, Zhao L, Zhao FH, Shao LY, Zuo JP. 2021b. An in-depth interpretation of definition and classification of macerals in coal (ICCP system 1994) for Chinese Researchers, II: Inertinite. Journal of China Coal Society, 46(7), 2212–2226 (in Chinese with English abstract).

Dai SF, Liu JJ, Tang YG, jiang YF, Ren DY, Zhao FH, Shao LY, Zhao L. 2021c. An in-depth interpretation of definition and classification of macerals in coal (ICCP system 1994) for Chinese Researchers, III: Huminite. Journal of China Coal Society, 46(8), 2623–2636 (in Chinese with English abstract).

Dai SF, Zhao L, Tang YG, Ren DY, Wei Q, Jiang YF, Liu JJ, Zhao FH. 2021d. An in-depth interpretation of definition and classification of macerals in coal (ICCP system 1994) for Chinese researchers, IV: Liptinite. Journal of China Coal Society, 46(9), 2965–2983 (in Chinese with English abstract).

Dehghanpour H, Lan Q, Saeed Y, Fei H, Qi Z. 2013. Spontaneous imbibition of brine and oil in gas shales: Effect of water adsorption and resulting microfractures. Energy & Fuels, 27(6), 3039–3049. doi: 10.1021/ef4002814.

Ding JH, Zhang JC, Huo ZP, Shen BJ, Shi G, Yang ZH, Li XQ, Li CX. 2021. Controlling factors and formation models of organic matter accumulation for the Upper Permian Dalong Formation black shale in the Lower Yangtze Region, South China: Constraints from geochemical evidence. ACS Omega, 6(5), 3681–3692. doi: 10.1021/acsomega.0c04979.

Ding WL, Xu CC, Jiu K, Li C, Zeng WT, Wu LM. 2011. The research progress of shale fracture. Advances in Earth Science, 26(02), 135–144 (in Chinese with English abstract). doi: 10.11867/j.issn.1001-8166.2011.02.0135.

Ding WL, Li C, Li CY, Hu CC, Jiu K, Ceng WT. 2012. Dominant factor of fracture development in shale and its relationship to gas accumulation. Earth Science Frontiers, 19(2), 212–220 (in Chinese with English abstract).

Dong DZ, Qiu Z, Zhang LF, Li SX, Zhang Q, Li XT, Zhang SR, Liu HL, Wang YM. 2021. Progress on sedimentology of transitional facies shales and new discoveries of shale gas. Acta Sedimentologica Sinica, 39(1), 29–45 (in Chinese with English abstract). doi: 10.14027/j.issn.1000-0550.2021.002.

Durand B. 1980. Sedimentary Organic Matter and Kerogen: Definition and Quantitative Importance of Kerogen. In: Durand B, (ed.), Kerogen: Insoluble Organic Matter from Sedimentary Rocks. Editions Technip, Paris, 13–34.

Dutton SP, Loucks RG. 2010. Diagenetic controls on evolution of porosity and permeability in lower Tertiary Wilcox sandstones from shallow to ultradeep (200–6700 m) burial, Gulf of Mexico Basin, USA. Marine and Petroleum Geology, 27(1), 69–81. doi: 10.1016/j.marpetgeo.2009.08.008.

EIA. 2015. https://www.eia.gov/analysis/studies/worldshalegas/.

Ehrenberg SN. 1997. Influence of depositional sand quality and diagenesis on porosity and permeability; examples from Brent Group reservoirs, northern North Sea. Journal of Sedimentary Research, 67(1), 197–211. doi: 10.1306/D4268531-2B26-11D7-8648000102C1865D.

Elburg MA, Bons PD, Foden J, Passchier CW. 2002. The origin of fibrous veins: Constraints from geochemistry. Geological Society, London, Special Publications, 200(1), 103–118. doi: 10.1144/GSL.SP.2001.200.01.0.

El-Shafeiy M, Chen DZ, Chu ZY, Liu M, El-Kahawy RM. 2024. Chemo- and bio-stratigraphic constraints on Cretaceous-Paleocene biotic turnover in the southern Tethys low-oxygen margin, Egypt. Gondwana Research, 129, 142–166. doi: 10.1016/j.gr.2023.12.007.

Emmanuel S, Day-Stirrat RJ. 2012. A framework for quantifying size dependent deformation of nano-scale pores in mudrocks. Journal of Applied Geophysics, 86, 29–35. doi: 10.1016/j.jappgeo.2012.07.011.

Engle MA, Reyes FR, Varonka MS, Orem WH, Ma L, Ianno AJ, Schell TM, Xu P, Carroll KC. 2016. Geochemistry of formation waters from the Wolfcamp and “Cline” shales: insights into brine origin, reservoir connectivity, and fluid flow in the Permian Basin, USA. Chemical Geology, 425, 76–92. doi: 10.1016/j.chemgeo.2016.01.025.

Ernst RE, Youbi N. 2017. How Large Igneous Provinces affect global climate, sometimes cause mass extinctions, and represent natural markers in the geological record. Palaeogeography, Palaeoclimatology, Palaeoecology, 478, 30–52. doi: 10.1016/j.palaeo.2017.03.014.

Falcieri FM, Benetazzo A, Sclavo M, Russo A, Carniel S. 2014. Po River plume pattern variability investigated from model data. Continental Shelf Research, 87, 84–95. doi: 10.1016/j.csr.2013.11.001.

Feng QQ, Qiu NS, Borjigin T, Wu H, Zhang J, Shen BJ, Wang JS. 2022. Tectonic evolution revealed by thermo-kinematic and its effect on shale gas preservation. Energy, 240, 122781. doi: 10.1016/j.energy.2021.122781.

Feng ZH, Liu B, Shao HM, Wang C, Hong SX, Wang JP, Pan HF, Wang YC, Zhang AD, Tian SS, Chi YA. 2020. Diagenetic evolution and reservoir performance of mud shale in Qingshankou Formation, Gulong area, Songliao Basin. Petroleum Geology and Development in Daqing, 39(3), 72–85. doi: 10.19597/J.ISSN.1000-3754.202004057.

Fisher DM, Brantley SL, Everett M, Dzvonik J. 1995. Cyclic fluid flow through a regionally extensive fracture network within the Kodiak accretionary prism. Journal of Geophysical Research: Solid Earth, 100(B7), 12881–12894. doi: 10.1029/94JB02816.

Friedrichs CT, Scully ME. 2007. Modeling deposition by wave-supported gravity flows on the Po River prodelta: From seasonal floods to prograding clinoforms. Continental Shelf Research, 27(3/4), 322–337. doi: 10.1016/j.csr.2006.11.002.

Gale JFW, Laubach SE, Olson JE, Eichhubl P, Fall A. 2014. Natural fractures in shale: A review and new observations. AAPG bulletin, 98(11), 2165–2216. doi: 10.1306/08121413151.

Gallego-Torres D, Martínez-Ruiz F, Paytan A, Jiménez-Espejo F, Ortega-Huertas M. 2007. Pliocene-Holocene evolution of depositional conditions in the eastern Mediterranean: Role of anoxia vs. productivity at time of sapropel deposition. Palaeogeography, Palaeoclimatology, Palaeoecology, 246, 424–439. doi: 10.1016/j.palaeo.2006.10.008.

Gao J, Li HL, HE ZL, Li SJ, Liu GX, Yuan YS, Li YQ, Li TY, He S. 2022. Pressure evolution, enrichment and preservation of normal-pressure shale gas in the Pengshui area of eastern Chongqing. Natural Gas Industry, 42(8), 124–135 (in Chinese with English abstract). doi: 10.3787/j.issn.1000-0976.2022.08.010.

Gao P, Xiao XM, Hu DF, Lash GG, Liu RB, Zhang BY, Zhao YM. 2024. Comparison of silica diagenesis between the lower Cambrian and lower Silurian shale reservoirs in the middle–upper Yangtze platform (southern China). AAPG Bulletin, 108, 6, 971–1003. doi: 10.1306/01242422096.

Ge XT, Chen DZ, Zhang GJ, Huang TY, Liu M, El-Shafeiy M. 2022. Marine redox evolution and organic accumulation in an intrashelf basin, NE Sichuan Basin during the Late Permian. Marine and Petroleum Geology, 140, 105633. doi: 10.1016/j.marpetgeo.2022.105633.

Geng LK, Duan S. 2022. Research progress of methane adsorption on water-bearing shale. Coal and Chemical Industry, 45(1), 135–140 (in Chinese with English abstract).

Goodarzi F, Norford BS. 1989. Variation of graptolite reflectance with depth of burial. International Journal of Coal Geology, 11(2), 127–141. doi: 10.1016/0166-5162(89)90002-5.

Gou QY, Xu S, Hao F, Yang F, Shu ZG, Liu R. 2021. The effect of tectonic deformation and preservation condition on the shale pore structure using adsorption-based textural quantification and 3D image observation. Energy, 219, 119579. doi: 10.1016/j.energy.2020.119579.

Grim RE. 1947. Relation of clay mineralogy to origin and recovery of petroleum. AAPG Bulletin, 31(8), 1491–1499.

Guan QZ, Dong DZ, Wang SF, Huang JL, Wang YM, Zhang CC. 2016. Analyses on differences of microstructure between marine and lacustrine facies shale reservoirs. Natural Gas Geoscience, 27(3), 524–531 (in Chinese with English abstract). doi: 10.11764/j.issn1672-1926.2016.03.0524.

Gudbrandsson S, Wolff-Boenisch D, Gislason SR, Oelkers EH. 2014. Experimental determination of plagioclase dissolution rates as a function of its composition and pH at 22°C. Geochimica et Cosmochimica Acta, 139, 154–172. doi: 10.1016/j.gca.2014.04.028.

Guo S, Sun J. 2020. Concentrations and sinking rates of transparent exopolymer particles (TEPs) in a coastal sea: The Changjiang River (Yangtze River) Estuary. Acta Oceanologica Sinica, 39, 58–69. doi: 10.1007/s13131-020-1660-7.

Guo SB, Mao WJ. 2019. Division of diagenesis and pore evolution of a Permian Shanxi shale in the Ordos Basin, China. Journal of Petroleum Science and Engineering, 182, 106351. doi: 10.1016/j.petrol.2019.106351.

Guo TL. 2016. Key geological issues and main controls on accumulation and enrichment of Chinese shale gas. Petroleum Exploration and Development, 43(3), 317–326. doi: 10.11698/PED.2016.03.01.

Guo W, Li XZ, Zhang XW, Lan CL, Liang PP, Shen WJ, Zheng MJ. 2022. Sedimentary microfacies and microrelief of organic-rich shale in deep-water shelf and their control on reservoirs: A case study of shale from Wufeng-Longmaxi formation in southern Sichuan Basin. Acta Petrolei Sinica, 43(8), 1089–1106 (in Chinese with English abstract). doi: 10.7623/syxb202208005.

Guo XW, Qin ZJ, Yang R, Dong T, He S, Hao F, Yi JZ, Shu ZG, Bao HY, Liu KY. 2019. Comparison of pore systems of clay-rich and silica-rich gas shales in the lower Silurian Longmaxi formation from the Jiaoshiba area in the eastern Sichuan Basin, China. Marine and Petroleum Geology, 101, 265–280. doi: 10.1016/j.marpetgeo.2018.11.038.

Guo XS, Ma XX, Li MW, Qian MH, Hu ZQ. 2023. Mechanisms for lacustrine shale oil enrichment in Chinese sedimentary basins. Oil & Gas Geology, 44(6), 1333–1349 (in Chinese with English abstract). doi: 10.11743/ogg20230601.

Guo YH, Zhao DF, Chen SY. 2021. Research progress and prospect of fine-grained sediments and palaeogeography. Journal of palaeogeography, 23(2), 263–283 (in Chinese with English abstract). doi: 10.7605/gdlxb.2021.02.020.

Hackley PC, Cardott BJ. 2016. Application of organic petrography in north American shale petroleum systems: A Review. International Journal of Coal Geology, 163, 8–51. doi: 10.1016/j.coal.2016.06.010.

Hackley PC, Walters CC, Kelemen SR, Mastalerz M, Lowers HA. 2017. Organic petrology and micro-spectroscopy of Tasmanites microfossils: Applications to kerogen transformations in the early oil window. Organic Geochemistry, 114, 23–44. doi: 10.1016/j.orggeochem.2017.09.002.

Hao F, Zou HY, Lu YC. 2013. Mechanisms of shale gas storage: Implications for shale gas exploration in China. AAPG Bulletin, 97(8), 1325–1346. doi: 10.1306/02141312091.

He WY, Zhao Y, Zhong JH, Sun NL. 2024. Characteristics and significance of micron pores and micron fractures in shale oil reservoirs of Cretaceous Qingshankou Formation in Gulong sag, Songliao Basin. Lithologic Reservoirs, 36(3), 1–18.

He ZL, Nie HK, Li SJ, Luo J, Wang H, Zhang GR. 2020. Differential enrichment of shale gas in upper Ordovician and lower Silurian controlled by the plate tectonics of the Middle-Upper Yangtze, south China. Marine and Petroleum Geology, 118, 104357. doi: 10.1016/j.marpetgeo.2020.104357.

Hilgers C, Urai JL, 2002. Experimental study of syntaxial vein growth during lateral fluid flow in transmitted light: First results. Journal of Structural Geology, 24(6–7), 1029–1043. doi: 10.1016/S0191-8141(01)00089-X.

Horsfield B, Douglas AG. 1980. The influence of minerals on the pyrolysis of kerogens. Geochimica et Cosmochimica Acta, 44(8), 1119–1131. doi: 10.1016/0016-7037(80)90066-6.

Hu WX, Yao SP, Lu XC, Wu HG, Sun FN, Jin J. 2019. Influence of organic matter evolution on reservoir property during diagenesis of typical continental shale oil series. Oil & Gas Geology, 40(5), 947–956,1047 (in Chinese with English abstract). doi: 10.11743/ogg20190501.

Hu ZQ, Zheng LJ, Shen BJ, Cheng G, Liu ZB. 2021. Preliminary study on unconventional and conventional oil-bearing gas systems. Geological Review, 67(3), 1007–1020 (in Chinese with English abstract). doi: 10.16509/j.georeview.2021.06.011.

Huang DF. 1996. Advances in hydrocarbon generation theory- (I) immature oils and generating hydrocarbon and evolutionary model. Advances in Earth Science, 4(11), 327–335 (in Chinese with English abstract). doi: 10.11867/j.issn.1001-8166.1996.04.0327.

Huang WK, Ma XF, Zhou XP, Liu JY, He TT, Tao HF, Li ST, Hao LW. 2023. Characteristics and controlling factors of pore structure of shale in the 7th member of Yanchang Formation in Huachi area, Ordos Basin, China. Journal of Natural Gas Geoscience, 8(5), 319–336. doi: 10.1016/j.jnggs.2023.09.001.

Ibach LEJ. 1982. Relationship between sedimentation rate and total organic carbon content in ancient marine sediments. AAPG Bulletin, 66, 170–183. doi: 10.11764/j.issn.1672-1926.2015.06.1076.

ICCP. 1998. The new vitrinite classification (ICCP System, 1994). Fuel, 77, 349–358. doi: 10.1016/S0016-2361(98)80024-0.

ICCP. 2001. The new inertinite classification (ICCP System, 1994). Fuel, 80, 459–471. doi: 10.1016/S0016-2361(00)00102-2.

Ilgen AG, Heath JE, Akkutlu IY, Bryndzia LT, Cole DR, Kharaka YK, Kneafsey TJ, Milliken KL, Pyrak-Nolte LJ, Suarez-Rivera R. 2017. Shales at all scales: Exploring coupled processes in mudrocks. Earth-Science Reviews, 166, 132–152. doi: 10.1016/j.earscirev.2016.12.013.

Ishii E, Sanada H, Iwatsuki T, Sugita Y, Kurikami H. 2011. Mechanical strength of the transition zone at the boundary between opal-A and opal-CT zones in siliceous rocks. Engineering Geology, 122, 215–221. doi: 10.1016/j.enggeo.2011.05.007.

Jasper K, Hartkopf-Fröder C, Flajs G, Littke R. 2010. Evolution of Pennsylvanian (Late Carboniferous) peat swamps of the Ruhr Basin, Germany: Comparison of palynological, coal petrographical and organic geochemical data. International Journal of Coal Geology, 83(4), 346–365. doi: 10.1016/j.coal.2010.05.008.

Jenkyns HC. 2010. Geochemistry of oceanic anoxic events. Geochemistry, Geophysics, Geosystems, 11(3), 1–30. doi: 10.1029/2009GC002788.

Ji LM, Wu YD, He C, Su L. 2016. High-pressure hydrocarbon-generation simulation and pore evolution characteristics of organic-rich mudstone and shale. Acta Petrolei Sinica, 37(2), 172–181 (in Chinese with English abstract). doi: 10.7623/syxb201602003.

Jiang ZX. 2003. Sedimentology 2nd edition. Beijing, Petroleum Industry Press, 345–351 (in Chinese)

Jiang ZX, Liang C, Wu J, Zhang JG, Zhang WZ, Wang YS, Liu HM, Chen X. 2013. Several issues in sedimentological studies on hydrocarbon-bearing fine-grained sedimentary rocks. Acta Petrolei Sinica, 34(6), 1031–1039 (in Chinese with English abstract). doi: 10.7623/syxb201306001.

Jiang ZX, Xu J, Liu T, Ma DX, Mu HS, Sun SL. 2023b. The Depositional Environment and Hydrocarbon Potential of the Mesoproterozoic Black Shale in the Western Liaoning Depression of the Yanliao Rift Zone. Acta Sedimentologica Sinica, 41(6), 1830–1846 (in Chinese with English abstract). doi: 10.14027/j.issn.1000-0550.2023.129.

Jiang ZX, Zhang JG, Kong XX, Xie HY, Cheng H, Wang L. 2023a. Research progress and development direction of continental shale oil and gas deposition and reservoirs in China. Acta Petrolei Sinica, 44(1), 45–71 (in Chinese with English abstract). doi: 10.7623/syxb202301004.

Jin ZJ, Wang XM, Wang HJ, Ye YT, Zhang SC. 2023. Organic carbon cycling and black shale deposition: An Earth System Science perspective. National Science Review, 10(11), nwad243. doi: 10.1093/nsr/nwad243.

Johns WD, Shimoyama A. 1972. Clay minerals and petroleum-forming reactions during burial and diagenesis. AAPG Bulletin, 56(11), 2160–2167. doi: 10.1306/819A41F4-16C5-11D7-8645000102C1865D.

Ju YW, Qi Y, Fang LZ, Zhu HJ, Wang GC, Wang GL. 2016. China shale gas reservoir types and its controlling factors. Advances in Earth Science, 31(8), 782–799 (in Chinese with English abstract). doi: 10.11867/j.issn.1001-8166.2016.08.0782.

Kidder DL, Worsley TR. 2010. Phanerozoic Large Igneous Provinces (LIPs), HEATT (Haline Euxinic Acidic Thermal Transgression) episodes, and mass extinctions. Palaeogeography, Palaeoclimatology, Palaeoecology, 295(1–2), 162–191. doi: 10.1016/j.palaeo.2010.05.036.

Klemme HD, Ulmishek GF. 1991. Effective petroleum source rocks of the world: stratigraphic distribution and controlling depositional factors. AAPG bulletin, 75(12), 1809–1851.

Kus J, Araujo CV, Borrego AG, Flores D, Hackley PC, Hámor-Vidó M, Kalaitzidis S, Kommeren CJ, Kwiecińska B, Mastalerz M, Mendonça Filho JG, Menezes TR, Misz-Kennan M, Nowak GJ, Petersen HI, Rallakis D, Suárez-Ruiz I, Sýkorová I, Životić D. 2017. Identification of alginite and bituminite in rocks other than coal. 2006, 2009, and 2011 round robin exercises of the ICCP Identification of Dispersed Organic Matter Working Group. International Journal of Coal Geology, 178, 26–38. doi:10.1016/j.coal.2017.04.013.

Lazar OR, Bohacs KM, Macquaker JHS, Schieber J, Demko TM. 2015. Capturing key attributes of fine-grained sedimentary rocks in outcrops, cores, and thin sections: Nomenclature and description guidelines. Journal of Sedimentary Research, 85(3), 230–246. doi: 10.2110/jsr.2015.11.

Lev SM, Filer JK, Tomascak P. 2008. Orogenesis *vs*. diagenesis: Can we use organic-rich shales to interpret the tectonic evolution of a depositional basin? Earth-Science Reviews, 86(1–4), 1–14. doi: 10.1016/j.earscirev.2007.07.001.

Lewan MD. 1997. Experiments on the role of water in petroleum formation. Geochimica et Cosmochimica Acta, 61(17), 3691–3723. doi: 10.1016/S0016-7037(97)00176-2.

Li JG, Batten DJ. 2005. Palynofacies: Principles and methods. Acta Palaeontologica Sinica, 44(1), 138–156 (in Chinese with English abstract).

Li MW, Jin ZJ, Dong MZ, Ma XX, Li ZM, Jiang QG, Bao YJ, Tao GL, Qian MH, Liu P, Cao TT. 2020. Advances in the basic study of lacustrine shale evolution and shale oil accumulation. Petroleum geology & experiment, 42(4), 489–505 (in Chinese with English abstract). doi: 10.11781/sysydz202004489.

Li MW, Ma XX, Jin ZJ, Li ZM, Jiang QG, Wu SQ, Li Z, Xu ZX. 2022. Diversity in the lithofacies assemblages of marine and lacustrine shale strata and significance for unconventional petroleum exploration in China. Oil & Gas Geology, 43(1), 1–25. doi: 10.11743/ogg20220101.

Li QQ, Xu S. 2022. Research status and prospects of marine-continental transitional shale reservoirs. Geological Bulletin of China, 41(8), 1417–1429 (in Chinese with English abstract). doi: 10.12097/j.issn.1671-2552.2022.08.009.

Li SJ, Li YQ, He ZL, Chen K, Zhou Y, Yan DT. 2020. Differential deformation on two sides of Qiyueshan Fault along the eastern margin of Sichuan Basin, China, and its influence on shale gas preservation. Marine and Petroleum Geology, 121, 104602. doi: 10.1016/j.marpetgeo.2020.104602.

Li SZ, Liu XF, Cen C, Yang SC, Xiao EZ, Zhang XT, He WH, Liu LX. 2023a. Sedimentary paleoenvironment and organic matter accumulation model of the Lower Silurian Gaojiabian Formation shales in the Lower Yangtze region, South China. Geoenergy Science and Engineering, 221, 211347. doi: 10.1016/j.geoen.2022.211347.

Li SZ, Zhou Z, Li F, Shen B, Xu QC, Song T, Zhang XT, Yang XG, Hu CZ, Wang C, Wei SY, Wang YL, Lu YX. 2024. Shale gas enrichment conditions and favorable exploration areas of Upper Permian Dalong Formation in the western Hubei and eastern Chongqing region. Natural Gas Industry, 44(5), 1–15. doi: 10.3787/j.issn.1000-0976.2024.05.001.

Li SZ, Zhou Z, Nie HK, Zhang LF, Song T, Liu WB, Li HH, Xu QC, Wei SY, Tao S. 2022. Distribution characteristics, exploration and development, geological theories research progress and exploration directions of shale gas in China. China Geology, 5(1), 110–135. doi: 10.31035/cg2021069.

Li SZ, Zhou Z, Nie HK, Liu M, Meng FY, Shen B, Zhang XT, Wei SY, Xi ZD, Zhang SS. 2023b. Organic matter accumulation mechanisms in the Wufeng-Longmaxi shales in western Hubei Province, China and paleogeographic implications for the uplift of the Hunan-Hubei Submarine high. International Journal of Coal Geology, 270, 104223. doi: 10.1016/j.coal.2023.104223.

Li T, Li HP, Xu LP. 2018. An experimental study of interaction between pure water and alkaline feldspar at high temperatures and pressures. Acta Geochimica, 37(1), 60–67. doi: 10.1007/s11631-017-0208-9.

Li WP, Liu SF, Wang Y, Qian T, Gao TJ. 2017. Duplex thrusting in the South Dabashan arcuate belt, central China. Journal of Structural Geology, 103, 120–136. doi: 10.1016/j.jsg.2017.09.007.

Li XS, Zhu HJ, Zhang KX, Li Z, Yu YX, Feng XQ, Wang ZX. 2021. Pore characteristics and pore structure deformation evolution of ductile deformed shales in the Wufeng-Longmaxi Formation, southern China. Marine and Petroleum Geology, 127, 104992. doi: 10.1016/j.marpetgeo.2021.104992.

Li YF, Schieber J, Fan TL, Li ZY, Zhang JP. 2017. Regional depositional changes and their controls on carbon and sulfur cycling across the Ordovician-Silurian boundary, northwestern Guizhou, South China. Palaeogeography, Palaeoclimatology, Palaeoecology, 485, 816–832. doi: 10.1016/j.palaeo.2017.07.039.

Liang JT, Huang WH, Wang HL, Blum MJ, Chen J, Wei XL, Yang GQ. 2020. Organic geochemical and petrophysical characteristics of transitional coal-measure shale gas reservoirs and their relationships with sedimentary environments: A case study from the Carboniferous-Permian Qinshui Basin, China. Journal of Petroleum Science and Engineering, 184, 106510. doi: 10.1016/j.petrol.2019.106510.

Liang ML, Wang ZX, Li CL, Li HJ, Zhang YL, Feng XQ, Zhang KX. 2020. Effect of structural deformation on permeability evolution of marine shale reservoirs. Journal of Geomechanics, 26(6), 840–851 (in Chinese with English abstract). doi: 10.12090/j.issn.1006-6616.2020.26.06.066.

Lin W, Guo W, Zhang JZ, Li MT. 2024. Organic matter pore-forming characteristic differences in complex lithofacies types of Longmaxi shales from southern Sichuan Basin. Natural Gas Geoscience, 35(1), 133–148 (in Chinese with English abstract). doi: 10.11764/j.issn.1672-1926.2023.07.004.

Liu B. 2023. Organic matter in shales: Types, thermal evolution, and organic pores. Earth Science, 48(12), 4641–4657 (in Chinese with English abstract). doi: 10.3799/dqkx.2022.130.

Liu B, Mastalerz M, Schieber J. 2022. SEM petrography of dispersed organic matter in black shales: A Review. Earth-Science Reviews, 224, 103874. doi: 10.1016/j.earscirev.2021.103874.

Liu GH. 2017. The Formation Mechanism of Authigenic Quartz in Lacustrine Shale and Influence to Reservoir Property. Beijing, China University of Petroleum (Beijing), PhD Thesis, 33–40 (in Chinese with English abstract).

Liu GH, Liu KY, Zhai GY, Zhao JH, Guo ZG. 2023. Crystallinity and formation of silica in Palaeozoic shales: A new quantification calculation method based on X-Ray diffraction. Marine and Petroleum Geology, 150, 106124. doi: 10.1016/j.marpetgeo.2023.106124.

Liu GH, Zhai GY, Huang ZL, Zou CN, Xia XH, Shi DS, Zhou Z, Zhang C, Chen R, Yu SF, Chen L, Zhang SH. 2019a. The effect of tuffaceous material on characteristics of different lithofacies: A case study on Lucaogou Formation fine-grained sedimentary rocks in Santanghu Basin. Journal of Petroleum Science and Engineering, 179, 355–377. doi: 10.1016/j.petrol.2019.04.072.

Liu GH, Zhai GH, Yang R, He TP, Wei B. 2021. Quartz crystallinity index: New quantitative evidence for biogenic silica of the Late Ordovician to Early Silurian organic-rich shale in the Sichuan Basin and adjacent areas, China. Science China Earth Sciences, 64(5), 773–787. doi: 10.1007/s11430-020-9718-2.

Liu GH, Zhai GY, Zou CN. 2019b. A comparative discussion of the evidence for biogenic silica in Wufeng-Longmaxi siliceous shale reservoir in the Sichuan basin, China. Marine and Petroleum Geology, 109, 70–87. doi: 10.1016/j.marpetgeo.2019.06.016.

Liu M, Philp RP. 2023. Utilization of pyrrolic compounds as indicators of secondary migration for woodford oils in the Anadarko Basin, Oklahoma, USA. Journal of Earth Science. doi: 10.1007/s12583-023-1811-9.

Liu HM, Yu BS, Xie ZH, Han SJ, Shen ZH, Bai CY. 2018. Characteristics and implications of micro-lithofacies in lacustrine-basin organic-rich shale: A case study of Jiyang depression, Bohai Bay Basin. Acta Petrolei Sinica, 39(12), 1328–1343. doi: 10.7623/syxb201812002.

Liu QY, Li P, Jin ZJ, Sun YW, Hu G, Zhu DY, Huang ZK, Liang XP, Zhang R, Liu JY. 2022. Organic-rich formation and hydrocarbon enrichment of lacustrine shale strata: A case study of Chang 7 Member. Science China Earth Sciences, 52(2), 270–290. doi: 10.1007/s11430-021-9819-y.

Liu QY, Zhu DY, Meng QQ, Liu JY, Wu XQ, Zhou B, Qi F, Jin ZJ. 2019. The basic connotation of hydrocarbon formation under deep fluid and organic-inorganic interaction. Science in China: Earth Sciences, 49(3), 499–520 (in Chinese with English abstract). doi: 10.1007/s11430-018-9281-2.

Liu R, Zhang K, Liu ZJ, Yan X, Yu JQ. 2021. Oil shale mineralization and geological events in China. Acta Sedimentologica Sinica, 39(1), 10–28. doi: 10.14027/j.issn.1000-0550.2020.104.

Liu W, Liu M, Yang T, Liu X, Them TR, Wang K, Bian CS, Meng QA, Li YX, Zeng X, Zhao W. 2022. Organic matter accumulations in the Santonian-Campanian (Upper Cretaceous) lacustrine Nenjiang shale

(K_2n) in the Songliao Basin, NE China: Terrestrial responses to OAE3? International Journal of Coal Geology, 260, 104069. doi: 10.1016/j.coal.2022.104069.
Liu WH, Huang DF, Xiong CW, Xu YC. 1999. The development of hydrocarbon generation theory and the distribution and research status of immature to low mature oil and gas abroad. Natural Gas Geoscience, 10(1–2), 1–22 (in Chinese). doi: 10.11764/j.issn.1672-1926.1999.01.1.
Liu WP, Zhang CL, Gao GD, Luo C, Wu W, Shi XW, Zhang J, Li WG, Deng XH, Hu XH. 2017. Controlling factors and evolution laws of shale porosity in Longmaxi Formation, Sichuan Basin. Acta Petrolei Sinica, 38(2), 175–184 (in Chinese with English abstract). doi: 10.7623/syxb201702005.
Loucks RG, Reed RM, Ruppel SC, Hammes U. 2012. Spectrum of pore types and networks in mudrocks and a descriptive classification for matrix-related mudrock pore. AAPG bulletin, 96(6), 1071–1098. doi: 10.1306/08171111061.
Luo W, Hou MC, Liu XC, Huang SG, Chao H, Zhang R, Deng X. 2018. Geological and geochemical characteristics of marine-continental transitional shale from the Upper Permian Longtan formation, Northwestern. Guizhou, China. Marine and Petroleum Geology, 89, 58–67. doi: 10.1016/j.marpetgeo.2017.06.029.
Ma BB, Cao YC, Wang YZ, Jia YC, Zhang SM. 2015. Diagenetic evolution and its influence on physical properties of Es_4^s reservoir in the northern steep zone of the Bonan Sag. Acta Sedimentologica Sinica, 33(1), 170–182 (in Chinese with English abstract). doi: 10.14027/j.cnki.cjxb.2015.01.018.
Ma J, Fang DZ, Zhang PX, Gu HT, Hu CF, Lu B, Cheng YY, Gao QF, Wan JY. 2022. Characteristics and genesis of shale fractures in Wufeng-Longmaxi formations of Yangchungou structural belt in Southeast Chongqing. Natural Gas Geoscience, 33(7), 1117–1131 (in Chinese with English abstract). doi: 10.11764/j.issn.1672-1926.2022.03.001.
Ma YS, Cai XY, Zhao PR. 2018. China's shale gas exploration and development: Understanding and practice. Petroleum Exploration and Development, 45(4), 589–603. doi: 10.1016/S1876-3804(18)30065-X.
Machel HG. 2001. Bacterial and thermochemical sulfate reduction in diagenetic settings-old and new insights. Sedimentary Geology, 140(1–2), 143–175. doi: 10.1016/S0037-0738(00)00176-7.
Macquaker JHS, Bentley SJ, Bohacs KM. 2010. Wave-enhanced sediment-gravity flows and mud dispersal across continental shelves: Reappraising sediment transport processes operating in ancient mudstone successions. Geology, 38(10), 947–950. doi: 10.1130/G31093.1.
Martin DP, Nittrouer CA, Ogston AS, Crockett JS. 2008. Tidal and seasonal dynamics of a muddy inner shelf environment, Gulf of Papua. Journal of Geophysical Research, 113(F1), F01S07. doi: 10.1029/2006JF000681.
Mastalerz M, Schimmelmann A, Drobniak A, Chen Y. 2013. Porosity of Devonian and Mississippian New Albany Shale across a maturation gradient: Insights from organic petrology, gas adsorption, and mercury intrusion. AAPG Bulletin, 97(10), 1621–1643. doi: 10.1306/04011312194.
Mastalerz M, Drobniak A, Stankiewicz AB. 2018. Origin, properties, and implications of solid bitumen in source-rock reservoirs: A review. International Journal of Coal Geology, 2018, 195. doi: 10.1016/j.coal.2018.05.013.
McLaughlin MR, Brooks JP, Adeli A. 2009. Characterization of selected nutrients and bacteria from anaerobic swine manure lagoons on sow, nursery, and finisher farms in the mid-south USA. Journal of Environmental Quality, 38(6), 2422–2430. doi: 10.2134/jeq2008.0468.
Mei JF, Liang C, Cao YC, Han Y. 2024. Types, genesis and significance of quartz in shales. Journal of palaeogeography (Chinese edition), 2024,26(2), 1–12. doi: 10.7605/gd1xb.2024.02.038.
Middelburg JJ, Meysman FJR. 2007. Burial at sea. Science, 316(5829), 1294–1295. doi: 10.1126/science.1144001.
Middleton NJ, Goudie AS. 2001. Saharan dust: Sources and trajectories. Transactions of the Institute of British Geographers, 26(2), 165–181. doi: 10.1111/1475-5661.00013.
Milliken KL, Olson T. 2017. Silica diagenesis, porosity evolution, and mechanical behavior in siliceous mudstones, Mowry Shale (Cretaceous), Rocky Mountains, USA. Journal of Sedimentary Research, 87(4), 366–387. doi: 10.2110/jsr.2017.24.
Mills BJW, Krause AJ, Jarvis I, Cramer BD. 2023. Evolution of atmospheric o_2 through the phanerozoic, revisited. Annual Review of Earth and Planetary Sciences, 51, 253–276. doi: 10.1146/annurev-earth-032320-095425.
Mort H, Jacquat O, Adatte T, Steinmann P, Föllmi K, Matera V, Berner Z, Stüben D. 2007. The Cenomanian/Turonian anoxic event at the Bonarelli level in Italy and Spain: Enhanced productivity and/or better preservation? Cretaceous Research, 28(4), 597–612. doi: 10.1016/j.cretres.2006.09.003.
Mulder T, Alexander J. 2001. The physical character of subaqueous sedimentary density flows and their deposits. Sedimentology, 48(2), 269–299. doi: 10.1046/j.1365-3091.2001.00360.x.
Mulder T, Syvitski JPM. 1995. Turbidity currents generated at river mouths during exceptional discharges to the world oceans. The Journal of Geology, 103(3), 285–299. doi: 10.1086/629747.
Murphy AE, Sageman BB, Hollander DJ, Lyons TW, Brett CE. 2000. Black shale deposition and faunal overturn in the Devonian Appalachian Basin: Clastic starvation, seasonal water-column mixing, and efficient biolimiting nutrient recycling. Paleoceanography, 15(3), 280–291. doi: 10.1029/1999PA000445.
Nie HK, Liu Q, Dang W, Li P, Su H, Bao H, Xiong L, Liu Z, Sun C, Zhang P. 2023. Enrichment mechanism and resource potential of shale-type helium: A case study of Wufeng Formation-Longmaxi Formation in Sichuan Basin. Science China Earth Sciences, 66(6), 1279–1288 (in Chinese with English abstract). doi: 10.1007/s11430-022-1045-3.
Nie HK, He ZL, Liu GX, Zhang GR, Lu ZY, Li DH, Sun CX. 2020a. Status and direction of shale gas exploration and development in China. Journal of China University of Mining & Technology, 49(1), 13–35 (in Chinese with English abstract). doi: 10.13247/j.cnki.jcumt.001096.
Nie HK, He ZL, Wang RY, Zhang GR, Chen Q, Li DH, Lu ZY, Sun CX. 2020b. Temperature and origin of fluid inclusions in shale veins of Wufeng–Longmaxi Formations, Sichuan Basin, south China: Implications for shale gas preservation and enrichment. Journal of Petroleum Science and Engineering, 193, 107329. doi: 10.1016/j.petrol.2020.107329.
Nygård R, Gutierrez M, Bratli RK, Høeg K. 2006. Brittle–ductile transition, shear failure and leakage in shales and mudrocks. Marine and Petroleum Geology, 23(2), 201–212. doi: 10.1016/j.marpetgeo.2005.10.001.
Okamoto A, Sekine K. 2011. Textures of syntaxial quartz veins synthesized by hydrothermal experiments. Journal of Structural Geology, 33(12), 1764–1775. doi: 10.1016/j.jsg.2011.10.004.
Oliver NHS, Bons PD. 2001. Mechanisms of fluid flow and fluid–rock interaction in fossil metamorphic hydrothermal systems inferred from vein–wallrock patterns, geometry and microstructure. Geofluids, 1(2), 137–162. doi: 10.1046/j.1468-8123.2001.00013.x.
Pan SQ, Zou CN, Li Y, Jing ZH, Liu ET, Yuan M, Zhang GS, Yang Z, Wu ST, Qiu Z, Liu HL. 2021. Major biological events and fossil energy formation: On the development of energy science under the earth system framework. Petroleum Exploration and Development, 48(3), 498–509 (in Chinese with English abstract). doi: 10.11698/PED.2021.03.06.

Parnell J, Honghan C, Middleton D, Haggan T, Carey P. 2000. Significance of fibrous mineral veins in hydrocarbon migration: Fluid inclusion studies. Journal of Geochemical Exploration, 69–70, 623–627. doi: 10.1016/S0375-6742(00)00040-6.

Parviainen A, Loukola-Ruskeeniemi K. 2019. Environmental impact of mineralised black shales. Earth-Science Reviews, 192, 65–90. doi: 10.1016/j.earscirev.2019.01.017.

Pattison SAJ. 2005. Storm-influenced prodelta turbidite complex in the Lower Kenilworth member at Hatch Mesa, Book Cliffs, Utah, U. S. A. : Implications for shallow marine facies models. Journal of Sedimentary Research, 75(3), 420–439. doi: 10.2110/jsr.2005.033.

Pedersen TF, Calvert SE. 1990. Anoxia vs. productivity: What controls the formation of organic-carbon-rich sediments and sedimentary rocks? AAPG Bulletin, 74(4), 454–466. doi: 10.1306/0C9B232B-1710-11D7-8645000102C1865D.

Peng J, Zeng Y, Yang YM, Yu LD, Xu TY. 2022. Discussion on classification and naming scheme of fine-grained sedimentary rocks. Petroleum Exploration and Development, 49(1), 106–115 (in Chinese with English abstract). doi: 10.11698/PED.2022.01.09.

Peng JW, Hu ZQ, Feng DJ. 2024. Influence of quartz types on rock fabrics and bulk physical properties in organic-rich mudstone: A review. Earth-Science Reviews, 249, 104670. doi: 10.1016/j.earscirev.2023.104670.

Petersen HI, Schovsbo NH, Nielsen AT. 2013. Reflectance measurements of zooclasts and solid bitumen in lower Paleozoic Shales, Southern Scandinavia: Correlation to vitrinite reflectance. International Journal of Coal Geology, 114, 1–18. doi: 10.1016/j.coal.2013.03.013.

Pickel W, Kus J, Flores D, Kalaitzidis S, Christanis K, Cardott BJ, Misz-Kennan M, Rodrigues S, Hentschel A, Hamor-Vido M, Crosdale P, Wagner N. 2017. Classification of liptinite—ICCP System 1994. International Journal of Coal Geology, 169, 40–61. doi: 10.1016/j.coal.2016.11.004.

Piper DZ, Calvert SE. 2009. A marine biogeochemical perspective on black shale deposition. Earth-Science Reviews, 95(1–2), 63–96. doi: 10.1016/j.earscirev.2009.03.001.

Planavsky NJ, McGoldrick P, Scott T, Li C, Reinhard CT, Kelly AE, Chu XL, Bekke A, Love GD, Lyons TW. 2011. Widespread iron-rich conditions in the mid-Proterozoic ocean. Nature, 477(7365), 448–451. doi: 10.1038/nature10327.

Pollastro RM. 1993. Considerations and applications of the illite/smectite geothermometer in hydrocarbon-bearing rocks of Miocene to Mississippian age. Clays Clay Miner, 41(2), 119–33. doi: 10.1346/CCMN.1993.0410202.

Qin JZ, Liu BQ. 2003. Study on the models of hydrocarbon generation and expulsion from various source rocks in coal-bearing environments. Petroleum Geology & Experiment, 25(6), 758–764 (in Chinese with English abstract). doi: 10.11781/sysydz200306758.

Qin JZ, Liu BQ. 2005. Models of hydrocarbon generation and expulsion from various marine source rocks. Petroleum Geology & Experiment, 27(1), 74–80 (in Chinese with English abstract). doi: 10.11781/sysydz200501074.

Qiu Z, Zou CN. 2020. Unconventional petroleum sedimentology: Connotation and prospect. Acta Sedimentologica Sinica, 38(1), 1–29 (in Chinese with English abstract). doi: 10.14027/j.issn.1000-0550.2019.116.

Rimmer SM. 2004. Geochemical paleoredox indicators in Devonian-Mississippian black shales, Central Appalachian Basin (USA). Chemical Geology, 206, 373–391. doi: 10.1016/j.chemgeo.2003.12.029.

Rimstidt JD, Chermak JA, Schreiber ME. 2017. Processes that control mineral and element abundances in shales. Earth-Science Reviews, 171, 383–399. doi: 10.1016/j.earscirev.2017.06.010.

Rong JY, Huang B. 2014. Study of Mass Extinction over the past thirty years: A synopsis. Scientia Sinica Terrae, 44, 377–404 (in Chinese with English abstract). doi: 10.1360/zd-2014-44-3-377.

Rose WI, Durant AJ. 2009. Fine ash content of explosive eruptions. Journal of Volcanology and Geothermal Research, 186(1/2), 32–39. doi: 10.1016/j.jvolgeores.2009.01.010.

Ross DJK, Bustin R. 2008. Characterizing the shale gas resource potential of devonian-mississippian strata in the Western Canada sedimentary basin: Application of an integrated formation evaluation. AAPG Bulletin, 92(1), 87–125. doi: 10.1306/09040707048.

Sageman BB, Murphy AE, Werne JP, er Straeten CA, Hollander DJ, Lyons TW. 2003. A tale of shales: The relative roles of production, decomposition, and dilution in the accumulation of organic-rich strata, Middle-Upper Devonian, Appalachian Basin. Chemical Geology, 195, 229–273. doi: 10.1016/S0009-2541(02)00397-2.

Schieber J. 2016. Mud re-distribution in epicontinental basins – Exploring likely processes. Marine and Petroleum Geology, 71, 119–133. doi: 10.1016/j.marpetgeo.2015.12.014.

Schieber J, Krinsley D, Riciputi L. 2000. Diagenetic origin of quartz silt in mudstones and implications for silica cycling. Nature, 406, 981–985. doi: 10.1038/35023143.

Scotese CR, Song HJ, Mills BJW, van der Meer DG. 2021. Phanerozoic paleotemperatures: The earth’s changing climate during the last 540 million years. Earth-Science Reviews, 215, 103503. doi: 10.1016/j.earscirev.2021.103503.

Sepkoski JJ. 1984. A kinetic model of Phanerozoic taxonomic diversity. III. Post-Paleozoic families and mass extinctions. Paleobiology, 10(2), 246–267. doi: 10.1017/S0094837300008186.

Shang FH, Miao K, Zhu YM, Wang M, Tang X, Wang Y, Feng GJ, Gao HT, Mi WT. 2023. Influence of tectonic deformation on pore structure of shale reservoir: A case study of Longmaxi Formation in northeastern Chongqing. Natural Gas Geoscience, 34(7), 1247–1259 (in Chinese with English abstract). doi: 10.11764/j.issn.1672-1926.2023.03.019.

Shao LY, Zhang TC. 2023. Discussion on definition and classification of mudrock. Journal of palaeogeography, 25(4), 742–751 (in Chinese with English abstract). doi: 10.7605/gdlxb.2023.04.058.

Shen SZ, Zhang H. 2017. What caused the five mass extinctions? Chinese Science Bulletin, 62, 1119–1135 (in Chinese with English abstract). doi: 10.1360/N972017-00013.

Shen YH, Ge HK, Meng MM, Jiang ZX, Yang XY. 2017. Effect of water imbibition on shale permeability and its influence on gas production. Energy & Fuels, 31(5), 4973–4980. doi: 10.1021/acs.energyfuels.7b00338.

Shi ZS, Qiu Z. 2021. Main Bedding Types of Marine Fine-Grained Sediments and their Significance for Oil and Gas Exploration and Development. Acta Sedimentologica Sinica, 39(1), 181–196 (in Chinese with English abstract). doi: 10.14027/j.issn.1000-0550.2020.097.

Slatt RM, Rodriguez ND. 2012. Comparative sequence stratigraphy and organic geochemistry of gas shales: Commonality or coincidence? Journal of Natural Gas Science and Engineering, 8, 68–84. doi: 10.1016/j.jngse.2012.01.008.

Stanley SM. 2015. Earth System History. New York, W. H. Freeman & Company, 245.

Su WB, Li ZM, Ettensohn FR, Johnson ME, Huff WD, Wang W, Ma C, Li L, Zhang L, Zhao HJ. 2007. Major controlling factors and implications of the spatiotemporal distribution of the black shale sequence in the Wufeng-Longmaxi Formations, South China. Journal of Earth Science—China University of Geosciences, 32(6), 819–827.

Sun LN, Tuo JC, Zhang MF, Wu CJ, Chai SQ. 2019. Pore structures and fractal characteristics of nano-pores in shale of Lucaogou formation from Junggar Basin during water pressure-controlled artificial pyrolysis. Journal of Analytical and Applied Pyrolysis, 140, 404–412. doi: 10.1016/j.jaap.2019.04.020.

Sun WJB, Zuo YJ, Wang SY, Wu ZH, Liu H, Zheng LJ, Lou YL. 2020. Pore structures of shale cores in different tectonic locations in the complex tectonic region: A case study of the Niutitang Formation in Northern Guizhou, Southwest China. Journal of Natural Gas Science and Engineering, 80, 103398. doi: 10.1016/j.jngse.2020.103398.

Sun WJB, Zuo YJ, Lin Z, Wu ZH, Liu H, Lin JY, Chen B, Chen QG, Pan C, Lan BF, Liu S. 2023. Impact of tectonic deformation on shale pore structure using adsorption experiments and 3D digital core observation: A case study of the Niutitang Formation in Northern Guizhou. Energy, 278, 127724. doi: 10.1016/j.energy.2023.127724.

Surdam RC, Crossey LJ, Hagen ES, Heasler HP. 1989. Organic-inorganic interactions and sandstone diagenesis. AAPG Bulletin, 73(1), 1–23.

Taylor GH, Teichmüller M, Davis ACFK, Diessel CFK, Littke R, Robert P. 1998. Organic Petrology. Gebrüder Borntraeger. Berlin, Stutgart, 1–30.

Teng J, Mastalerz M, Liu B. 2021. Petrographic and chemical structure characteristics of amorphous organic matter in marine black shales: Insights from Pennsylvanian and Devonian black shales in the Illinois Basin. International Journal of Coal Geology, 235, 103676. doi: 10.1016/j.coal.2021.103676.

Thyberg B, Jahren J, Winje T, Bjørlykke K, Faleide JI, Marcussen Ø. 2010. Quartz cementation in Late Cretaceous mudstones, northern North Sea: Changes in rock properties due to dissolution of smectite and precipitation of micro-quartz crystals. Marine and Petroleum Geology, 27(8), 1752–1764. doi: 10.1016/j.marpetgeo.2009.07.005.

Tissot B, Durand B, Espitalie J, Combaz A. 1974. Influence of nature and diagenesis of organic matter in formation of petroleum. AAPG Bulletin, 58, 499–506. doi: 10.1306/83d91425-16c7-11d7-8645000102c1865d.

Tissot BP, Welte DH. 1984. Petroleum Formation and Occurrence, 2nd. Springer-Verlag, Berlin, 131–198.

Trabucho-Alexandre J. 2015. Organic matter-rich shale depositional Environments. Fundamentals of Gas Shale Reservoirs, 21–45. doi: 10.1002/9781119039228.ch2.

Tyson RV, Pearson TH. 1991. Modern and ancient continental shelf anoxia: an overview. Geological Society, London, Special Publications, 58(1), 1–24.

Tyson RV. 2001. Sedimentation rate, dilution, preservation and total organic carbon: Some results of a modelling study. Organic Geochemistry, 32, 333–339. doi: 10.1016/S0146-6380(00)00161-3.

Van Kranendonk MJ. 2006. Volcanic degassing, hydrothermal circulation and the flourishing of early life on Earth: A review of the evidence from c. 3490–3240 Ma rocks of the Pilbara Supergroup, Pilbara Craton, Western Australia. Earth-Science Reviews, 74(3–4), 197–240. doi: 10.1016/j.earscirev.2005.09.005.

Wan XF, Liu CC, Zhao DF, Ge X. 2023. Hotspot and development trend of shale oil research. Earth Science, 48(2), 793–813 (in Chinese with English abstract). doi: 10.3799/dqkx.2022.443.

Wang EZ, Guo TL, Li MW, Xiong L, Dong XX, Zhang NX, Wang T. 2022. Depositional environment variation and organic matter accumulation mechanism of marine-continental transitional shale in the upper Permian Longtan Formation, Sichuan Basin, SW China. ACS Earth and Space Chemistry, 6(9), 2199–2214. doi: 10.1021/acsearthspacechem.2c00101.

Wang M, Chen Y, Song GQ, Steele-MacInnis M, Liu Q, Wang XJ, Zhang XJ, Zhao ZY, Liu WY, Zhang HJ, Zhou ZZ. 2018. Formation of bedding-parallel, fibrous calcite veins in laminated source rocks of the Eocene Dongying Depression: A growth model based on petrographic observations. International Journal of Coal Geology, 200, 18–35. doi: 10.1016/j.coal.2018.10.004.

Wang RY, Hu ZQ, Long SX, Du W, Wu J, Wu ZH, Nie HK, Wang PW, Sun CX, Zhao JH. 2022. Shale reservoir characteristics and evolution mechanism of Upper Ordovician Wufeng Formation and Lower Silurian Longmaxi Formation in Sichuan Basin. Oil & Gas Geology, 43(2), 353–364 (in Chinese with English abstract). doi: 10.11743/ogg20220209.

Wang WY, Pang XQ, Wang YP, Chen ZX, Li CR, Ma XH. 2022. Hydrocarbon expulsion model and resource potential evaluation of high-maturity marine source rocks in deep basins: Example from the Ediacaran microbial dolomite in the Sichuan Basin, China. Petroleum Science, 19(6), 2618–2630. doi: 10.1016/j.petsci.2022.11.018.

Wang XF, Liu QY, Liu WH, Li XB, Tao C, Li XF, Zhao D, Zhang JY, Zhu DY, Meng QQ, Xu HY, Wu XQ. 2023. Helium accumulation in natural gas systems in Chinese sedimentary basins. Marine and Petroleum Geology, 150, 106155. doi: 10.1016/j.marpetgeo.2023.106155.

Wang XX, Cai JG, Bao YJ. 2006. Catalysis of clay miner al to organic matter in hydrocarbon genesis. Marine Origin Petroleum Geology, 11(3), 27–38 (in Chinese with English abstract).

Wang Y. 2020. Hydrocarbon Generation and Diagenetic Evolution of Shale and Their Influences on Gas Occurrence in Wufeng-Longmaxi Formation, Southern Sichuan Basin. Beijing, China University of Petroleum (Beijing), Master Thesis, 1–105 (in Chinese with English abstract).

Wang ZL, Yang XG, Guo SB. 2024. Evolution of pore spaces in marine organic-rich shale: Insights from multi-scale analysis of a Permian–Pennsylvanian sample. Minerals, 14, 392. doi: 10.3390/min14040392.

Warrick JA, DiGiacomo PM, Weisberg SB, Nezlin NP, Mengel M, Jones BH, Ohlmann JC, Washburn L, Terrill EJ, Farnsworth KL. 2007. River plume patterns and dynamics within the southern California Bight. Continental Shelf Research, 27(19), 2427–2448. doi: 10.1016/j.csr.2007.06.015.

Wen ZX, Tong XG, Zhang GY, Wang ZM, Yang SF, Chen HL, Song CP. 2014. Earth Science Frontiers, 21(3), 26–37 (in Chinese with English abstract). doi: 10.13745/j.esf.2014.03.004.

Wei W, Ling SX, Li XN, Wu XY. 2024. Enrichment characteristic and health risk assessment of heavy metals in soils derived from black shale in Chengkou area, Chongqing. Environmental Chemistry, 2024,43(7), 1–10 (in Chinese with English abstract). doi: 10.7524/j.issn.0254-6108.2023011601.

Wei XF, Li YP, Wei ZH, Liu RB, Yu GC, Wang QB. 2017. Effects of preservation conditions on enrichment and high yield of shale gas in Sichuan Basin and its periphery. Petroleum Geology & Experiment, 39(2), 147–153 (in Chinese with English abstract). doi: 10.11781/sysydz201702147.

Weight RWR, Anderson JB, Fernandez R. 2011. Rapid mud accumulation on the central Texas shelf linked to climate change and sea-level rise. Journal of Sedimentary Research, 81(10), 743–764. doi: 10.2110/jsr.2011.57.

Wen HJ, Zhou ZB, Ma WP, Zhu Y. 2024. Research progresses and main scientific issues of strategically critical minerals in black rock series. Bulletin of Mineralogy, Petrology and Geochemistry (in Chinese with English abstract). doi: 10.3724/j.issn.1007-2802.20240008.

Wille M, Nebel O, Van Kranendonk MJ, Schoenberg R, Kleinhanns IC and Ellwood MJ. 2013. Mo-Cr isotope evidence for a reducing Archean atmosphere in 3.46–2.76 Ga black shales from the Pilbara, Western Australia. Chemical Geology, 340, 68–76. doi: 10.1016/j.chemgeo.2012.12.018.

Worden RH, Armitage PJ, Butcher AR, Churchill JM, Csoma AE, Hollis C, Lander RH, Omma JE. 2018. Petroleum reservoir quality prediction: overview and contrasting approaches from sandstone and carbonate communities. Geological Society, London, Special Publications, 435, 421–435. doi: 10.1144/SP435.2.

Woulds C, Cowie GL, Levin LA, Andersson JH, Middelburg JJ, Vandewiele S, Lamont PA, Larkin KE, Gooday AJ, Schumacher S, Whitcraft C, Jeffreys RM, Schwartz M. 2007. Oxygen as a control on sea floor biological communities and their roles in sedimentary carbon cycling. Limnology and Oceanography, 52(4), 1698–1709. doi: 10.4319/lo.2007.52.4.1698.

Wu AB, Zhang JK, Wang JL, Luo JG, Luo Q, Jiang ZX. 2020. Genesis, diagenetic model and geological significance of calcite veins in organic-rich shale: A case study of the Longmaxi Formation, southern Sichuan basin, China. Geological Review, 66(1), 88–100 (in Chinese with English abstract). doi: 10.16509/j.georeview.2020.01.006.

Wu P, Cao D, Zhu GH, Liu XQ, Li Y, Li YB, Hu WQ, Liu ZZ, Kong W, Fei JL. 2021. Geological characteristics and reservoir-forming potential of shale gas of transitional facies in Linxing area, eastern margin of Ordos Basin. Coal Geology & Exploration, 49(6), 24–34. doi: 10.3969/j.issn.1001-1986.2021.06.003.

Xiang J, Chen SB, Wang Y, Jiang TG, Xue XH, Wang XQ, Zhu YM. 2021. Effect of fault system on shale gas preservation: A case study ofthe Wufeng-Longmaxi Formation in Northeast Yunnan area. Journal of China Coal Society, 46(11), 3599–3612 (in Chinese with English abstract).

Xie SC, Jiao NZ, Luo GM, Li DD, Wang PX. 2022. Evolution of biotic carbon pumps in Earth history: Microbial roles as a carbon sink in oceans. Chinese Science Bulletin, 67, 1715–1726 (in Chinese with English abstract). doi: 10.1360/TB-2021-0672.

Xie XM, Tenger, Qian JZ, Zhang QZ, Bian LZ, Yin LM. 2015. Depositional environment organisms components and source rock formation of siliceous rocks in the base of the Cambrian Niutitang Formation Kaili Guizhou. Acta Geologica Sinica, 89(2), 425–439 (in Chinese with English abstract).

Xie XN, Cheng JM, Meng YL. 2009. Basin fluid flow and associated diagenetic processes. Acta Sedimentologica Sinica, 27(5), 863–871 (in Chinese with English abstract).

Xiong YQ, Geng AS, Wang YP, Liu DH, Jia RF, Shen JG, Xiao XM. 2001. Experimental study on dynamic simulation of secondary hydrocarbon generation from kerogen. Science in China, 31(4), 315–320 (in Chinese). doi: 10.1360/zd2001-31-4-315.

Xu HM, Lin YX, Xi FY, Fang LF. 2000. The organic acid evolution and distribution of Eogene in Mangya depression. Petroleum Exploration and Development, 27(6), 23–25 (in Chinese with English abstract).

Xu L, Yang W, Jiang ZX, Chen DX, Wang YH, Lu JK, Zhao MZ, Li L. 2022. Evolution and genesis of organic pores in Triassic Xujiahe Formation shale, Western Sichuan Depression, Sichuan Basin. Oil & Gas Geology, 43(2), 325–340 (in Chinese with English abstract). doi: 10.11743/ogg20220207.

Xu LW, Wang Y, Liu LF, Chen L, Chen J. 2019. Evolution characteristics and model of nanopore structure and adsorption capacity in organic-rich shale during artificial thermal maturation: A pyrolysis study of the Mesoproterozoic Xiamaling marine shale with type II kerogen from Zhangjiakou, Hebei, China. Energy Exploration & Exploitation, 37(1), 493–518. doi: 10.1177/0144598718810.

Xue LH, Shi JA, Jin HJ. 1996. Study of controlling mechanism of carbonate cementation on porosity evolution in Lower Tertiary Sandstones of the Liaohe Basin. Acta Sedimentologica Sinica, 14(2), 102–109 (in Chinese with English abstract).

Yang T, Cao YC, Friis H, Liu KY, Wang YZ, Zhou LL, Zhang SM, Zhang HN. 2018. Genesis and distribution pattern of carbonate cements in lacustrine deep-water gravity-flow sandstone reservoirs in the third member of the Shahejie Formation in the Dongying Sag, Jiyang Depression, Eastern China. Marine and Petroleum Geology, 92, 547–564. doi: 10.1016/j.marpetgeo.2017.11.020.

Yang XG, Guo SB. 2020. Porosity model and pore evolution of transitional shales: An example from the Southern North China Basin. Petroleum Science, 17(6), 1512–1526. doi: 10.1007/s12182-020-00481-7.

Yasser MM, Evgeni MC. 2012. Clay mineral transformation as a major source for authigenic quartz in thermo mature gas shale. Applied Clay Science, 55, 138–150. doi: 10.1016/j.clay.2011.11.007.

Yawar Z, Schieber J. 2017. On the origin of silt laminae in laminated shales. Sedimentary Geology, 360, 22–34. doi: 10.1016/j.sedgeo.2017.09.001.

Yu BS. 2013. Classification and characterization of gas shale fore system. Earth Science Frontiers, 20(4), 211–220 (in Chinese with English abstract).

Yu GC, Wei XF, Li F, Liu ZJ. 2020. Disruptive effects of faulting on shale gas preservation in Upper Yangtze region. Petroleum Geology & Experiment, 42(3), 355–362 (in Chinese with English abstract). doi: 10.11781/sysydz202003355.

Yuan K, Huang WH, Wang T, Li SZ, Sun XC, Fang XX, Xiao JP, Guo J. 2023. Tectonic evolution and accumulation characteristics of Carboniferous shale gas in Yadu-Ziyun-Luodian aulacogen, Guizhou Province, South China. China Geology, 6, 646–659. doi: 10.31035/cg2022059.

Zelt FB. 1985. Natural Gamma-ray spectrometry, lithofacies, and depositional environments of selected upper cretaceous marine mudrocks, western United States, including tropic shale and tununk member of mancos shale. Princeton, Princeton University, 372.

Zeng LB, Ma SJ, Tian H, Xue M, Liu GP, Lü WY. 2023. Research progress of natural fractures in organic rich shale. Earth Science, 48(7), 2427–2442 (in Chinese with English abstract). doi: 10.3799/dqkx.2022.190.

Zhang D, Zhou MZ, Xiong KN, Gu BQ, Yang H, Li WY, Yao CB, Yang LS. 2021. Assessment of pollution and human health risk from heavy metals in soils and crops in the lower Cambrian black shale area, Zunyi, Guizhou Province. Research of Environmental Sciences, 34(5), 1247–1257 (in Chinese with English abstract). doi: 10.13198/j.issn.1001-6929.2021.01.10.

Zhang GJ, Chen DZ, Huang KJ, Liu M, Huang TY, Yeasmin R, Fu Y. 2021. Dramatic attenuation of continental weathering during the Ediacaran-Cambrian transition: Implications for the climatic-oceanic-biological co-evolution. Global and Planetary Change, 203, 103518. doi: 10.1016/j.gloplacha.2021.103518.

Zhang P. 2020. Study on the interaction between organic matter and inorganic minerals and pore characteristcs in shale of Dongying Depression. Qingdao, China University of Petroleum (East China), Master Thesis, 1–99 (in Chinese with English abstract).

Zhang SC, Zhang B, Wang XM, Feng ZH, He K, Wang HJ, Fu XL, Liu YK, Yang CL. 2023. Gulong shale oil enrichment mechanism and orderly distribution of conventional–unconventional oils in the Cretaceous Qingshankou Formation, Songliao Basin, NE China. Petroleum Exploration and Development, 50(5), 911–923. doi: 10.1016/S1876-3804(23)60448-3.

Zhang YF, Yu BS, Sun MD. 2017. Diagenesis and its effect on pores of the Niutitang Formation shale in southeast Chongqing, China. Journal of Chengdu University of Technology (Science & Technology Edition), 44(1), 48–56 (in Chinese with English abstract).

Zhao JH, Jin ZJ. 2021. Mudstone diagenesis: Research advances and prospects. Acta Sedimentologica Sinica, 39(1), 58–72 (in Chinese with English abstract). doi: 10.14027/j.issn.1000-0550.2020.133.

Zhao JH, Jin ZJ, Jin ZK, Hu QH, Hu ZQ, Du W, Yan CN, Geng YK. 2017. Mineral types and organic matters of the Ordovician-Silurian Wufeng and Longmaxi Shale in the Sichuan Basin, China: Implications for pore systems, diagenetic pathways, and reservoir quality in fine-grained sedimentary rocks. Marine and Petroleum Geology, 86, 655–674. doi: 10.1016/j.marpetgeo.2017.06.031.

Zhao JZ, Li J, Xu ZY. 2017. Advances in the origin of overpressures in sedimentary basins. Acta Petrolei Sinica, 38(9), 973–998 (in Chinese with English abstract). doi: 10.7623/syxb201709001.

Zhao WZ, Wang XM, Hu SY, Zhang SC, Wang HJ, Guan SW, Ye YT, Ren R, Wang TS. 2019. Hydrocarbon generation characteristics and exploration prospects of Proterozoic source rocks in China. Science China Earth Sciences, 62, 909–934. doi: 10.1007/s11430-018-9312-4.

Zheng YJ, Liao YH, Wang J, Xiong YQ, Wang YP, Peng PA. 2024. Factors controlling the heterogeneity of shale pore structure and shale gas production of the Wufeng–Longmaxi shales in the Dingshan plunging anticline of the Sichuan Basin, China. International Journal of Coal Geology, 282, 104434. doi: 10.1016/j.coal.2023.104434.

Zhu HJ, Ju YW, Qi Y, Huang C, Zhang L. 2018. Impact of tectonism on pore type and pore structure evolution in organic-rich shale: Implications for gas storage and migration pathways in naturally deformed rocks. Fuel, 228, 272–289. doi: 10.1016/j.fuel.2018.04.137.

Zhu HJ, Ju YW, Huang C, Han K, Qi Y, Shi MY, Yu K, Feng HY, Li WY, Ju LT, Qian J. 2019. Pore structure variations across structural deformation of Silurian Longmaxi Shale: An example from the Chuandong Thrust-Fold Belt. Fuel, 241, 914–932. doi: 10.1016/j.fuel.2018.12.108.

Zhu RX, Wang HJ, Wang HJ, Wang XM, Wan B, Zhang W, Zhu HQ, Liu YK, Liu JL, Meng QR, Hao F, Jin ZJ. 2024. Multi-spherical interactions and mechanisms of hydrocarbon enrichment in the Southeast Asian archipelagic tectonic system. Science China Earth Sciences, 67, 566–583. doi: 10.1007/s11430-023-1254-4.

Zou C, Wu Y, Liang X, Jiang ZX, Wang GC, Zhang JH, Zhang C, He Y, Duan XG, Gong HJ. 2023. Control effect of formation water on shale gas enrichment in the background of strike-slip fault activity in western Chongqing. Petroleum Geology & Oilfield Development in Daqing, 42(3), 11–19 (in Chinese with English abstract). doi: 10.19597/j.issn.1000-3754.202210006.

Zou CN, Ma F, Pan SQ, Zhang XS, Wu ST, Fu GY, Wang HJ, Yang Z. 2023. Formation and distribution potential of global shale oil and the developments of continental shale oil theory and technology in China. Earth Science Frontiers, 30(1), 128–142(in Chinese with English abstract). doi: 10.13745/j.esf.sf.2022.8.29.

Zou CN, Qiu Z, Zhang JQ, Li ZY, Wei HY, Liu B, Zhao JH, Yang T, Zhu SF, Tao HF, Zhang FY, Wang YM, Zhang Q, Liu W, Liu HL, Feng ZQ, Liu D, Gao JL, Liu R, Li YF. 2022. Unconventional Petroleum Sedimentology: A Key to Understanding Unconventional Hydrocarbon Accumulation. Engineering, 18, 62–78. doi: 10.1016/j.eng.2022.06.016.